2018

Active and Reactive Power Control of Flexible Loads for Distribution-Level Grid Services

Jingyuan Wang
Michigan Technological University, jwang11@mtu.edu

ACTIVE AND REACTIVE POWER CONTROL OF FLEXIBLE LOADS FOR DISTRIBUTION-LEVEL GRID SERVICES

By

Jingyuan Wang

A DISSERTATION

Submitted in partial fulfillment of the requirements for the degree of

DOCTOR OF PHILOSOPHY

In Electrical Engineering

MICHIGAN TECHNOLOGICAL UNIVERSITY

2018

This dissertation has been approved in partial fulfillment of the requirements for the Degree of DOCTOR OF PHILOSOPHY in Electrical Engineering.

Department of Electrical and Computer Engineering

Dissertation Advisor: *Dr. Sumit Paudyal*

Committee Member: *Dr. Bo Chen*

Committee Member: *Dr. Lucia Gauchia*

Committee Member: *Dr. Seyed A. Zekavat*

Department Chair: *Dr. Daniel R. Fuhrmann*

Contents

List of Figures

List of Tables

Preface

This dissertation is submitted for the degree of Doctor of Philosophy at Michigan Technological University. The research described herein was conducted under the supervision of Dr. Sumit Paudyal in the Department of Electrical and Computer Engineering, Michigan Technological University, between September 2013 and December 2018. Part of this work was carried out in collaboration with the University of Vermont and the University of Alabama.

Content of Chapter 3 has been published in *J. Wang, G. R. Bharati, S. Paudyal, O. Ceylan, B. P. Bhattarai, and K. S. Myers, "Coordinated Electric Vehicle Charging With Reactive Power Support to Distribution Grids," IEEE Transactions on Industrial Informatics, 2018.* Contents of Chapter 3 of this dissertation are my original contributions.

Content of Chapter 4 is under review for publications. Content of this chapter is developed in collaboration with Dr. M. C. Kisacikoglu and his group from the University of Alabama. The detailed EV/charger models have been provided by them, and are implemented in real-time simulator in this work. Rest of the contents in Chapter 4 of this dissertation are my original contributions.

Part of Chapter 5 is under preparation for a journal. This work has been carried out

in collaboration with Dr. M. R. Almassalkhi and his group from the University of Vermont. The server and the Packetized Load Management algorithm are developed by the University of Vermont. Rest of the contents in Chapter 5 of this dissertation are my original contributions.

Acknowledgments

I would like to thank my PhD advisor, Dr. Sumit Paudyal, for supporting me in the past five years. He is the nicest advisor and one of the smartest people I've ever seen. I hope that I could be as passionate and efficient as he is. I appreciated every single insightful discussion about my research with him and every single piece of suggestion that he ever gave me. He is my primary resource to learn, understand and appreciate power systems.

I would like to thank Dr. Mads R. Almassalkhi, Adil Khurram, and Mahraz Amini from the University of Vermont for the collaboration opportunity that helped to complete Chapter 5 of this dissertation. I would like to acknowledge support provided through ARPA-E Award No. DE-AR0000694.

I would like to thank Dr. Mithat C. Kisacikoglu and Emin Y. Ucer from the University of Alabama for the collaboration opportunity that helped to complete Chapter 4 of this dissertation. I would like to thank all my committee members, Dr. Bo Chen, Dr. Lucia Gauchia, and Dr. Seyed (Reza) A. Zekavat, for their suggestions on my research.

I take this opportunity to express my gratitude to my parents for their love, unfailing encouragement and support.

Abstract

Electric vehicle (EV) charging/discharging can take place in any P-Q quadrants, which means EVs could provide reactive power at any state-of-charge (SOC). This dissertation shows four-quadrant operation of EVs and aggregation of EVs for support of grid operations.

First, this work develops hierarchical coordination frameworks to optimally manage active and reactive power dispatch of number of spatially distributed EVs incorporating distribution grid level constraints. This work demonstrates benefits of coordinated dispatch of active and reactive power from EVs using a 33-node distribution feeder with large number of EVs (more than 5,000). Case studies demonstrate that, in constrained distribution grids, coordinated charging reduces the average cost of EV charging if the charging takes place at non-unity power factor mode compared to unity power factor. Similarly, the results also demonstrate that distribution grids can accommodate charging of increased number of EVs if EV charging takes place at non-unity power factor mode compared to the unity power factor.

Next, this work utilizes detailed EV battery model that could be leveraged for its four-quadrant operations. Then, the developed work coordinates the operations of EVs and distribution feeder to support voltage profile on the grid in real time. The

grid level problem is devised as a distribution optimal power flow model to compute voltage regulation signal to dispatch active/reactive power setpoints of individual EVs. The efficacy of the developed models are demonstrated by using a LV secondary feeder, where EVs' operating in all four quadrants are shown to compensate the feeder voltage fluctuations caused by daily time varying residential loads, while honoring other operational constraints of the feeder.

Furthermore, a novel grid application, called virtual power plant (VPP), is developed. Traditional nonlinear power flow problems are nonconvex, hence, time consuming to solve. In order to be used in real time simulation in VPP, an efficient linearized optimal power flow model is developed. This linearization method is used to solve a 534-bus power system with 3 VPPs in real-time. This work also implements VPP scheduling in real-time using OPAL-RT's simulator in hardware-in-the-loop (HIL), where the loads are emulated using micro-controller devices.

Chapter 1

Introduction

1.1 Motivation

Electric vehicles (EVs) are increasingly used due to their clean nature. Fossil fuel generates a lot of greenhouse gas emission and EVs are one of the solutions to reduce it. According to [1], EV sales in USA by year and month as for 2016 is shown in Fig. 1.1. Over 159,000 new EVs hit the road, and sales were 38% more than the numbers in 2015. 2016 EV sales by state is shown in Fig. 1.2. California is leading overwhelmingly, representing over 50% of the total EV sales in the USA. The other 9 states including CT, ME, MD, MA, NJ, NY, OR, RI, VT account for another 25%.

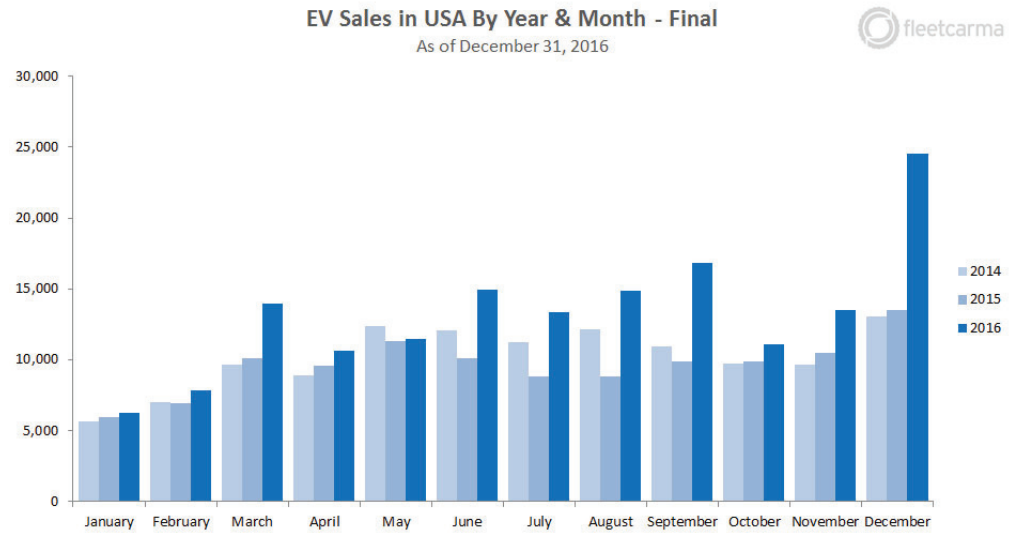

Figure 1.1: 2016 EV sales in USA by year and month [1].

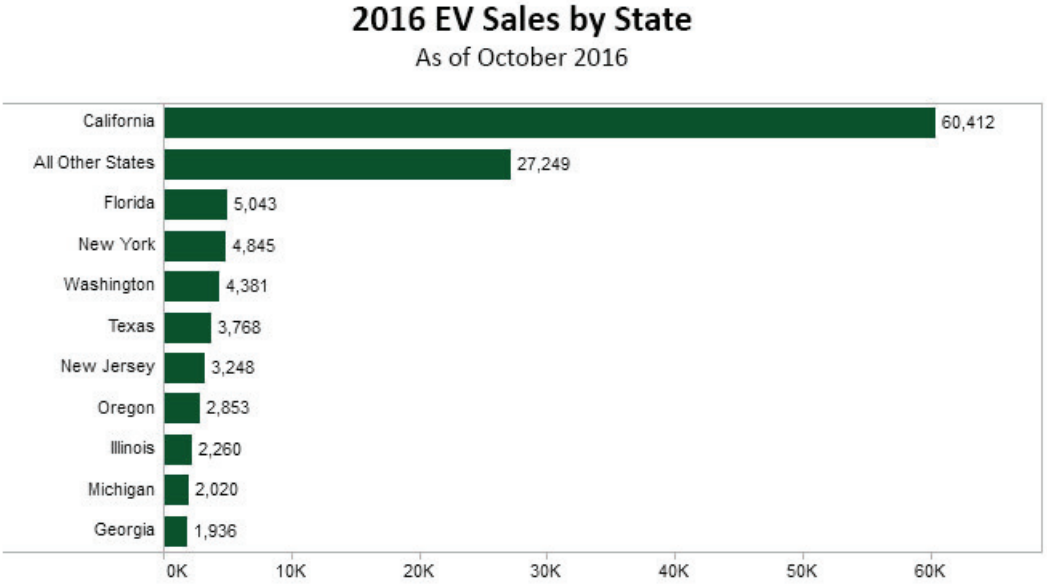

Figure 1.2: 2016 EV sales by state [1].

EVs, due to their sizable power ratings and flexibility of charging, possess great demand response potential in electric power grids. EV aggregation not only benefits the operations of distribution grids, this could support system-wide frequency regulation, load following services, etc [7, 8, 9]. Despite the benefits EVs provide to the

grids [10, 11, 12, 13, 14], high penetration of EVs adversely impact power grids in case of uncoordinated charging. High penetration of EV leads to several issues on distribution feeders including increased energy losses, voltage deviations, and transformer overloading. Studies showed that about 50% penetration of EV leads to 50% overloading of distribution transformers [15] and causes 25% more energy losses in the feeders [16]. Uncoordinated EV charging requires replacing most 50 kVA distribution transformers if EV penetration level reaches 40% [17]. To reduce the negative impacts of EVs on grid operations and equipment, coordinated charging schemes can be devised, in which distribution system operator (DSO) would coordinate the charging of EVs [10, 18, 19, 20, 21, 22].

This dissertation concentrates around solving distribution level operational problems by utilizing the flexibility of EV loads.

1.2 Smart Grid and Demand Response

Smart grid refers to the communication and computer-based technologies which are used for remote and automatic control of electric power grids, from generation all the way through transmission and distribution systems, in order to improve efficiency, reliability and security of the grids [23]. Smart grid also helps to optimize grid operations, to apply 'smart' meters and other sensors for measuring system conditions,

to encourage demand response activities, and to accommodate high penetration of EVs and distributed energy resources (DERs) into systems. Generally, smart grid is intelligent, efficient, accommodating, quality-focused, resilient, and 'green' [24].

With the help of smart meters, advanced metering infrastructure (AMI), and advanced computing capabilities, it becomes possible to predict the peak loads on the grids and to take demand response actions to avoid overload on the grids, which otherwise might lead to power failure. Although DERs such as wind and solar are growing due to environmental reasons, they are generally non-dispatchable and intermittent compared to the demand response resources [25]. Demand response, also known as demand-side management, is a recent trend in smart grids. This means consumers can make corresponding interactions and responses to grid operators power adjustments while respecting their own choices and privacy, such as consuming less energy during peak periods or shifting power consumption to a different time. Demand response not only means lowering peak demand, rather, it also represents demand increase when there is high power production [26]. Without demand response, independent system operators (ISOs) and regional transmission operators (RTOs) determine the electricity price in power markets with the assumption that customers could not adjust their power usages even when the price is very high. Such markets result in fixed energy price and there will be no motivation for customers to defer using energy intensive appliances such as EVs, air conditioners, water heating, and clothes dryers, at peak

hours [27].

There are several options to implement demand response, such as price options, incentive options, and demand reduction bids. Time of use rates (TOU), critical peak pricing (CPP) and real-time pricing (RTP) are popular price options. TOU refers to different fixed rates for different times of a day. CPP refers to an extra-high rate which is planned by utilities during a limited time period. RTP refers to real-time changing rates in response to wholesale market prices. For incentive options, customers receive incentive payments for load reduction or load curtailment. For a demand bidding program, customers could bid to reduce or curtail loads in real-time market when wholesale market prices are high [26]. By getting compensations, various rates and other financial incentives, consumers can be engaged in the grid operations by reducing their electricity usage or even send electricity back to the grid at the peak power usage periods.

The main purpose of demand response is to balance the supply and demand with the help of demand itself [28]. All the generation, transmission, distribution systems and customers can get benefits from demand response programs. For generation systems, they can produce less power and at peak time, decrease power spinning reserves and reduce capital cost investments. For transmission and distribution systems, demand response can relieve congestion, increase reliability and decrease power losses. For customers, demand response and load shifting help them to reduce electricity bills

[26, 27].

Demand response also has its own limitations. For instance, it can affect customers' comfort to some extent and may impact the grid adversely if not coordinated. Reference [29] proposed comfort indices such as severity indices, scale indices and duration indices to measure how severely and how long consumer's comfort is violated. Reference [30] proposed a demand response strategy as a load shaping tool to solve distribution transformer overloading problem by operating home appliances without violating customers' comfort and privacy. Reference [31] proposed an intelligent home energy management (HEM) algorithm to keep power consumption of the whole house under demand limit. A HEM system helps with demand response applications for end-use costumers. HEM system could monitor, control, manage and operate home appliances to reduce, shift or curtail loads in response to system requirements. References [29, 30, 31] only considered high power consumption home appliances in the research, such as water heaters, air conditioners, clothes dryers, and EVs, ignoring the detailed modeling of grid for analysing the impact of demand response on the grids.

1.3 Electric Vehicle Loads

EVs provide excellent demand response potential due to their size and flexibility. Not only distribution grids benefit from demand response of EVs, but also EV consumers could get monetary incentives from the grid operators. The benefits are mutual, which could motivate the EV owners to get involved in demand response activities.

EVs require regular charging due to the limited battery capacities. The time and power EV takes to charge depend on charging infrastructure. Table 1.1 shows three EV charging levels and ratings. Level 1 charging is 1-phase slow charging, level 2 charging comes with 3-phase slow and fast charging, and level 3 charging is fast charging.

Table 1.1
Levels of EV charging[6].

Levels of charging	Ampere (A)	Voltage (V)	Power (kW)
Level 1 charging **AC plug, single phase, slow**	$12 - 16$	120	$1.3 - 1.9$
Level 2 charging **AC plug, 3-phase, slow and fast**	≤ 80	240	≤ 19.2
Level 3 charging **DC charging, 3-phase, fast**	≤ 80	480	≤ 130

The demand response from EVs come from controlling or deferring the charging of EVs. Therefore, efficient EV battery charging algorithms should be emphasized and studied for an effective demand response program from the EVs. Some research has

already been carried out in this area in recent years, and according to [6], EV charging schemes can be classified into two main categories: uncontrolled and controlled smart charging.

Uncontrolled Charging, also called uncoordinated charging, refers to start serving and charging EVs right after they are plugged in, without arranging and organizing their charging schedules. An uncontrolled charging flow chart is shown in Figure 1.3. Uncontrolled charging can lead to several issues including large voltage deviations, peak load increasing, transformer/feeder overload, etc [6].

Controlled Charging, which is also referred to as coordinated charging, tries to solve the charging schedules while keeping the power grids from overloading issues, limiting load profile valley, or anything that can decrease power quality and reliability. The control objectives are either optimal economic objectives, such as minimum cost, minimum power losses or maximum profit, or optimal operational objectives, such as valley-filling/peak shaving/flattening of the load profiles or even maximizing the grid load factor. According to [6], controlled charging schemes can further be classified into indirectly-controlled charging, smart charging, and bidirectional charging. For indirectly-controlled charging, directly-controlled parameters such as charging rate and charging duration are not used. Instead, any other indirect factors, such as incentives, which can help EV owners make their decisions are used. For smart charging, directly-controlled parameters are used. Charging power can vary from

time to time, place to place depending on system's requirement; thus, the EV totally turns to a flexible load in this case. However, the energy may only flow from grid to vehicle (G2V), not the other way around. The majority of EV coordinations are about unidirectional charging between EVs and power grids. For bidirectional

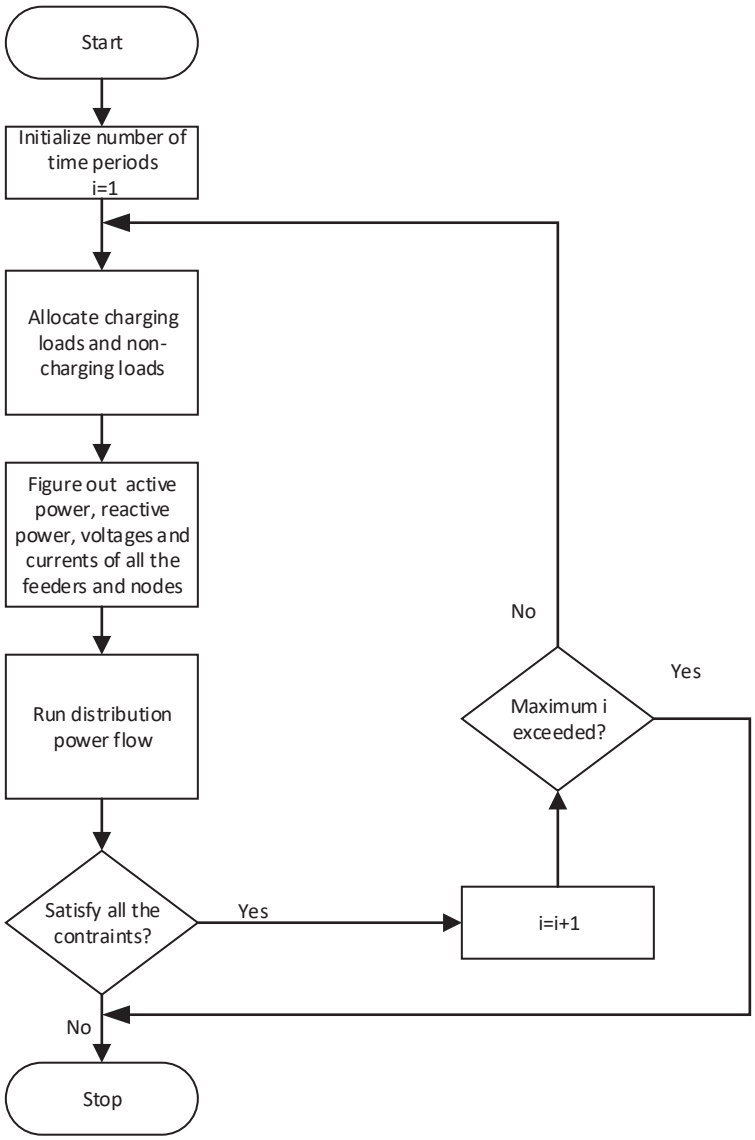

Figure 1.3: Flow chart for uncontrolled charging of EVs.

charging [32, 33, 34, 35, 36, 37, 38], the power electronic devices make it possible for electricity to flow from vehicle to grid (V2G) at the same time as G2V. In that case, EVs are not only consumers or flexible loads, but moving energy sources. With V2G options, EVs can participate in frequency regulation and many power markets such as bulk energy markets and spinning reserve markets. They could flatten the load profile by taking energy from EV loads when there is a high load demand in the system and charging EV loads when the demand is low.

1.4 State-of-the-art

Coordinated charging of EVs is an active area of research. References [11, 39] proposed coordinated EV charging to minimize the power losses and maximize the grid load factor with quadratic programming (QP) and dynamic programming (DP) approaches. The QP can optimize quadratic function while satisfying linear constraints. DP is the shortest path technique and it has to store every possible passes through stages so it takes more time than QP. Reference [40] proposed a new charging technique to optimize the total power delivered to EVs within the constrains set. Reference [41] used smart charging to carry out unidirectional V2G regulation. The proposed method requires communication between EVs and aggregator, and the aggregator sends all the combined data of EVs to markets to bid. The method finds the preferred operating point (POP) which is the target average power consumption

around which the EV could be charged. However, this work only discussed EV power dispatch ignoring the distribution grid constraints. Reference [9] discussed a novel algorithm for bidirectional charging and discharging of EVs. The authors in [9] proposed optimal schedule of EVs to minimize total costs in each group of EVs. They proved that the performance of this approach is close to the global one. Reference [42] proposed a coordinated real-time smart load management (RT-SLM) algorithm based on maximum sensitivities selection (MSS) to minimize power losses. The RT-SLM allows EVs to charge as soon as possible within priority-charging time zones and all grid constrains. Reference [43] developed an optimal charging/discharging control of EVs to minimize operation costs which includes energy costs and battery degradation costs, and also considers system voltage constrains and line current constrains. Reference [12] proposed an optimal charging and V2G control of EVs to minimize the total charging costs subject to demand constrains. This paper focused on the EV dispatch issues and didn't explicitly modeled the grid constraints.

Possible coordination charging scheduling can be classified into two categories: centralized charging and decentralized charging [44]. For centralized charging scheduling, the control center (e.g., grid control center) decides precise charging time and charging rate of each EV while decentralized charging scheduling, also called distributed charging, allows each EV to make their own charging decision. Centralized algorithms optimize the charging profile of all the EVs with all the relevant information collected at a centralized location. Their objective functions include minimize power loss, load

variance minimization, and EV penetration maximization [11, 45, 46].

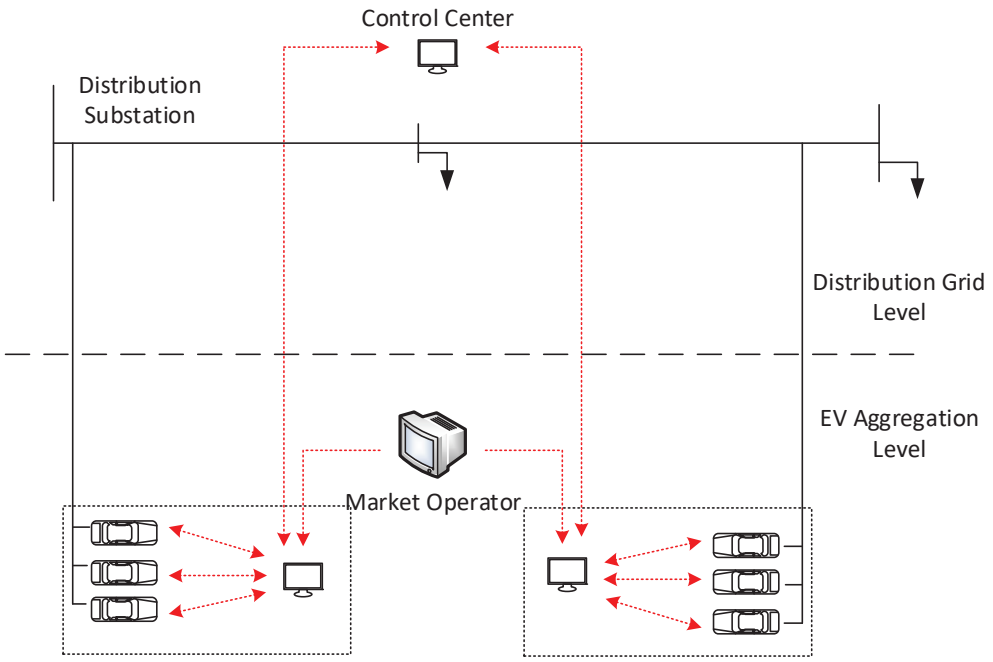

Figure 1.4: Hierarchical Control of Distribution Grid and EVs.

1.4.1 Distributed EV Charging Algorithms

Thanks to smart meters, AMI and communication techniques, EVs are able to decide their own charging profile, which is called decentralized algorithm. Decentralized control can effectively reduce computational complexities due to decomposition of the large centralized scheduling problem. Reference [47] proposed algorithms to solve optimal decentralized charging (ODC) models, which use synchronous, asynchronous, and real-time ODC algorithms. Those algorithms can help solve valley filling and

flatten load profiles. EVs update their charging schedule profile in each iteration depending on the control signals obtained from the control center. Control center also updates its control signal to help EVs adjust their schedules. Reference [44] is also solving valley-filling with decentralized charging control. However, the papers [44, 47] do not consider modeling of the grid side. Similarly, in [48] a decentralized algorithm is proposed which is based on iterative water-filling and the objective is to flatten the total demand profile with bidirectional energy flow and decentralized control. This paper also focused on load demand and EV dispatch problems but didn't explicitly model the power grid. Reference [49] developed a droop-based control and novel distributed V2G dispatch algorithm to maximize revenues of aggregators from ancillary services. Reference [50] developed a decentralized bidirectional EV coordination charging method to carry out valley-filling, aiming to minimize load variance. Similarly, the decentralized charging mechanism in [51] minimize aggregate load variance to avoid system overloading with overload cost functions.

Hierarchical computing approaches was brought up by [47, 52, 53]. There can be several levels and necessary information can be exchanged among different levels. A big demand dispatch problem can be split into several small problems which can reduce computational complexity to a great extent. Reference [54] proposed a bi-level hierarchical vehicle-to-grid optimization framework, as showed in Figure 1.4. There are both distribution grid level and EV aggregation level involved in the hierarchy.

Information such as each EV owners preferences, EVs state of charge (SOC), distribution system control commands and market operators strategies are supposed to exchange among every member inside this hierarchy.

A centralized approach to solve EV scheduling problem is computationally involving in a practical sized distribution system. To reduce the computational complexity, distributed and hierarchical computing approaches can be used with information exchange among various levels in the hierarchy. It is shown that computational complexity can be reduced by using distributed approach, which leads to small manageable problems. Therefore, in this proposed work distributed algorithm, particularly ADMM, will be used to solve optimal scheduling of large number of EVs in distribution grids.

1.4.2 Reactive Power Support from EVs

Every single customer device consumes some amount of reactive power. Reactive power flow affects voltages throughout the system, and helps improve voltage profile, grid reliability, and security. It also helps increase transferring power factor and improve real power transfer capability. Traditionally, reactive power is generated by synchronous generators, synchronous condensers, capacitors, static VAR compensators

(SVCs), static synchronous compensators (STATCOMs), flexible ac transmission systems (FACTS) and distributed generation. But, the shortcomings are the reactive power capacity they generate is limited and reactive power needs to be transmitted from a fixed place to the loads [55, 56]. Currently, most of the reactive power gets to the load all the way through generation, transmission and distribution systems, which causes more power losses and make transformers get overloaded.

Even though the optimal EV scheduling has been an active research topic recently, reactive power dispatch of EVs is not discussed much. Grid applications, such as frequency regulation, load following, etc. [7, 8, 57] can be obtained from active power dispatch of EVs, while reactive power dispatch could provide ancillary services for voltage support [3, 58]. With power-electronics based charging infrastructure, the EV charging/discharging could be operated in any P-Q quadrants, as shown in Figure 1.5. In fact, the EVs could generate/consume reactive power at any SOC level without impacting lifecycle of the batteries [3, 59, 60]. With this control flexibility, EVs can support reactive power and voltage control applications in the power grid [61].

According to [62], EVs can respond to the system demand locally and fast, and provide reactive power back to the grid even without battery. Reference [63] also pointed out that EVs can participate in ancillary service market and demand response by providing reactive power to the grid. Reference [64] pointed out that there is no battery degradation in reactive power market, and presented both decoupled and

coupled energy and reactive power markets with EVs integrated. Therefore, EVs provide an efficient way to support power systems with reactive power. In addition, EV owners can receive compensation for providing reactive power support to the grid. With reactive power, bidirectional power occurs [52, 65] with EV charging process taking place in any of the P-Q quadrants, as shown in Figure 1.5.

Usually, V2G refers to active power flowing from vehicles to grids. However, chargers can also provide reactive power support back to the grid whenever they get a chance to plug in outlets. Reference [66] designed a bidirectional battery charger which enables EV itself send reactive power back to the grid, and balances the reactive power between supply and demand. This on-site reactive power can reduce the reactive power transmission through the entire grid and take advantage of several operation modes of the EVs. However, most of the papers on reactive power from EVs focus on designing electronic circuit interface. For instance, [65] designed a battery charger for V2G reactive power compensation with inverter dc-link capacitor and [67] developed several non-isolated bi-directional DC-DC converters for EV charging.

Some paper focus on the battery level, such as in [68]. Other papers such as [55, 56, 69] focus on the reactive power market level. Reference [55] proposed a stochastic scheme for clearing of reactive power market with EVs involved in, and solved it as a mixed integer non-linear programming (MINLP) problem. Reference [69] came up with a decentralized EV on-street parking and charging scheduling method for V2G reactive

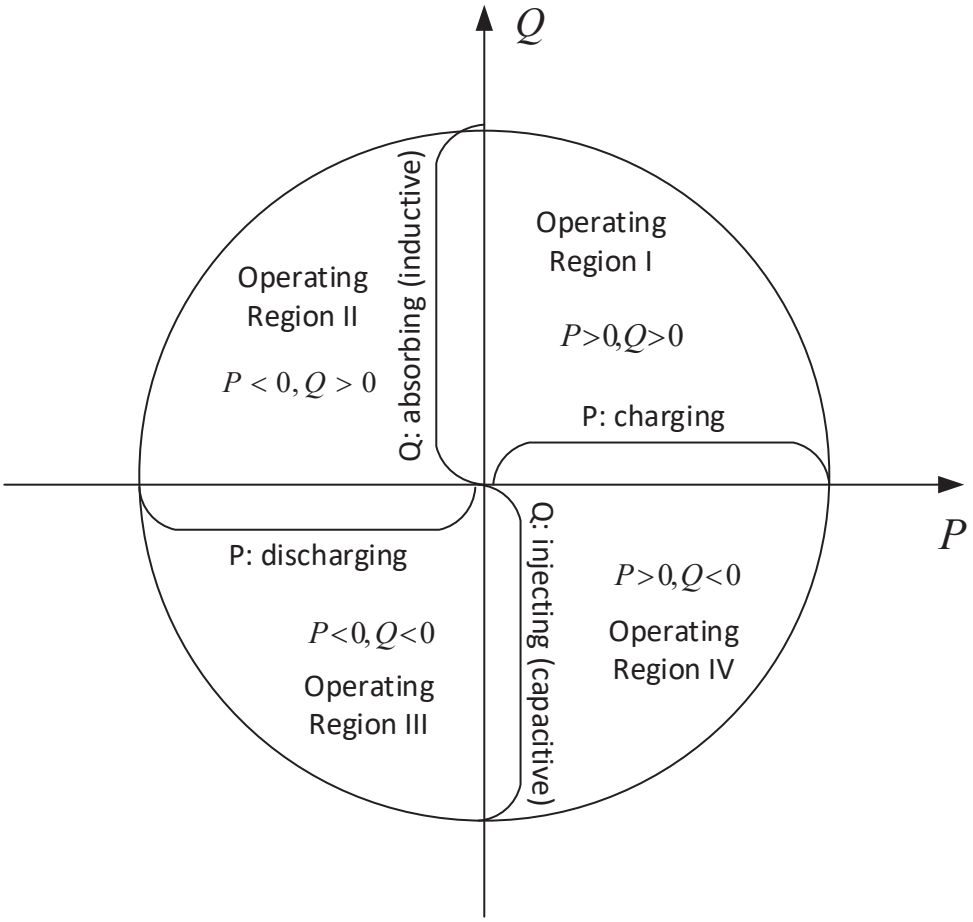

Figure 1.5: Operation modes of the EVs.

power compensation. EVs are used as mobile reactive power resources in this scheme.

Since reactive power support is an important issue in power grids, in this proposal, the reactive power support from the EVs will be included while solving the optimal scheduling of EVs.

1.5 Literature Review

1.5.1 Coordinated EV Charging with Reactive Power Support to Distribution Grids

DSO can limit charging power for EVs based on existing system peak load in coordinated scheme [70, 71]. DSO may use operational limits on voltage drop, feeder current rating, etc., to coordinate EV charhing [72, 73]. In constrained feeders, EV coordination helps maintain distribution grid operational limits [74, 75]. However, when DSO imposes limits on charging power for the EVs to maintain the grid constraints, the cost of charging EVs may increase. This can happen when dynamic energy pricing scheme is used.

Centralized approach to solve EV scheduling problem on practical-sized grid with large penetration of EVs becomes computationally challenging task due to mixed-integer non-linear nature of the problem [76, 77]. In [72], EV scheduling with grid constraints is simplified to a linear programming (LP) problem; however, the resulting LP problem may be infeasible to the original nonlinear model. Distributed and hierarchical computing approaches have also been used to achieve computational efficiency [48, 77]. However, references [48, 77] did not consider modeling of the grid.

Even though a rich literature exists for optimal active power scheduling of EVs, reactive power dispatch is not discussed often. Grid applications, such as frequency regulation, load following, etc. [7, 8, 57] can be obtained from active power dispatch of EVs, while reactive power dispatch could provide ancillary services for voltage support [3, 58]. EV could be charged/discharged in any P-Q quadrants with advanced charging infrastructure. In fact, the EVs could generate/consume reactive power at any state-of-charge (SOC) level without impacting life cycle of the batteries [3, 59, 60, 78, 79]. With this control flexibility, EVs can support reactive power and voltage control applications in the power grid [61]. According to [3], EVs can respond to the system demand locally and fast, and provide reactive power back to the grid even without battery. It was also pointed out in [59] EVs can participate in ancillary service market and demand response by providing reactive power to the grid. The authors in [64] specified that there is no battery degradation when EVs participate in reactive power markets, and presented both decoupled and coupled energy and reactive power markets for EVs. Hence, EVs provide an efficient way to support power grids with reactive power.

1.5.2 Four Quadrant Operation of EVs for Voltage Support and Real Time Implementation

Uncontrolled charging of large number of EVs leads to increased feeder losses, voltage deviations, overloading of distribution transformers, and the need for network reinforcements [22, 80, 81]. Studies showed that 45% EV penetration will lead to 50% overloading on the transformers and 25% increase in the energy losses in the distribution system [82]. Similar observation is made in [17] that uncoordinated charging of EVs will require replacing all 50 kVA transformers when EV penetration exceeds 40%.

In coordinated charging, DSO could restrict charging of EVs based on existing system peak load [70, 71], or using operational limits on voltage drop, feeder current rating, etc. [72, 73]. In previous studies [74], it is shown that in constrained distribution grids, coordinated charging of EVs help maintain distribution grid operational limits; however, average cost of charging EVs may increase. This could happen particularly when EVs are subscribed to dynamic energy prices and DSO imposes limits on charging power for the EVs to maintain the grid constraints.

The peak loads caused by EV charging can be restrained either by unidirectional

EV charging management [22, 83] or by discharging EV batteries into the grid using vehicle-to-grid (V2G) technology [84, 85, 86]. In coordinated charging schemes, distribution system operator (DSO) would coordinate the charging to minimize the adverse impacts of EVs on grid operations and equipment [18, 20, 22, 73]. DSO could restrict charging of EVs based on existing system peak load [70, 71], or using operational limits on voltage drop, feeder current rating, etc. [72, 73]. The DSO could use full-fledged optimization model with objectives such as load profile optimization, loss/cost/emission minimization [87, 88], and revenue maximization [32] to coordinate the charging of EVs. Contrary to the problems due to large EV penetration, there is also a great potential for demand response management and grid ancillary services in distribution feeders due to flexibility of EVs' charging and their sizable power ratings [10, 89, 90, 91].

At the distribution level, EVs can provide Volt/Var support [63, 86, 89, 92, 93]. Traditionally, this service is provided only by utilizing load tap changers (LTCs) and capacitor banks at the distribution level [94, 95]. Even though the optimal EV scheduling has been an active research topic recently, reactive power dispatch of EVs is not discussed much. Grid applications, such as frequency regulation, load following, etc., can be obtained from active power dispatch of EVs [7, 8], while reactive power dispatch could provide ancillary services for voltage support [3, 63]. According to [3], EVs can respond to the system demand locally and fast, and provide reactive power back to the grid even without battery. With advanced power-electronics based

charging infrastructure, the EV charging/discharging could be operated in any P-Q quadrants. In fact, the EVs could generate/consume reactive power at any state-of-charge (SOC) level without impacting life cycle of the batteries [3, 63, 64, 78]. With this control flexibility, EVs can support reactive power and voltage control applications in the power grids.

Reactive power potential of EVs using a residential 3.3 kVA and a commercial 30 kVA charging station is demonstrated in [86, 93]. Recent work in [96] utilized EVs and LTCs to regulate voltage in distribution feeder. Similarly, reactive power dispatch of EVs [97] and 4-quadrant operations of EVs [98, 99] for voltage control are recently proposed. Even though these studies focus on reactive power control of EVs for grid voltage support, modeling is primarily focused on grid side, while battery and charger models are overly simplified.

1.5.3 Real-time Virtual Power Plant Coordination at Distribution Level

With large penetration of Distributed Energy Resources (DERs), storage, and flexible loads on low voltage grid, the concept of virtual power plant (VPP) is becoming reality. VPP is an efficient way to couple small DG units with demand response (DR) and distributed energy storage into one large aggregation which can participate on

real-time power balancing. VPP is a power plant with dynamic and limited power and energy capacity constraints. VPP's operating bounds are based on several factors in the VPP including heterogeneity of devices, customers' preferences, distribution network constraints, etc. Therefore, modeling of network constraints in VPP coordination is very crucuial, as the resources are spatially distributed on the low voltage network [100, 101]. Recent works in VPPs [101, 102] demonstrates VPP dispatch using individual DER constraints and system constraints. Reference [103] developed an optimization framework for DER aggregation to emulate a VPP, which can provide regulation services. In other related work on VPPs, optimal scheduling of VPPs are presented in [104, 105], and value of energy storage devices into VPP is shown in [106].

With the help of advanced metering infrastructure and advanced information and communication technologies, parameters and status of smart grids can be accurately monitored and controlled [107]. On-load tap changers (OLTC), step voltage regulators (SVR), and shunt capacitors (SC) can be remotely controlled to help power systems operate within constraints and optimize objective functions (such as loss minimization). Mathematically, this could be achieved through distribution level Optimal Power Flow (DOPF). DOPF in accurate formulation is non-liner and non-convex, and may involve integer control. DOPF has inherent computational challenges that prohibits its application in real-time control [108]. Therefore, a non-convex version of DOPF may not be suitable for VPP dispatch, if a fast grid service is sought from

the VPP. In this context, a linearized version of DOPF model could be a possible solution to dispatch VPP in real time.

Several recent works have used linearization approaches for DOPF, to convert non-linear problem to linear programming (LP) problem. A piece-wise linear approximation is used in [109, 110, 111, 112, 113]. A curve-fitting technique is used in [114] to obtain linear equivalents. Sensitivity coefficients are used in [115, 116] to linearize the relationship between voltages and control variables. DistFlow method is used in [113, 117, 118, 119, 120] to approximate power flow model assuming line losses are negligible and voltage deviations are small. Further, simplified-DistFlow method is used in a linear approximation of branch flow model in [121, 122] by dropping the second order terms. Truncated Taylor series is used in [112, 123] to linearize power flow equations. It used first-order approximation of P, Q and V around the operating point to transform non-linear constraints to linear constraints.

1.6 Contribution of the Dissertation

The main contributions of this dissertation are:

† Bi-level EV and grid optimization models are developed; Inclusion of reactive power in the formulation of optimal EV charge scheduling and to the best of the

author's knowledge, this is the first work that considers both active and reactive power in the optimal EV scheduling formulation; Modeling of comprehensive distribution optimal power flow with inclusion of flexible reactive power support from EVs, load shifting, and curtailment as demand response options; Applications that demonstrate coordinated reactive power dispatch of EVs combined with active power can result in higher EV penetration without impacting the grid.

† Inclusion of reactive power in the formulation of optimal EV charge scheduling problems at distribution grid level and, integration to the detailed EV charger/-battery model for grid services such as voltage support applications; Real-time implementation of 4-quadrant operation of EV.

† A novel linearized optimal power flow approach is proposed by taking first order of Taylor series expansion; Voltage regulation signals in terms of active and reactive power dispatch are generated by linearizing about the operation points; Distribution level VPP coordinator is developed to reschedule VPPs against distribution constraints; Real-time hardware-in-the-loop (HIL) simulation is implemented.

Chapter 2

Background

2.1 Introduction

This chapter describes background information required to understand the contents provided in Chapters 3,4, and 5. Specifically, this chapter describes mathematical models of distribution power flow with operational constraints, EV model, and EV charger model.

2.2 Nomenclature

Subscripts

ag	EV aggregator
c	curtailment
g	grid
i	node number/EV aggregator number
$init$	initial value
j	branch number which connects node i and node $i+1$
nom	nominal value
ph	phase, ph=a,b,c
rv	receiving end
s	shifting
sd	sending end
t	time

Superscripts

$base$	base load
c	curtailment
Cap	capacitor load
$consI$	constant current load
$consP$	constant power load
$consZ$	constant impedance load
EV	EV loads
max	maximum value/upper limit
min	minimum value/lower limit
R	rating value
req	minimum requirement
s	shifting
Var	variable load
Xfm	transformer

Parameters

Δ_{step}	$\Delta_{step} = 0.00625$ per unit

Δ_t	time interval
η	efficiency
γ	trade-off parameter
λ	penalty factor/birth rate
μ	death rate
ρ	augmented Lagrangian parameter, penalty factor
A, B, C, D	three phase ABCD parameter matrices
B	binary number
$c(t)$	price per unit
E	state
k	population of a size/ current iteration number
N	number of EVs/ number of agents
P	probability
tap	tap number, tap=-16,-15,...,15,16
SOC	state of charge
SOD	state of discharge
TP	total active power
TS	total apparent power
u	scaled price vector

Variables

I	complex current vector
$\bar{I}$	complex conjugate of current vector
P	active power
Q	reactive power
S	apparent power
V	complex voltage vector
x	load profile, which is a vector
$\bar{x}$	average load profile of all the agents
Z	impedance

Functions

$\int$	integral
f	cost function
$\Re$	real part of a complex number
$\Im$	imaginary part of a complex number

2.3 Distribution Power Flow Model

Kirchhoff's circuit law (KCL) and Kirchhoff's voltage law (KVL) are used to formulate the distribution circuit equation [124]. The diagram of component connection is shown in Figure 2.1.

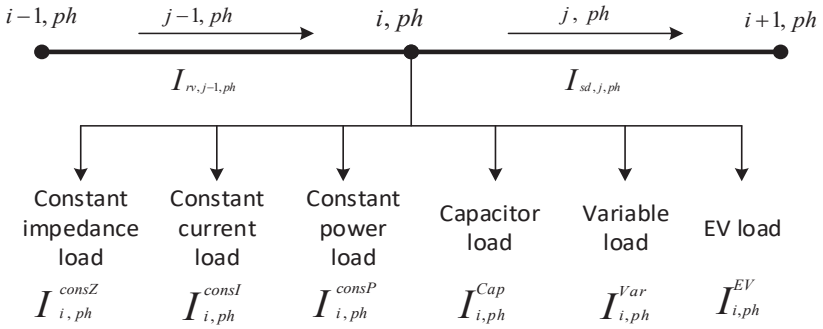

Figure 2.1: The diagram of components.

The series elements such as cables, transformers, conductors and load tap changers are modeled with ABCD parameters, which can be formulated as,

$$\begin{bmatrix} V_{i,ph}(t) \\ I_{sd,j,ph}(t) \end{bmatrix} = \begin{bmatrix} A_j & B_j \\ C_j & D_j \end{bmatrix} \begin{bmatrix} V_{i+1,ph}(t) \\ I_{rv,j,ph}(t) \end{bmatrix} \tag{2.1}$$

The equation constrains above is based on KVL.

Three phase transformers are modeled based on either delta connection or wye connection. Distribution cables and conductors are modeled based on pi-equivalent circuits. Load tap changers (LTC) enable voltage regulation of output by adjusting discrete numbers of turns to get different output voltage ratios. The voltage range being used in this paper is [0.9, 1.1] per unit, and 32 steps included in the tap changer. So there is 0.00625 per unit difference between each step. The LTC is also modeled with the equation above, and the ABCD parameters are represented as follows,

$$A_{LTC}(t) = \begin{bmatrix} 1 + \Delta_{step} \times tap_{Aph} & 0 & 0 \\ 0 & 1 + \Delta_{step} \times tap_{Bph} & 0 \\ 0 & 0 & 1 + \Delta_{step} \times tap_{Cph} \end{bmatrix} \tag{2.2}$$

$$B_{LTC}(t) = C_{LTC}(t) = [0] \tag{2.3}$$

$$D_{LTC}(t) = A_{LTC}^{-1}(t) \tag{2.4}$$

Shunt components refer to constant impedance load, constant current load, constant power load, capacitor banks, and variable loads. Capacitor banks are modeled as constant impedance load. The models and equations for those loads are represented below, and V_{nom} stands for nominal voltage for single phase.

For single-phase constant impedance load,

$$Z = \frac{V_{nom}^2}{\overline{S}} = \frac{V_{nom}^2}{P - jQ} \tag{2.5}$$

For constant current load,

$$\overline{I} = \frac{S}{V} = \frac{P + jQ}{V} \tag{2.6}$$

For constant power load,

$$S = P + jQ = V_{nom} * \overline{I} \tag{2.7}$$

For capacitive loads, they could be modeled as constant impedance loads but the active power is always zero.

For three-phase, all the single-phase nominal voltages, currents, and impedance should be changed to line to line values.

EV loads can be modeled as follows,

$$S^{EV} = V(t) \times \overline{I^{EV}(t)} \tag{2.8}$$

Where $P^{EV} = \Re(S^{EV})$ and $Q^{EV} = \Im(S^{EV})$.

Those models are based on single phase. As for three-phase, phase voltages and currents should be replaced by line to line voltages and currents.

Based on KCL, the equation constrain is as follows,

$$I_{rv,j,ph} - I_{sd,j+1,ph} = I^{consZ}_{i+1,ph}(t) + I^{consI}_{i+1,ph}(t) + I^{consP}_{i+1,ph}(t) + I^{cap}_{i+1,ph}(t) + I^{EV}_{i+1,ph}(t) + I^{var}_{i+1,ph}(t) \tag{2.9}$$

2.4 Distribution Operational Constraints

Distribution operational constrains refer to operation limits such as voltage, current, power capacity limits. These constrains are inequality constrains for the optimization problem.

The voltage limit means the node voltage should be neither over maximum voltage nor lower than minimum voltage to ensure power quality and grid reliability. It is defined below,

$$V_i^{min} < |V_{i,ph}(t)| < V_i^{max} \tag{2.10}$$

Similarly, current limit is defined as follows,

$$|I_{j,ph}(t)| \leq I_j^{max} \tag{2.11}$$

And transformer capacity limit is shown below,

$$\sum_{ph} \left| V_{i,ph}(t) \times \overline{I_{sd,ph}^{Xfm}(t)} \right| \leq S^{Xfm} \tag{2.12}$$

2.5 Electric Vehicle Load Model

State of Charge (SOC) is an energy gauge for the battery in EVs. The percentage range is from 0%(empty) to 100%(fully charged). The left driving miles can be predicted with SOC. The equation for SOC is shown below,

$$SOC = \frac{Q_{init} \pm \int i_{bc} dt}{Q_{nom}} \times 100 \tag{2.13}$$

where Q_{init} is the initial electric energy before charging the EV, Q_{nom} is the nominal electric energy capacity of the EV, and i_{bc} is the battery current of the EV. If i_{bc} is positive, it means the current is going to the EV direction and the SOC is increasing. It can be figured out from the equation above that SOC is a normalized value.

Similarly, state of discharge (SOD) stands for how much electricity has been discharged. The equation is shown below,

$$SOD = 1 - SOC \tag{2.14}$$

2.6 EV Charging Model

The charger and components of battery system model used in this dissertation are shown in Fig. 2.2 to Fig. 2.6 [2, 59, 63, 65, 66, 78, 79, 83, 86, 93, 125][1]. DC and AC system dynamics of EVs are included in the model. More specifically, detailed DC battery cell model as shown in Fig. 2.3 and AC grid connection model as shown in Fig. 2.2 are used to represent EV grid integration system accurately. Constant current (CC)/constant voltage (CV) control of DC battery system is shown in Fig. 2.5; AC system response, as shown in Fig. 2.6, is used which is based on a second-order transfer function.

An open-circuit cell voltage and an equivalent internal resistance are included in the battery cell model, and they are in series with each other. The functions of open-circuit voltage (OCV) and equivalent resistance (R_{eq}) in terms of battery SOC are shown in Fig. 2.4.

CC and CV modes are the two operating regions of the charge control model as shown in Fig. 2.5. The battery voltage gradually increases as shown in Fig. 2.3, and the battery terminal voltage (V_{bt}) plays a key role in determining the time to switch from CC to CV mode. In CC mode, the commanded active power (P^{ev}) controls the

[1]This work is developed by Dr. M. C. Kisacikoglu's group from the University of Alabama, and is used in Chapter 4 for real-time implementation.

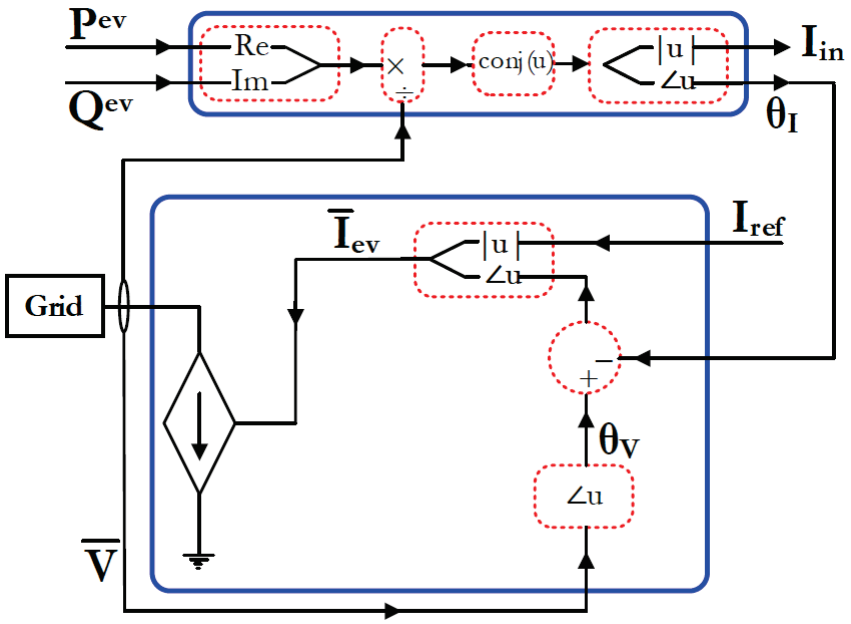

Figure 2.2: Power Control Block.

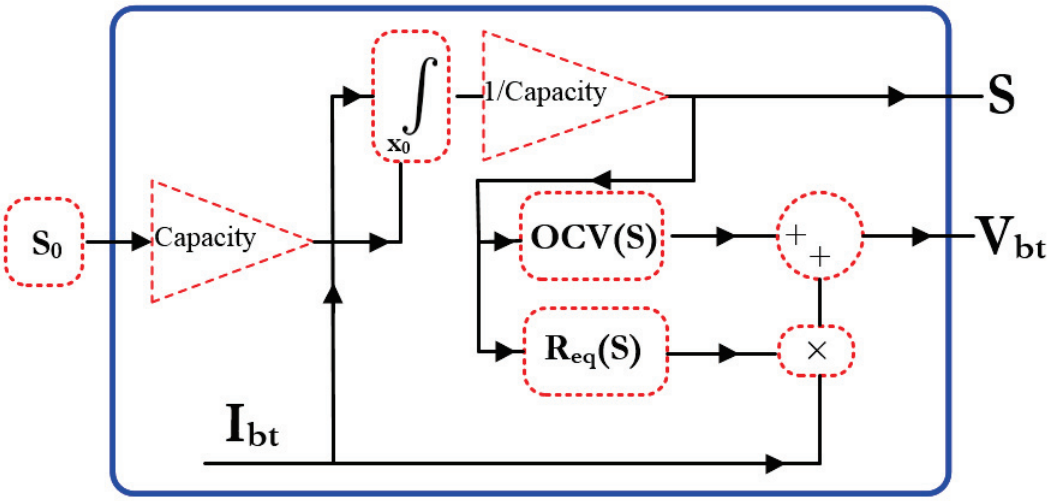

Figure 2.3: SOC Dynamics Block.

DC battery current I_{bt}. The battery cell switches to CV charging mode when V_{bt} becomes 4.0 V at time t_{cv} in the models of this work. The battery current is reduced exponentially and the model maintains the constant battery voltage at $V_{bt,max}$ at the same time after switching to CV charging mode.

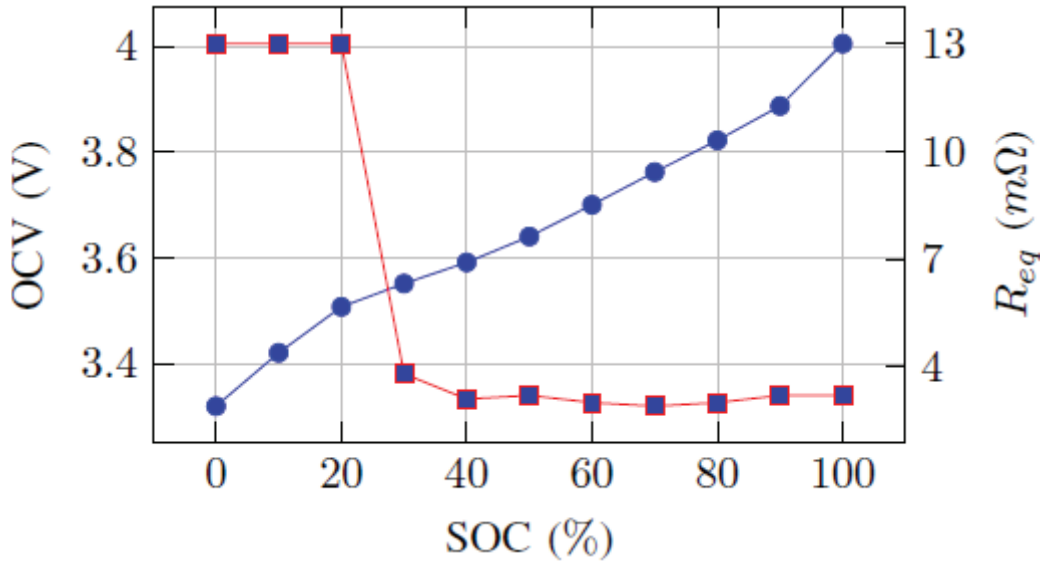

Figure 2.4: Battery Characteristics [2].

This model consists essential features of on-board charger and EV battery, and it has the ability to track active and reactive power set-points sent by DSO.

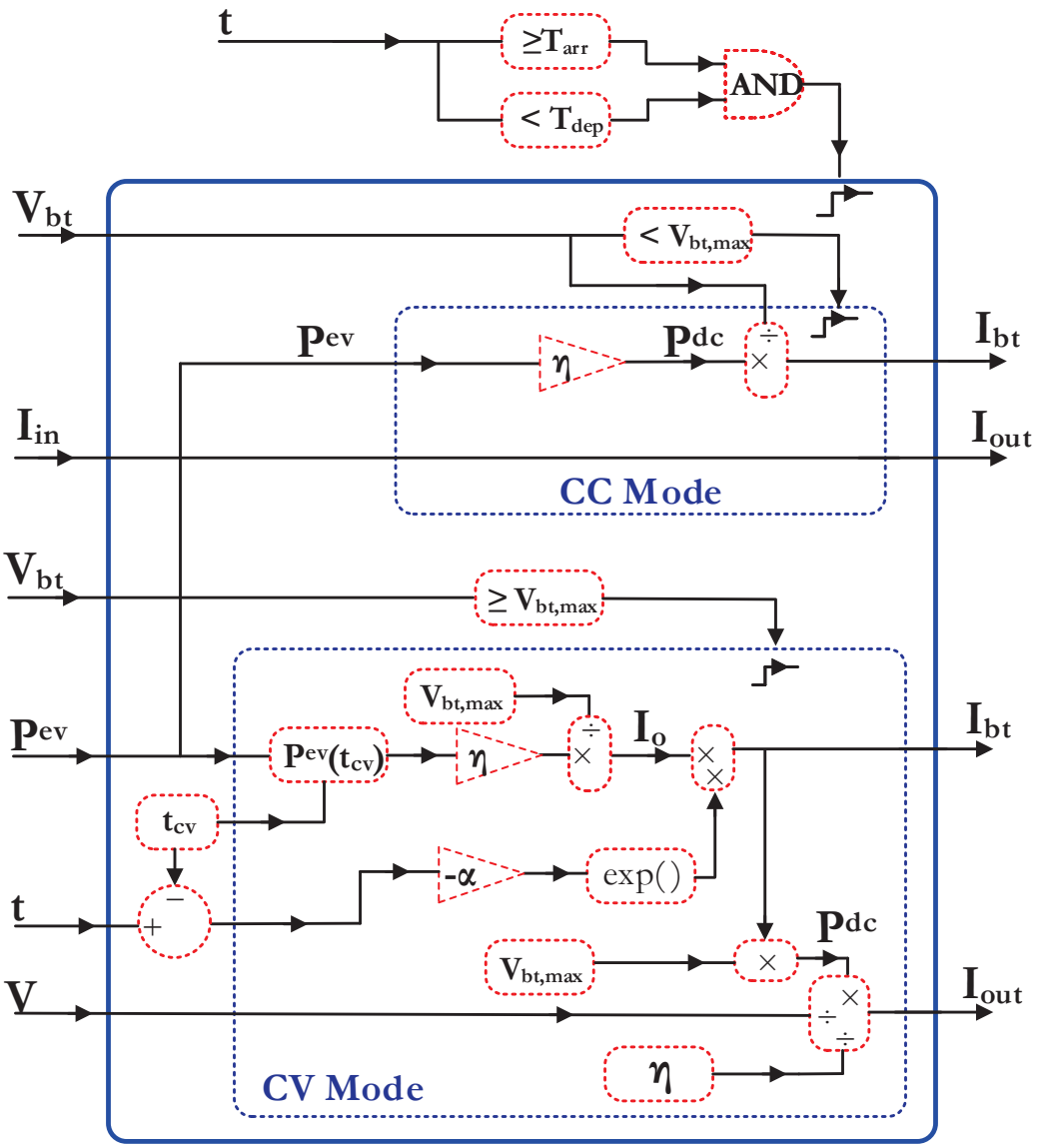

Figure 2.5: Charge Control Block.

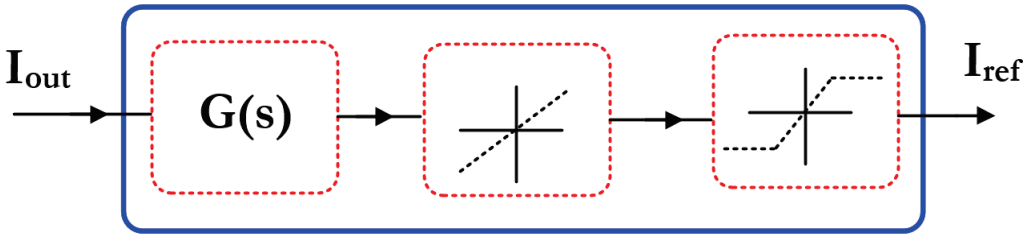

Figure 2.6: Current Response Block.

Chapter 3

Coordinated Electric Vehicle Charging with Reactive Power Support to Distribution Grids

3.1 Introduction

In this chapter, hierarchical coordination frameworks are developed to optimally manage active and reactive power dispatch of number of spatially distributed EVs incorporating distribution grid level constraints[1]. The frameworks consist of detailed

[1]This work has been published in IEEE Transactions on Industrial Informatics.

mathematical models, which can benefit the operation of both entities involved, i.e., the grid operations and EV charging. The first model comprises of a comprehensive optimal power flow model at the distribution grid level, while the second model represents detailed optimal EV charging with reactive power support to the grid.

3.2 Nomenclature

Subscripts

e EV number, $eset = \{e \,|\, e \in \mathbb{Z}, 0 < e \leq e^{max}\}$.

i Node number, $iset = \{i \,|\, i \in \mathbb{Z}, 0 < i \leq i^{max}\}$.

j Series element between node i and $i+1$,

$jset = \{j \,|\, j \in \mathbb{Z}, 0 < j \leq j^{max}\}$.

k Time interval, $kset = \{k \,|\, k \in \mathbb{Z}, 0 < k \leq k^{max}\}$.

m Node with base loads, $m \in iset$.

r Receiving end.

s Sending end.

t Time when EVs are grid connected, $t \in kset$.

t' Time when EVs are off grid, $t' \in kset$.

Superscripts

ba Base load.

ct Load curtailment.

ev EV loads.

fl Flexible loads.

il Constant current load.

$loss$ Loss.

max Maximum value.

min Minimum value.

pl Constant power load.

sh Load shift.

ss Substation.

zl Constant impedance load.

Parameters

Δk Time interval.

η Efficiency.

λ_1, λ_2 Weighting factor.

ρ Energy price.

θ Power factor angle.

A, B, C, D ABCD parameter matrices.

E EV battery's energy.

$I0$ Constant current.

$P0$ Constant active power.

$Q0$ Constant reactive power.

R Socket rating.

S State of charge.

$S0$ Desired SOC.

$Z0$ Constant impedance.

Variables

Ψ, Ω_1, Ω_2 Objective function values.

F Fairness index.

I Complex current vector.

$\bar{I}$ Complex conjugate of current vector.

P Active power.

Q Reactive power.

V Complex voltage Vector.

Functions

$\Re$ Real part of a complex number.

$\Im$ Imaginary part of a complex number.

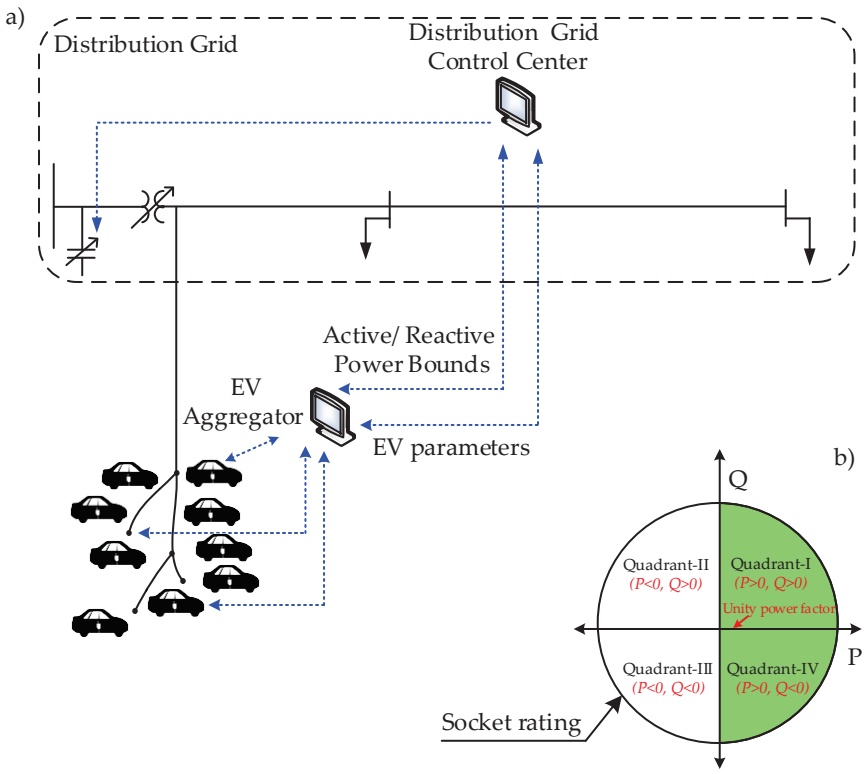

Figure 3.1: a) High-level overview of the proposed active/reactive power scheduling of EVs, and b) Charging region of EVs [3, 4].

3.3 Solution Approach

In this work, EVs are deployed on the first and fourth P-Q quadrants, i.e., EVs inject/withdraw reactive power from the grid while charging, as shown in Fig. 3.1-b). This allows DSO to raise charging power limits for the EVs without violating the grid operating constraints, compared to the case when EVs are dispatched at the unity power factor. The higher EV charging power limit means reduced energy costs for the EV owners in dynamic pricing scheme. The EVs could participate in reactive power market to maximize the revenue; however, reactive power market is a bit futuristic.

Thus, this work demonstrates immediate benefits of dispatching reactive power from grid constraint management point of view.

Fig. 3.1-a) shows a high-level schematic of the proposed coordinated EV charging, where EVs support reactive power to the grid while charging the EVs at lowest possible costs. Two coordinated versions are proposed. In the first coordinated framework, EV aggregators (EVAs) submit EVs' preferences and parameters (such as socket rating, SOC, etc.) to the DSO. Then, DSO solves an optimal power flow (OPF) model at the grid level and generates upper bounds on active power consumption and reactive power injection at each aggregated node on the feeder. At the aggregation level, optimal EV scheduling models are solved, in which the bounds obtained from the DSO are used as additional constraints to ensure feasible operations of the grid.

In the second coordinated framework, models at the EV aggregation level are solved first and optimal EV charging profiles from each node are sent to the grid control center. Then, the grid control center solves distribution OPF with an objective to minimize the deviation of EV charging scheduling through load shifting and load curtailment.

In this work, EVs are considered operating on the first and fourth P-Q quadrants to demonstrate the concept, i.e., EVs can inject/withdraw reactive power while charging. The main contributions of this chapter are as follows:

a) inclusion of reactive power in the formulation of optimal EV charge scheduling. This is a substantial extension to [4], and to the best of the authors' knowledge, this is the first paper that considers both active and reactive power in the optimal EV scheduling formulation,

b) modeling of comprehensive distribution optimal power flow with inclusion of flexible reactive power support from EVs, load shifting, and curtailment as demand response options, and

c) applications that demonstrate coordinated reactive power dispatch of EVs combined with active power can result in higher EV penetration without impacting the grid.

3.4 Mathematical Modeling

At the grid level, we have extended prior work in [108] on distribution optimal power flow (DOPF) model to create upper bounds on net active and reactive powers for EVs, load shifting, and load curtailment on EV charging. At the EV aggregation level, we have extended previous work in [14, 74, 75] on optimal EV scheduling models by including reactive power support from the EVs. Key mathematical modeling and constraints are discussed next.

3.4.1 Distribution Grid Component Model

The DOPF model is built using individual grid components and circuit laws. The mathematical models are developed in terms of branch current and nodal voltages. The conductors and cables are modeled using π-equivalent circuits. Detailed descriptions of these models can be found in [108].

For each series element, ABCD parameters are used to model sending/receiving end currents and voltages,

$$\begin{bmatrix} V_{i,k} \\ \\ I_{s,j,k} \end{bmatrix} = \begin{bmatrix} A_j & B_j \\ \\ C_j & D_j \end{bmatrix} \begin{bmatrix} V_{i+1,k} \\ \\ I_{r,j,k} \end{bmatrix} \tag{3.1}$$

Loads are modeled as shunt components. Impedance-current-power (ZIP) load model is used for the base loads which are non-flexible loads in the system. For base loads,

$$V_{m,k} = Z0_{m,k}\, I^{zl}_{m,k} \tag{3.2}$$

$$\left|I^{il}_{m,k}\right| \left(\angle V_{m,k} - \angle I^{il}_{m,k}\right) = \left|I0^{il}_{m,k}\right| \angle\theta_{m,k} \tag{3.3}$$

$$V_{m,k}\, \overline{I^{pl}_{m,k}} = P0_{m,k} + \sqrt{-1}\, Q0_{m,k} \tag{3.4}$$

Equation (3.2), (3.3), and (3.4) represent constant impedance, constant current, constant power part of the ZIP loads.

To represent the current balance at node, the following equation is used,

$$\overbrace{I_{r,j-1,k} = I_{s,j,k}}^{\text{Branch currents}} + \overbrace{I^{zl}_{i,k} + I^{il}_{i,k} + I^{pl}_{i,k}}^{\text{ZIP load currents}} + I^{fl}_{i,k} \tag{3.5}$$

where superscript fl is used to denote flexible loads, such as EVs. The flexible loads in (3.5) are assumed to be connected at nodes where base loads are connected, i.e., at nodes m.

3.4.2 Electric Vehicle Load Optimization Model

Total cost of charging EVs are minimized from EVA's

point of view. The objective function can be written as,

$$\Psi_m = \sum_k \rho_k \sum_e P^{ev}_{m,e,k}\, \Delta k \tag{3.6}$$

Equation (3.6) represents cost of charging EVs at node m on the distribution grid.

The mathematical model of EVs are developed based on SOC, initial SOC, final SOC

desired by the EV owners, and the time instances when EVs are connected to the grid. The SOC of EVs are given by,

$$S_{m,e,t} = S_{m,e,t-1} + \eta_{m,e} \frac{P^{ev}_{m,e,t} \Delta k}{E^{max}_{m,e}} \tag{3.7}$$

Electric power consumed by the EV must always be within the rating of the charging socket,

$$P^{ev^2}_{m,e,k} + Q^{ev^2}_{m,e,k} \leq R^2_{m,e} \tag{3.8}$$

where R represents the rating of charging socket.

SOC at the instance EV is off the grid must meet the SOC desired by the EV owner,

$$S_{m,e,t'} \geq S0_{m,e} \tag{3.9}$$

Minimum and maximum allowed SOC are represented as,

$$S^{min}_{m,e} \leq S_{m,e,t} \leq S^{max}_{m,e} \tag{3.10}$$

Grid constraints, i.e., upper bounds on active power consumption and reactive power

injection from the EVs, which are computed from the model given in Section III.C, are also incorporated using the following equations,

$$\sum_{e} P^{ev}_{m,e,t} \leq P^{fl}_{m,t} \tag{3.11}$$

$$\sum_{e} Q^{ev}_{m,e,t} \geq Q^{fl}_{m,t} \tag{3.12}$$

3.4.3 Distribution Grid Optimization Model-I

This model is used to find maximum penetration of flexible loads on the distribution grid, which can be written as,

$$\Omega_1 = \sum_{m,k} P^{fl}_{m,k} \tag{3.13}$$

where,

$$P^{fl}_{m,k} = \Re\Big(V_{m,k}\,\overline{I^{fl}_{m,k}}\Big) \tag{3.14}$$

The reactive power of the flexible load is represented as,

$$Q_{m,k}^{fl} = \Im\left(V_{m,k}\,\overline{I_{m,k}^{fl}}\right) \tag{3.15}$$

DSO sends P^{fl} and Q^{fl} to the aggregators at each node m, which represent upper bounds on active power consumption and reactive power injection from the EVs. Equation (13) may not result in a fair allocation of EV active and reactive power bounds at all nodes. Thus, we introduce a fairness index based on base load,

$$F_k = \frac{P_{m,k}^{fl}}{P_{m,k}^{zl} + P_{m,k}^{il} + P_{m,k}^{pl}} \tag{3.16}$$

where F is called the fairness index, which ensures that the EV load penetration at all nodes is allowed in the same proportion corresponding to the base loads. However, F is kept as variable in the optimization model.

The voltage limits at load buses are modeled as,

$$V_m^{min} \leq |V_{m,k}| \leq V_m^{max} \tag{3.17}$$

Similarly, feeder current limits are defined as follows,

$$|I_{s,j,k}| \leq I_j^{max} \tag{3.18}$$

$$|I_{r,j,k}| \leq I_j^{max} \tag{3.19}$$

The distribution grid optimization model-I consists of the objective function given in (3.13), equality constraints (5.2)-(3.5), (3.14)-(3.16), and inequality constraints (3.17)-(3.19). Other constraints such as transformer capacity limits, can also be easily incorporated in the model.

3.4.4 Distribution Grid Optimization Model-II

The optimization objective of this model is to minimize the total power loss on the distribution grid as well as the active power shifting and curtailment of EV loads.

$$\Omega_2 = P^{loss} + \sum_{m,k}(\lambda_1 P^{sh}_{m,k} + \lambda_2 P^{ct}_{m,k}) \tag{3.20}$$

where,

$$P^{loss} = \sum_{k} \Re\left(V^{ss}_{k}\ \overline{I^{ss}_{k}}\right) - \sum_{m,k,e} P^{ev}_{m,e,k} - \sum_{m,k}(P^{ba}_{m,k} - P^{ct}_{m,k}) \tag{3.21}$$

where P^{sh} stands for active power shifting and P^{ct} stands for active power curtailment. Power shifting means EV loads can change their time to charge while connected at the same charging nodes. If active power shifting couldn't satisfy the grid constraints, then the active power curtailment will be carried out. λ_1 and λ_2 are the weighting factors used to prioritize P^{sh} over P^{ct}. A higher weighting factor for P^{ct} ensures that active power shifting is prioritized compared to the curtailment.

EVs can provide reactive support back to distribution grid. There are lower and upper limits for reactive power which EVs could provide, which can be mathematically modeled as following,

$$Q_{m,k}^{min} \leq Q_{m,e,k} \leq Q_{m,k}^{max} \tag{3.22}$$

where

$$Q_{m,k}^{min} = -\sum_{e} \sqrt{R_{m,e,k}^2 - P_{m,e,k}^{ev^2}} \tag{3.23}$$

$$Q_{m,k}^{max} = \sum_{e} \sqrt{R_{m,e}^2 - P_{m,e,k}^{ev^2}} \tag{3.24}$$

Regulation of reactive power injection to the grid is essential. Q^{min} is the reactive power injection limit and constraint (3.22) ensures that the reactive power injection/-consumption in each node supports an optimal operation of the grid and EVs. In case of utility regulations requiring mandatory minimum reactive power support from EVs, Q^{min} must be set to the minimum of the regulation requirement and the reactive power capability of EVs obtained using (3.23). The distribution grid optimization model-II consists of the objective function given in (20), constraints (21)-(24), and other constraints similar to the grid optimization model-I, i.e., (1)-(5), (14)-(16), and (17)-(19).

The EV load optimization model and grid optimization models are non-linear programming problem (NLP) in nature.

3.5 Case Studies

The mathematical models described in Section III are developed in GAMS and solved using KNITRO solver. For the case studies, a modified single phase 33-node distribution feeder is considered [5], as shown in Fig. 3.2, which serves residential customers. EV departure time, arrival time, initial SOC, and final desired SOC are modeled using truncated Gaussian distribution functions [126]. The EVs are assumed grid connected at home from evening to the morning. Socket rating of 3.3 kW is used, which in this case is taken as kVA rating. Charging efficiency of the EVs is assumed in the range of 90-95%. The maximum energy capacity of EVs is assumed 30 kWh. Simulation is run for 24 hours with 15-minute intervals.

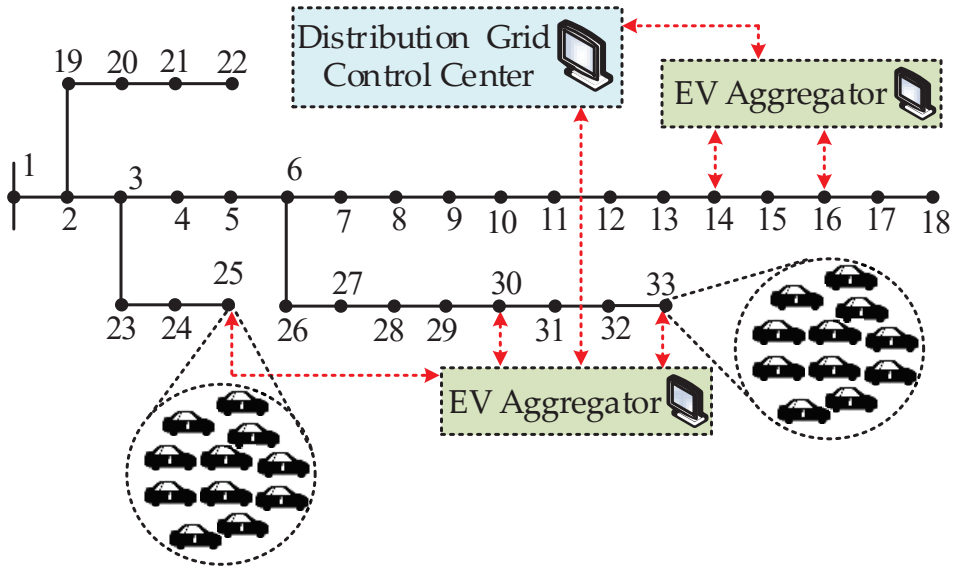

Figure 3.2: 33-node feeder [5] which is used to demonstrate the optimal active/reactive power dispatch of EVs.

3.5.1 Case Studies: Grid Optimization Model-I and EV Optimization Model

To avoid the consequences of uncontrolled charging, the DSO coordinates the charging of the EVs. DSO first solves the distribution grid optimization model described in the Section II-C. For this case studies, the price of electricity in a 24-hour period is shown in Fig. 3.3, which is based on locational marginal price (LMP) from ISO-NE system. The solutions to this model provide two set of bounds for each node, i.e., maximum allowable active power consumption and maximum allowable reactive power injection from EVs. DSO sends this information to the EV aggregators. Fig. 3.4 shows active power bounds for EV charging sent to the aggregators designated for node-25 and node-33 along with the base loads. These bounds are obtained when EVs operate in unity power factor mode, i.e., the reactive power injection from EVs is zero. Fig. 3.5 shows similar bounds when EV charging takes place in non-unity power factor mode. The active power bounds in Fig. 3.5 are higher than that in Fig. 3.4 for the same base loads, EV parameters, and the grid constraints. This shows that if EVs agree to inject reactive power into the grid, in coordinated charging scheme, DSO can permit more active power withdrawal from the EV charging.

At the aggregation level, signals from the DSO are incorporated into the EV optimization model described in the Section II-B. Here, we present the case studies for

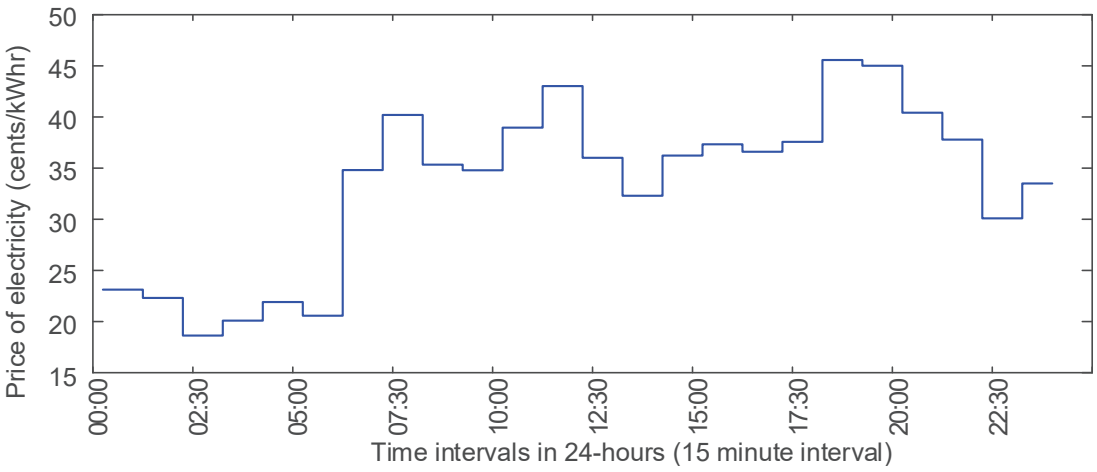

Figure 3.3: Dynamic electricity price.

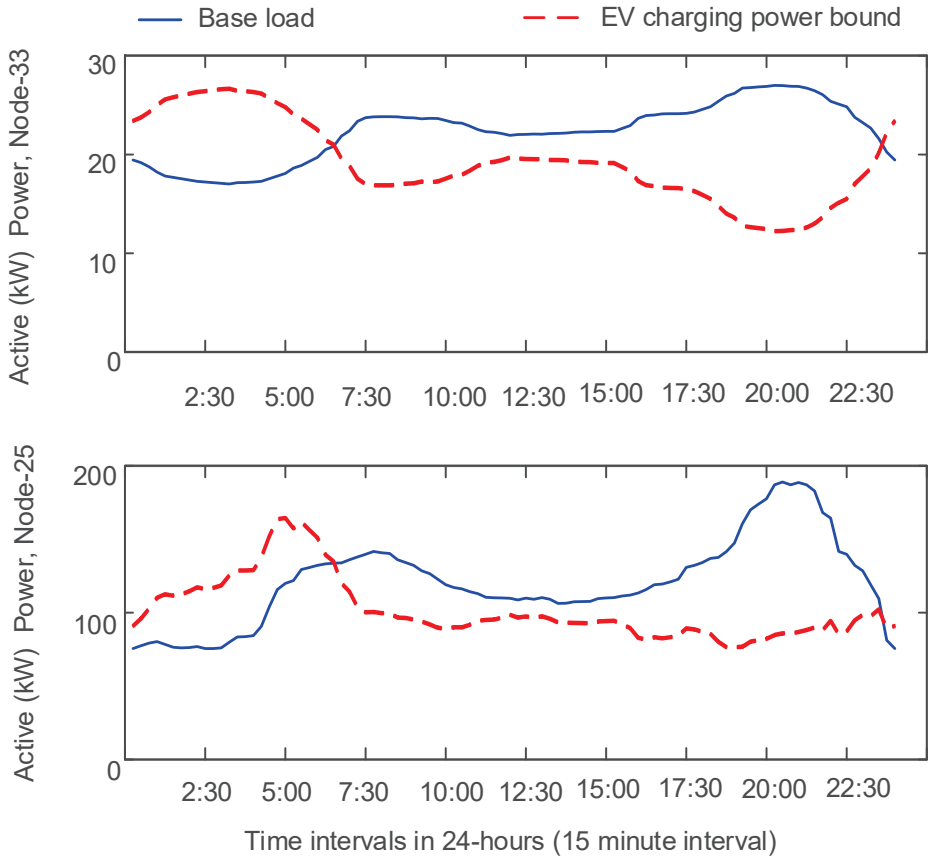

Figure 3.4: Active power injection bounds at node-25 and -33 when EVs charging operate on unity power factor mode.

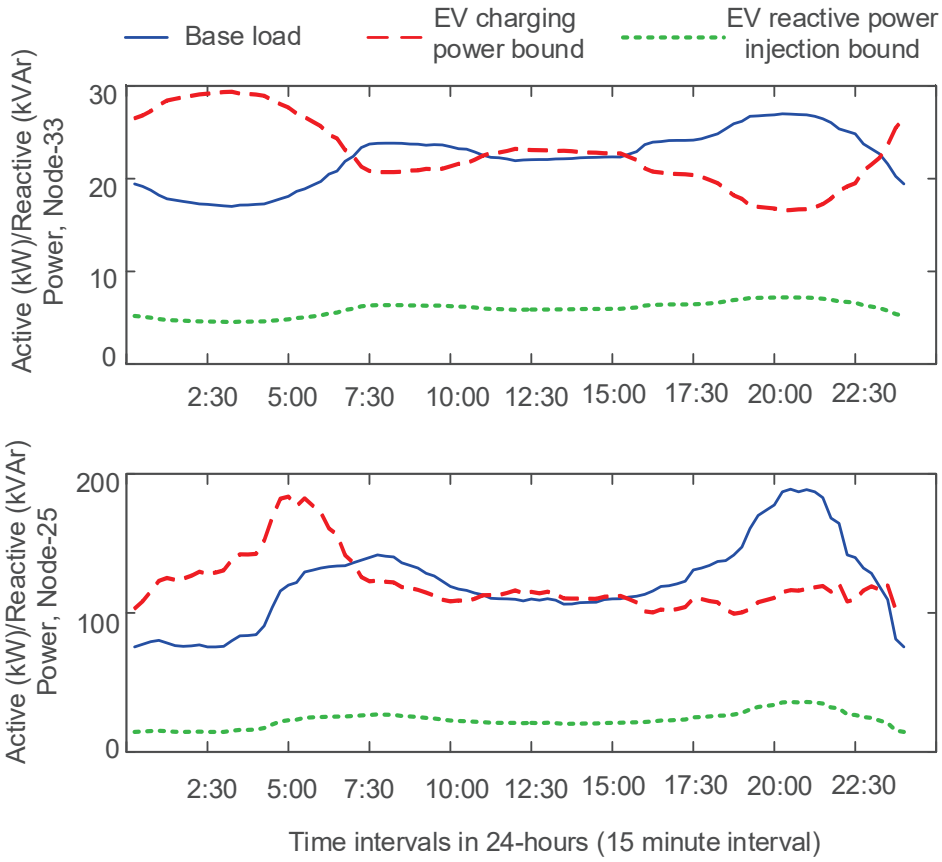

Figure 3.5: Active/reactive power injection bounds at node-25 and -33 when EVs charging operate on the fourth quadrant.

165 EVs connected at node-25; however, a total of 1,500 EVs are connected to the feeder which is used to solve the grid level optimization model discussed above.

At node-25, first, the EV optimization model is solved without grid constraints, which represents an uncontrolled charging scheme. On a dynamic energy pricing, most of the EVs are charged during 1:00-2:30 and 21:00-22:30 (see Fig. 3.6) when energy prices are low. The peak EV charging load exceeds 500 kW. In fact, all EVs charge at 3.3 kW during those time slots. From EV owners' perspective, uncontrolled charging

yields the best solution as the average cost of charging one EV is the lowest (30 /day). In an uncontrolled charging, when optimal EV load profiles from all nodes are integrated and power flow is solved for the feeder, some of the nodes show under voltage issues.

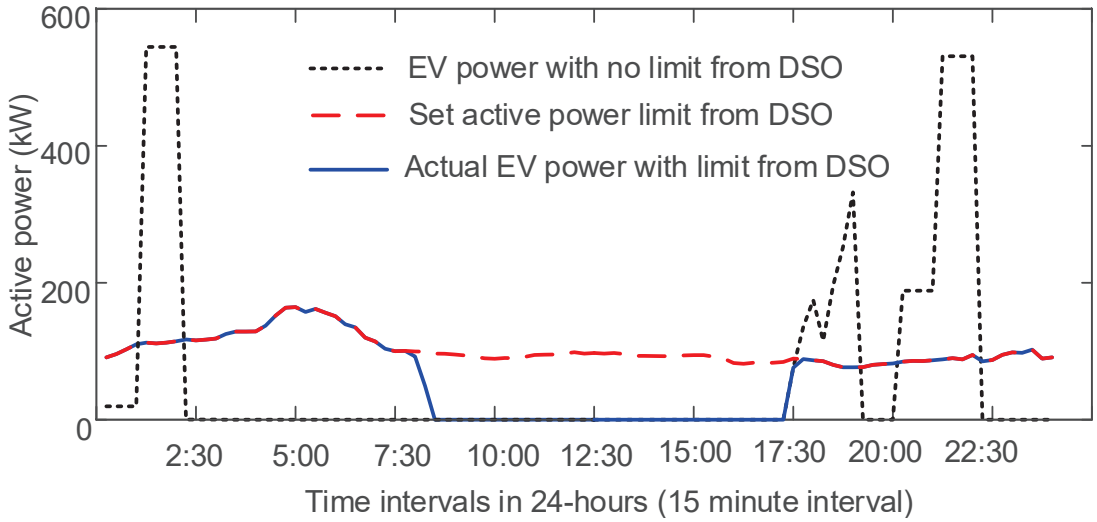

Figure 3.6: Active power profile in uncoordinated charging scheme, and on coordinated scheme when EVs operate on unity power factor at node-25.

Next, active power withdrawal bounds from the DSO, shown in Fig. 3.4, are incorporated into the EV optimization model. This case represents EVs operating on unity power factor mode. Fig. 3.6 shows that the EV charging is now constrained by the bounds from the DSO; the maximum power allowed for EV charging is about 164 kW. With these optimized EV load profiles, the grid constraints are not violated. In Fig. 3.6, when EVs are grid connected, it can be seen that the EVs charging always hits the bounds set by the DSO. All the EVs are off the grid between 8:15 to 17:15. With the grid constraints, the average cost of charging one EV is 52 /day at node-25.

If the number of EVs are increased further from 165 at node-25, grid operations become infeasible. Therefore, for higher number EVs, the requested amount of energy may not be delivered to EVs at the node-25.

If EVs agree to operate in non-unity power factor mode, the DSO sends two set of bounds to each node, as shown in Fig. 3.5, that represent active power withdrawal and reactive power injection bounds. The bounds on reactive power injection are also necessary to avoid any overvoltage issues that excessive reactive power injection may cause. Fig. 3.7 shows EV charging with the grid constraints. From the optimized EV charging profile of 165 EVs at node-25, it is clear that there is still room to charge more EVs if required. With reactive power injection from the EVs, the active power limits set by the DSO are higher (max 183 kW) compared to EVs charging at unity power factor mode (max 164 kW). This reduces average charging cost to 42 /day from 52 . It should be noted that the observed cost reduction is not representative and depends on several factors including the variation of dynamic pricing over the day, base loads, and several grid parameters. However, the key point here is that reactive power injection can subside the adverse impacts of active power withdrawal to some extent, which provides benefits both DSO and EV owners. DSO benefits by obtaining the reactive power support from the distributed EVs, while EVs benefit with the reduced charging costs in coordinated EV charging schemes.

In this proposed model, we have not considered direct financial model to compensate

EVs' participating for the grid level services. However, we have demonstrated indirect benefit of this on the charging costs of EVs. Without reactive power support to the grid, the maximum power limit set by DSO for EVs is less compared to the case when EVs support reactive power to the grid. The later allows charging EVs at less expensive costs.

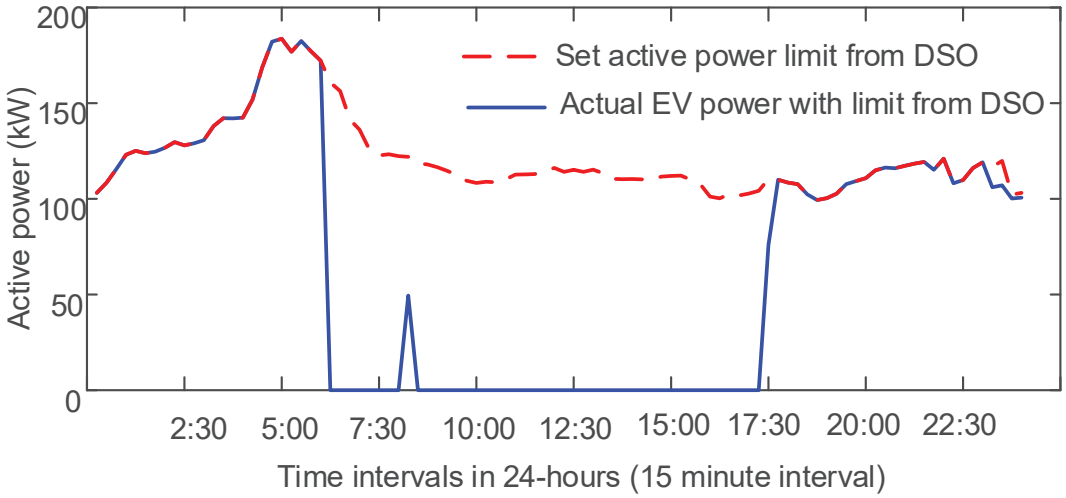

Figure 3.7: Active power profile in coordinated charging scheme when EVs operate on the fourth quadrant at node-25.

3.5.2 Case Studies: Grid Optimization Model-II and EV Optimization Model

The same 33-node system is used in these case studies. First, the EV aggregator at each node solves an optimization model based on minimization of EV charging costs. For this case studies, dynamic energy price taken from ISO-NE system on 09/07/2017 is used as shown Fig. 3.8. The optimized load profile along with the

reactive power support capability of each EVs are sent to the grid control center. The grid control center incorporates the optimized load profiles (active power) obtained from all the nodes, the reactive power capability limits from EVs, and solves the grid level optimization problem. The grid optimization model first tries to accommodate the optimized load profile of the EVs, and in doing so it may dispatch negative reactive power from EVs (injection). If the reactive power is not sufficient to fix the constraint violations particularly when EV penetration is high, then the optimization model will first time shift the charging of EVs, and then will curtail the active power dispatch of EVs. We use $\lambda_1 = 10^4$, and $\lambda_2 = 10^{10}$ for the case studies. Higher value of λ_2 ensures that customer's quality of service is given priority as EV curtailment takes only as the last resort. The EVs are connected at all nodes, except at node-1; however, the case studies on this chapter will be presented only for EVs connected at node-18 and the total aggregation of EVs seen from the substation, i.e., node-1.

No Adverse Impact from EVs: Total of 160 EVs are connected to the 33-node distribution grid. There are 5 EVs at node-18. Since the EV penetration is low, the optimized EV load profiles from each node did not lead to constraint violation on the grid. Fig. 3.9 shows EV charging are scheduled during time slots when price of electricity is low. Fig. 10 shows that the voltage of the nodes are within the limit with or without reactive power support from EVs. When EVs are not fixed to operate on unity power factor, some reactive power dispatch is seen due to the objective chosen, i.e., the loss minimization. The reactive power injection from EVs help to reduce

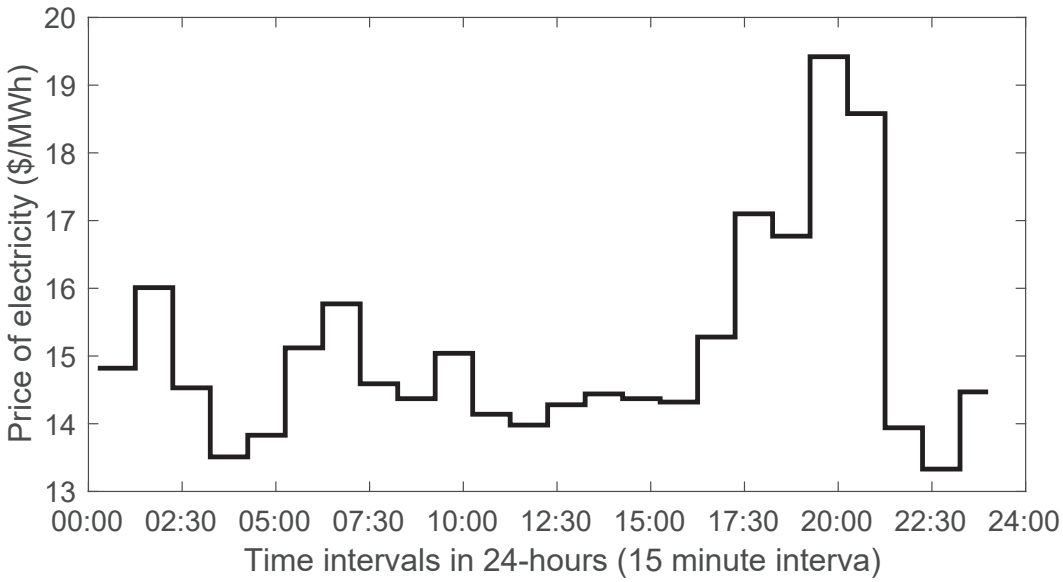

Figure 3.8: Dynamic electricity price.

the losses on the grid without impacting the costs of charging of EVs. Since the EV penetration was low, the grid control center did not require to move or curtail the EV charging schedules. The energy served from the substation in this case is summarized in the Table I along with the results form other case studies.

Load Shifting of EVs: The total number of EVs is set to 1,925. There are 50 EVs at node-18. EV optimization is solved at each node first. Then, the resulting data from EV optimization are imported to distribution grid optimization. Since, the number of EVs in this case is large, the grid optimization needed to shift some of EV charging power from peak to off-peak (see Fig. 3.11) but no curtailment was necessary (with $Q \neq 0$ from EVs).

When we set $Q = 0$ for this case study, solution yields some energy curtailment (see

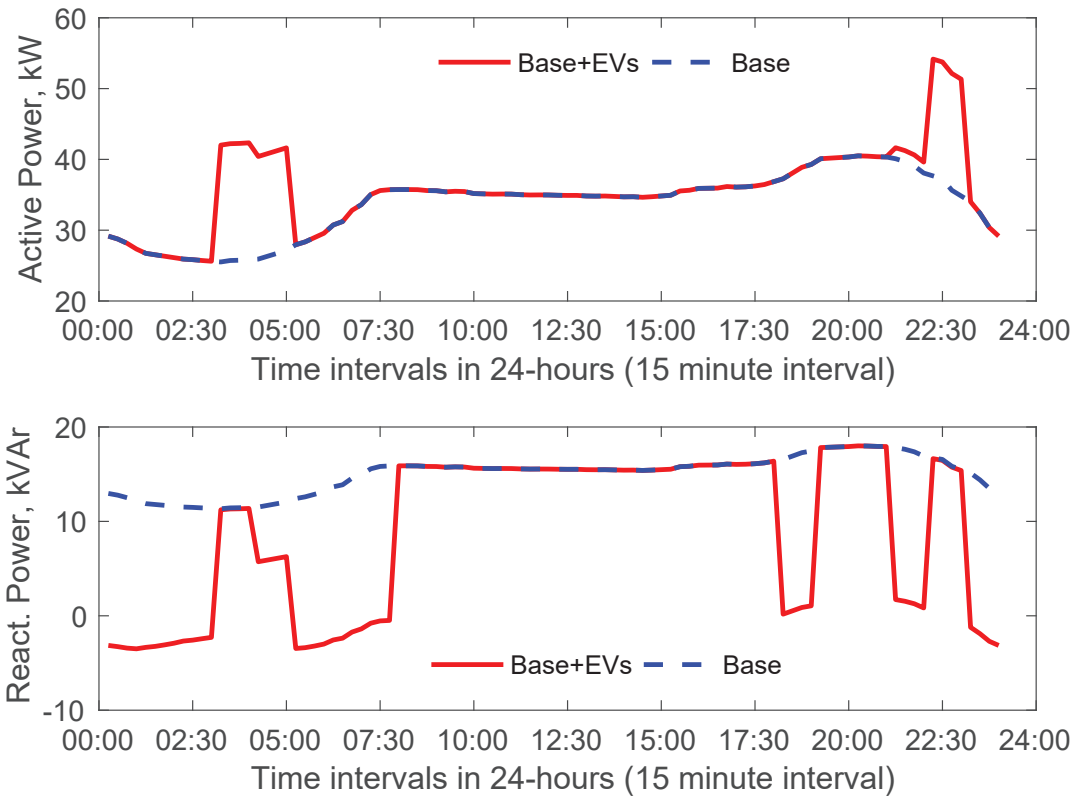

Figure 3.9: Active and reactive power dispatch of EV and base loads at node-18.

Table I). Also, voltage at node-18 becomes below 0.95 (refer to Fig. 3.12) at some time intervals. Voltage at node-18 are within the range from 0.95 p.u to 1.05 p.u. as long as reactive power support from EVs take place. Therefore, the reactive power of EV loads are of great importance to keep grid voltages within limits. It was also observed that power shifting is large when EVs are operating at non-unity power factor. Total active power consumption of all the loads are shown in Fig. 3.13.

This case demonstrates that EV loads can have both positive and negative impacts on the system. A large number of EVs consuming active power can make the system

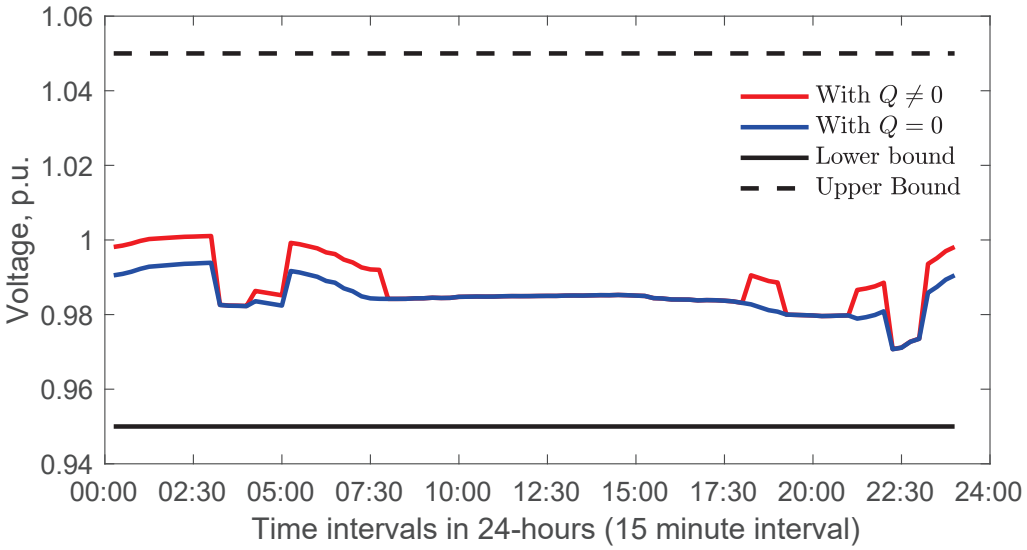

Figure 3.10: Voltage profile at node-18 with and without reactive power support from EVs.

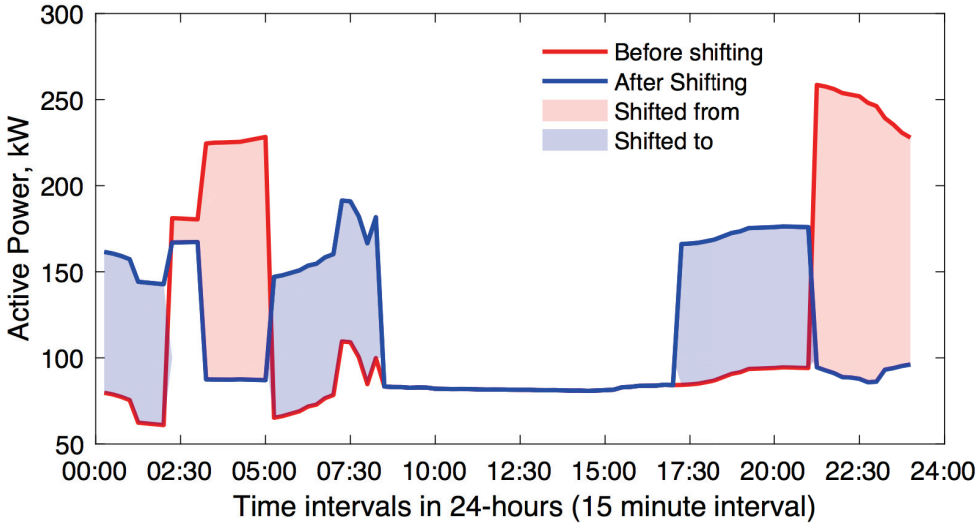

Figure 3.11: Active power of EV loads at node-18 with and without load shifting and $Q \neq 0$ from EVs.

overload and violate operational constraints of distribution grid. In this case, power shifting is of great importance to keep the distribution system feasible. Moreover, EV loads can operate in non-unity power factor mode, which enables them to provide reactive power support back to the grid.

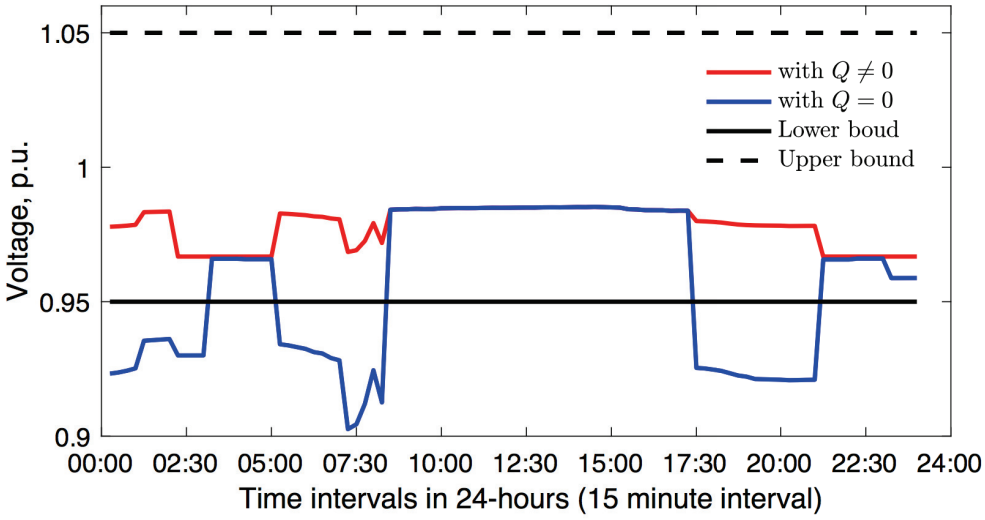

Figure 3.12: Voltage profile at node-18 with and without reactive power support.

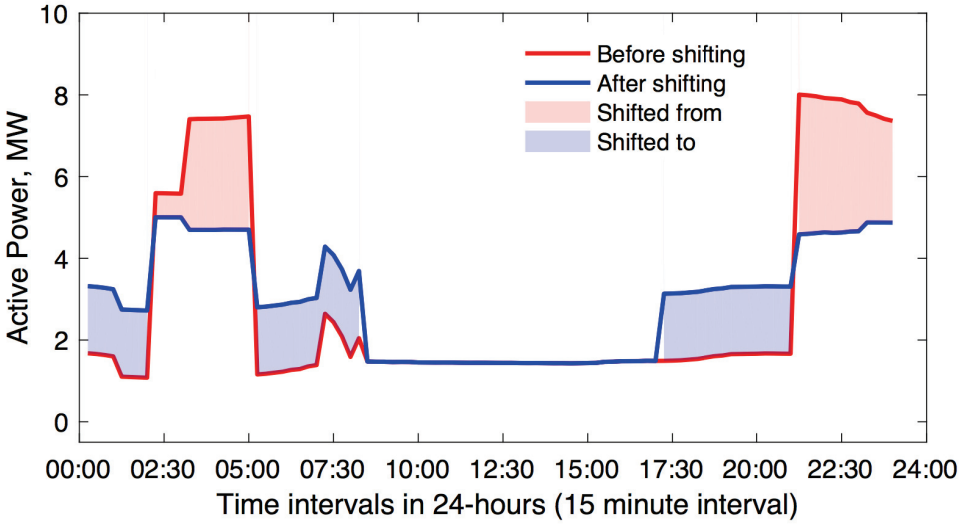

Figure 3.13: Total active power of all the loads seen from substation with and without load shifting and $Q \neq 0$ from EVs.

Load Shifting and Load Curtailment of EVs: The total number of EVs are increased to 5,450. There are 150 EVs both at node-18 and node-32. Since the number of EVs are large in this case, load shifting of EV charging itself is not sufficient to ensure feasibility of the grid operations; therefore, the grid optimization model comes up

Table 3.1
Summary of Total Energy Shift and Curtailment with and without Reactive Power.

	Without React. Power			With React. Power		
No. of EVs	Energy Served MWhr	Energy Shift MWhr	Energy Curt. MWhr	Energy Served MWhr	Energy Shift MWhr	Energy Curt. MWhr
160	36.52	0	0	36.52	0	0
1,925	64.01	9.69	6.81	70.82	15.20	0
5,450	87.69	11.84	51.35	121.84	39.70	17.20

with load curtailment from EVs. Fig. 3.14 shows the active and reactive power of EV loads at node-18 with power shifting and curtailment. Some EV loads are curtailed at two peak hours as shown in Fig. 3.14 in order to keep the distribution grid feasible.

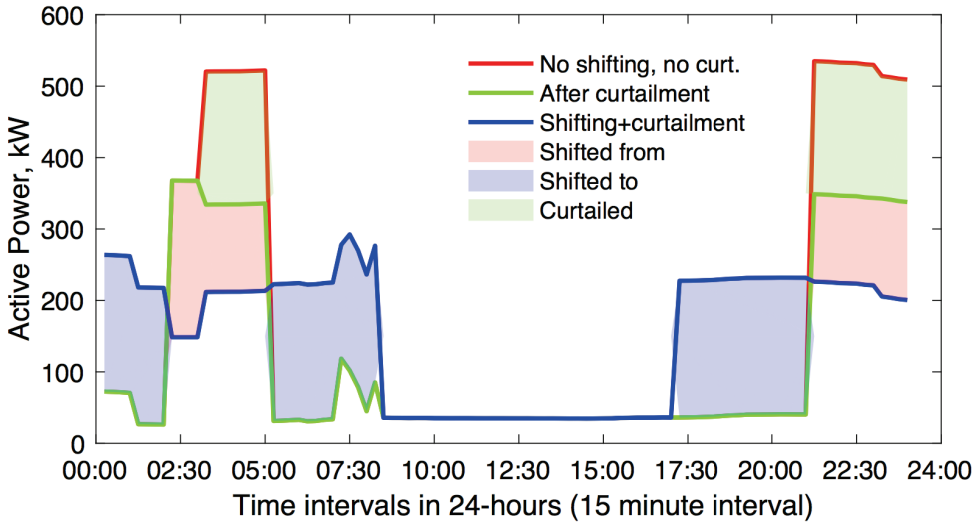

Figure 3.14: Active power of EVs and base loads at node-18 with power shifting and curtailment.

Voltage profile of node-18 in case 3 is shown in Fig. 3.15. Voltages at node-18 are within the limit from 0.95 p.u to 1.05 p.u. when EVs operate in non-unity power factor mode. When EVs operate at unity power factor mode, voltages at node-18 (and other nodes) are below 0.95 p.u. at some of the time intervals. Table I summarizes the results of the case studies.

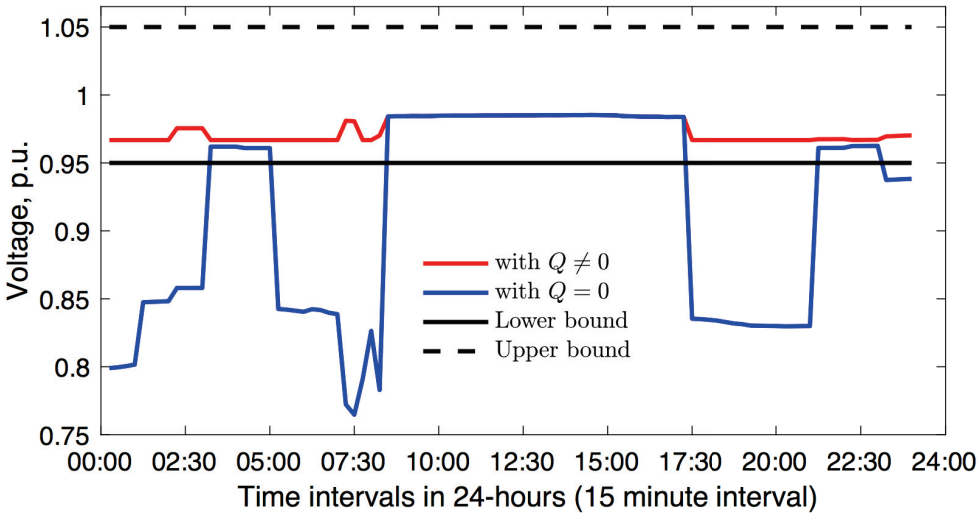

Figure 3.15: Voltage profile at node-18 with and without reactive power support.

This case demonstrates that reactive power support from EVs, load shifting of EVs, and load curtailment of EVs should be coordinated to improve power system operational feasibility. If coordinated, it leads to increased EV penetration and optimal operation of the grid as well as EVs. Based on our preliminary studies it seems this idea is promising and could open new avenues to optimally aggregate EVs for reactive power support to the grid.

The EV aggregation model is a non-linear programming (NLP) problem and is solved on nodal basis; thus, this could be solved in parallel. The maximum solution time for one node was recorded 3.2 seconds using KNITRO solver in a Windows machine with 6 GB memory and 2.80 GHz processor. The grid level model is an NLP problem and needs to be solved twice: once to obtain the active/reactive bounds as shown in Figs. 3 and 4, and once to ensure that the optimal EV profiles from all nodes,

when aggregated, are feasible for the grid. Using KNITRO solver, and with the same computing specifications as above, the grid level problem was solved in 15.23 seconds. Note that the grid level problem is cast as an NLP; hence, it does not consider the integer variables associated with tap changers and switched capacitor banks. Note that the grid level optimal power flow problem is a NP-hard problem, and since the model is non-convex, KNITRO does not guarantee a global optimal solution. Recent advancements in convexification of optimal power flow may be applicable in this context to achieve global optimal solution and also to speed up the computation further [127].

3.6 Conclusion

In this chapter, optimal distribution power flow and optimal EV charging models are developed first, which utilize reactive power injection capability of the EVs to support the grid. The benefits of dispatching reactive power from EVs to the grid operation and also to the EV owners are demonstrated. Reactive power dispatch from EVs could help manage distribution grid constraints, e.g., undervoltage issues caused by the active power consumption during the EV charging. This work has shown that in coordinated charging scheme, if EVs agree to inject reactive power into the grid, it benefits EVs by reducing the costs of charging the EVs in dynamic energy pricing schemes. This work also demonstrates that the reactive power injection from EVs

can be coordinated with the load shifting and load curtailment in demand response applications to help accommodate increased number of EVs on constrained grids.

Chapter 4

Four Quadrant Operation of Electric Vehicles for Voltage Support and Real-Time Implementation

4.1 Introduction

In this chapter, detailed EV battery model that could be leveraged for its 4-quadrant operations is integrated into coordination of the operations of EVs and distribution

feeder to support voltage profile on the grid. The grid level problem is devised as a distribution optimal power flow model to compute voltage regulation signal to dispatch active/reactive power set points of individual EVs. The whole integrated system is implemented in real time simulation with OPAL-RT OP5600[1].

4.2 Nomenclature

$\boldsymbol{\Delta t}$	Time interval.
$\boldsymbol{\eta}$	EV efficiency.
$\boldsymbol{\Phi}$	Objective function value.
$\boldsymbol{E^{cap}}$	Battery capacity.
$\boldsymbol{I}$	Nodal current injection.
$\boldsymbol{j, k}$	EV number, $\{\boldsymbol{j, k} \in \boldsymbol{N}\}$.
$\boldsymbol{m}$	set of nodes with EVs and loads, $\{\boldsymbol{m} \in \boldsymbol{N}\}$.
$\boldsymbol{P^c}$	EV charging power.
$\boldsymbol{P^d}$	EV discharging power.
$\boldsymbol{P^{ev}}$	EV power on grid side.
$\boldsymbol{P^L}$	Active power of load.
$\boldsymbol{Q^{ev}}$	Reactive power of EV on grid side.

[1]Contents of this chapter is developed in collaboration with Dr. M. C. Kisacikoglu's group from the University of Alabama. The detailed EV/charger models were provided by them, and are implemented in real-time simulator in this work.

$\boldsymbol{Q^L}$	Reactive power of load.
$\boldsymbol{R^{ev}}$	Charger rating.
$\boldsymbol{s^{max}}$	Max. SOC.
$\boldsymbol{s^{min}}$	Min. SOC.
$\boldsymbol{t}$	Time index, $\{\boldsymbol{t} \in \boldsymbol{T}\}$.
$\boldsymbol{u^c}, \boldsymbol{u^d}$	Charging/discharging status of EV.
$\boldsymbol{V}$	Nodal voltage.
$\boldsymbol{V^{max}}$	Max. nodal voltage limit.
$\boldsymbol{V^{min}}$	Min. nodal voltage limit.
$\boldsymbol{Y}$	Y-bus matrix.

4.3 Solution Approach

In this proposed work, a high fidelity EV charging model described in Chapter 2 is used to deploy EVs in all four P-Q quadrants for voltage control in distribution grids. Figure 4.1 shows a high-level schematic of the proposed coordinated EV charging, where EVs support reactive power to the grid for voltage support. In this coordinated framework, EVs send EVs' preferences and parameters (such as power rating, SOC, etc.) to the DSO. Then, DSO solves an optimal power flow (OPF) model at the

grid level and generates voltage regulation signals that each EVs are recommended to follow. Figure 4.2 shows an overview of the real time setup in this chapter. The main contributions of this chapter are as following:

† Inclusion of reactive power in the formulation of optimal EV charge scheduling problems at distribution grid level and, integration to the detailed EV charger/battery model for grid services such as voltage support applications.

† Real-time implementation of 4-quadrant operation of EV.

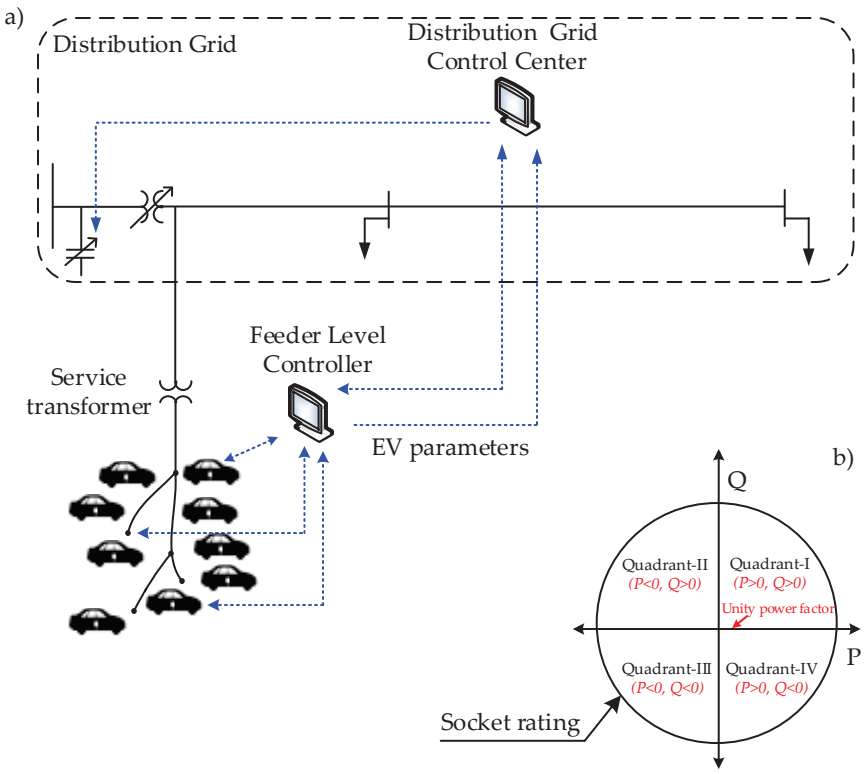

Figure 4.1: a) High-level overview of the proposed active/reactive power scheduling of EVs, and b) Charging region of EVs [3].

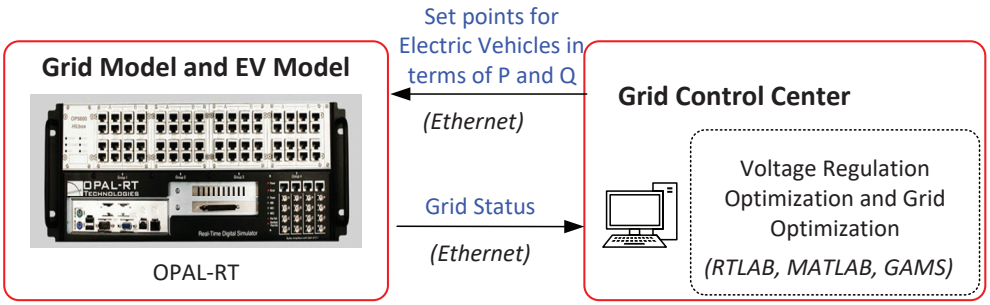

Figure 4.2: Overview of the real time simulation setup and optimization models.

4.4 Mathematical Modeling: Optimal Voltage Regulation Model

This work has extended prior work on distribution optimal power flow (DOPF) model in [108] to create voltage regulation signals (in terms of active power and reactive power dispatch of EVs) from the DSO's point of view. The DOPF model is built using individual grid components and circuit laws. The mathematical models are developed in terms of branch current and nodal voltages. The conductors and cables are modeled using π-equivalent circuits. Detailed descriptions of these models can be found in [108].

$$\textbf{Min:} \quad \Phi = \sum_{m \in N,\, t \in T} \left(V_{m,t} - V^{min} \right)^2 \tag{4.1}$$

subject to:

(Grid Level Constraints)

$$\boldsymbol{V_{j,t}} = \sum_{k \in N} \boldsymbol{Y_{j,k}}\, \boldsymbol{I_{k,t}} \;\; \forall\, \boldsymbol{j \in N, t \in T} \tag{4.2}$$

$$\boldsymbol{P^{ev}_{j,t}} + \boldsymbol{P^{L}_{j,t}} = \mathbb{R}\left(\boldsymbol{V_{j,t}}\; \boldsymbol{I^{*}_{j,t}}\right) \;\; \forall\, \boldsymbol{j \in N, t \in T} \tag{4.3}$$

$$\boldsymbol{Q^{ev}_{j,t}} + \boldsymbol{Q^{L}_{j,t}} = \mathbb{I}\left(\boldsymbol{V_{j,t}}\; \boldsymbol{I^{*}_{j,t}}\right) \;\; \forall\, \boldsymbol{j \in N, t \in T} \tag{4.4}$$

$$\boldsymbol{V^{min}} \leq \boldsymbol{V_{m,t}} \leq \boldsymbol{V^{max}} \;\; \forall\, \boldsymbol{m \in N, t \in T} \tag{4.5}$$

(EV Level Constraints)

$$\boldsymbol{P^{ev}_{m,t}} = \boldsymbol{u^{c}_{m,t}}\, \boldsymbol{P^{c}_{m,t}}\, (\boldsymbol{\eta_{m,t}})^{-1} - u^{d}_{m,t}\, P^{d}_{m,t}\, \eta_{m,t} \;\; \forall\, m \in N, t \in T \tag{4.6}$$

$$\boldsymbol{Q^{ev}_{m,t}} \leq \sqrt{\left(\boldsymbol{R^{ev}_{m,t}}\right)^{2} - \left(\boldsymbol{P^{ev}_{m,t}}\right)^{2}} \;\; \forall\, \boldsymbol{m \in N, t \in T} \tag{4.7}$$

$$\boldsymbol{Q^{ev}_{m,t}} \geq -\sqrt{\left(\boldsymbol{R^{ev}_{m,t}}\right)^{2} - \left(\boldsymbol{P^{ev}_{m,t}}\right)^{2}} \;\; \forall\, \boldsymbol{m \in N, t \in T} \tag{4.8}$$

$$\boldsymbol{s^{ev}_{m,t}} = \boldsymbol{s^{ev}_{m,t-1}} + \boldsymbol{\Delta t}\, (\boldsymbol{E^{cap}})^{-1}\left(\boldsymbol{u^{c}_{m,t}}\, \boldsymbol{P^{c}_{m,t}}\, (\boldsymbol{\eta_{m,t}})^{-1} - u^{d}_{m,t}\, P^{d}_{m,t}\, \eta_{m,t}\right) \;\; \forall\, m \in N, t \in T \tag{4.9}$$

$$\boldsymbol{s^{ev}_{m,t}} = \boldsymbol{s^{ev}_{m,0}} + \boldsymbol{\Delta t}\, (\boldsymbol{E^{cap}})^{-1}\left(\boldsymbol{u^{c}_{m,t}}\, \boldsymbol{P^{c}_{m,t}}\, (\boldsymbol{\eta_{m,t}})^{-1} - u^{d}_{m,t}\, P^{d}_{m,t}\, \eta_{m,t}\right) \;\; \forall\, m \in N, t = 1 \tag{4.10}$$

$$\boldsymbol{s^{min}} \leq \boldsymbol{s_{m,t}} \leq \boldsymbol{s^{max}} \;\; \forall\, \boldsymbol{m \in N, t \in T} \tag{4.11}$$

$$u^c_{m,t} + u^d_{m,t} \leq 1 \ \forall m \in N, t \in T \tag{4.12}$$

$$u^c_{m,t}, u^d_{m,t} \in \{0, 1\} \ \forall m \in N, t \in T \tag{4.13}$$

Equation 4.1 minimizes the voltage deviation from minimum allowed limit at EV nodes. This objective function ensures EVs get opportunity to charge when the base load is not causing excessive voltage drop issue (i,e., EVs operate in I and IV P-Q quadrants). At times, when voltage with base load goes below the minimum limit, the objective function will also force EV to discharge (i.e., EVs operate in II and III P-Q quadrants). Equation 4.2 represents the network model. Equations 4.3 and 4.4 represent the load models. Equation 4.5 ensures the nodal voltage limits. Equation 4.6 represents EV power in terms of charging and discharging powers. Equations 4.7 and 4.8 calculate and bound the reactive power of EVs based on socket KVA rating and EVs' active power. Equation 4.9 and 4.10 represent SOC dynamics, and 4.11 represents SOC limits. Equations 4.12 ensures charging and discharging would not take place simultaneously, and 4.13 ensures the binary values on charging/discharging decision. This model is non-linear mixed integer in nature, and the variables $P^{ev}_{m,t}$ and $Q^{ev}_{m,t}$ represent the dispatch signals send to EVs in order to maintain voltage profile on the feeder.

4.5 Case Studies

4.5.1 EV Charger/Battery Model Validation

The mathematical model [2, 59, 63, 65, 66, 78, 79, 83, 86, 93, 125] of the battery is implemented in Simulink. The EVs are connected to a distribution feeders and are operated in 4-quadrant based on arbitrary P,Q set points sent to the EVs for 60 minutes. The set points are limited between -3.3 to 3.3 kVA (which is the rated capacity of the battery). Fig. 4.3 to Fig. 4.7 show response of the battery looking at active power tracking, SOC dynaimcs, battery current, battery voltage, and reactive power tracking, respectively.

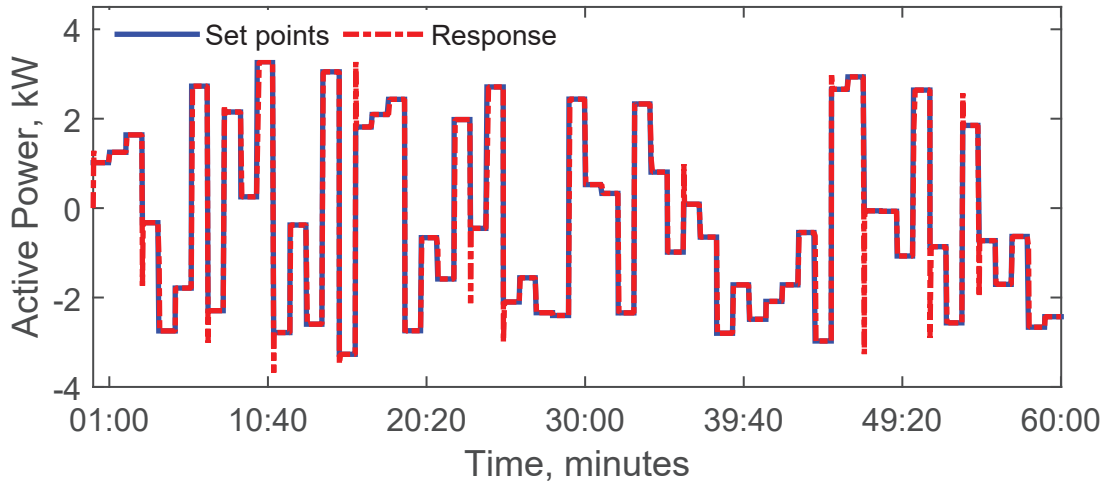

Figure 4.3: Response of battery model for dynamic active power set points.

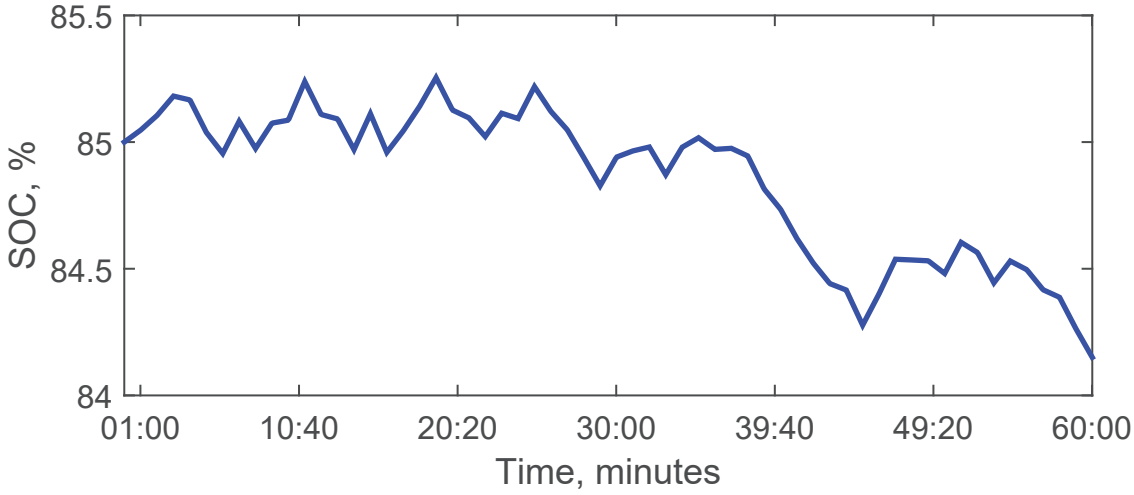

Figure 4.4: SOC as battery model trakcs dynamic active power set points.

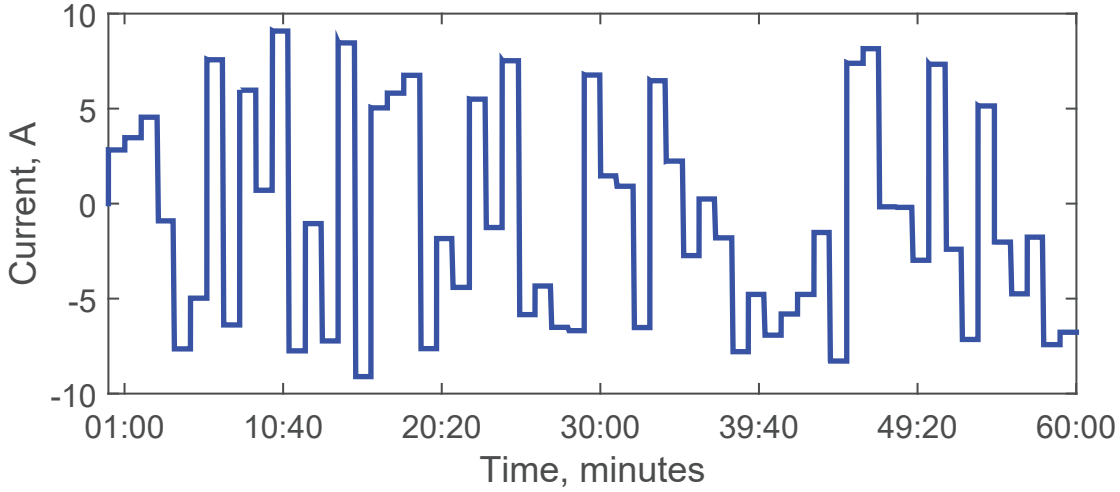

Figure 4.5: Battery current (DC side) as the battery tracks dynamic active power set points.

4.5.2 Feeder Level Simulation

For analysis purpose, the 240 V lateral in [128] is modified. It is considered that the feeder is supplied by a 175 kVA, 14.4/0.24 kV transformer as shown in Fig. 4.8. The

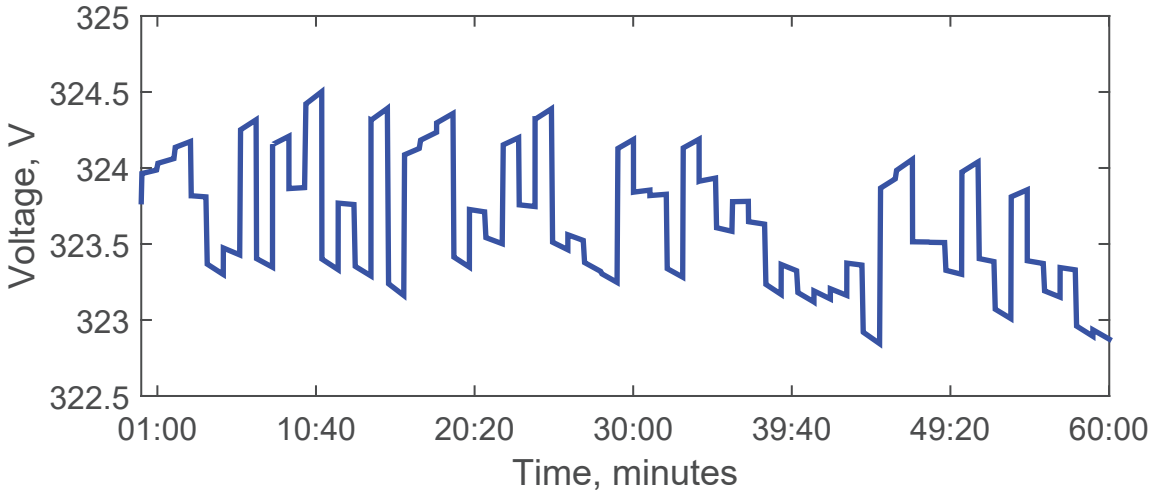

Figure 4.6: Battery internal voltage (DC side) as the battery tracks dynamic active power set points.

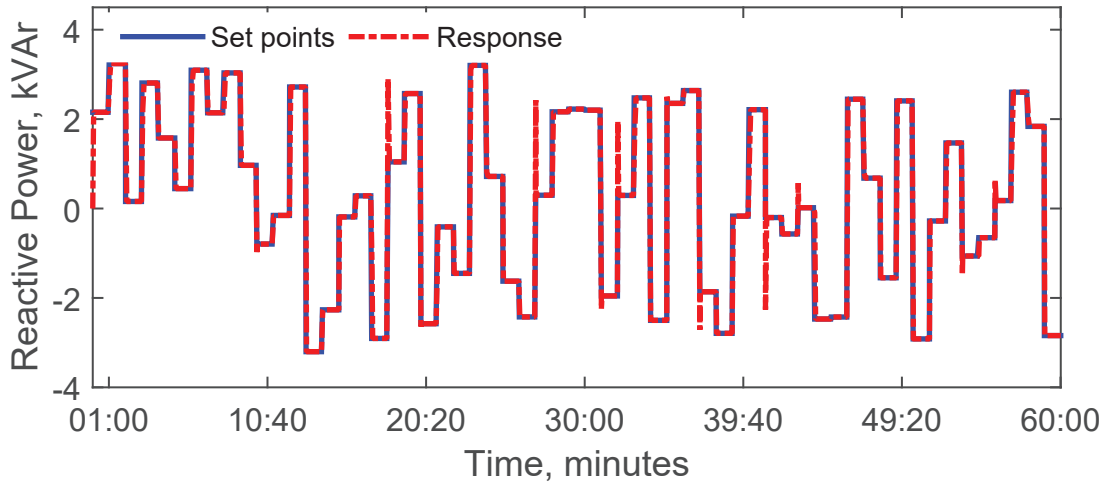

Figure 4.7: Response of battery for dynamic reactive power set points.

feeder supplies 24 houses (node 1 through 24) through service drops. The impedances of lateral sections, i.e., branch 52-53 through 62-63, are assumed identical and equal to $0.0069+\mathrm{j}\,0.0018\Omega$. Similarly, the impedances of the service drops, i.e., branch 52-1 through 63-24, are also assumed identical and equal to $0.011+\mathrm{j}\,0.0017\Omega$. Transformer

has an impedance of $0.0143 + j0.0357\Omega$ referred to LV side. The grid and EV models are solved using ePHASORSIM solver in OPAL-RT. The optimal voltage regulation model is built in GAMS and solved using KNITRO solver. Each house has different daily base load profiles (EV load excluded), and the total consumption of the 24 houses for a typical summer day beginning from noon is shown in Fig. 4.9. Voltage profile at 24-houses are shown in Fig. 4.10, which are obtained by solving power flow using 1-minute resolution load profiles. Fig. 4.10 shows during the evening time, when the loads are high, houses far away from the service transformer experience undervoltage issues.

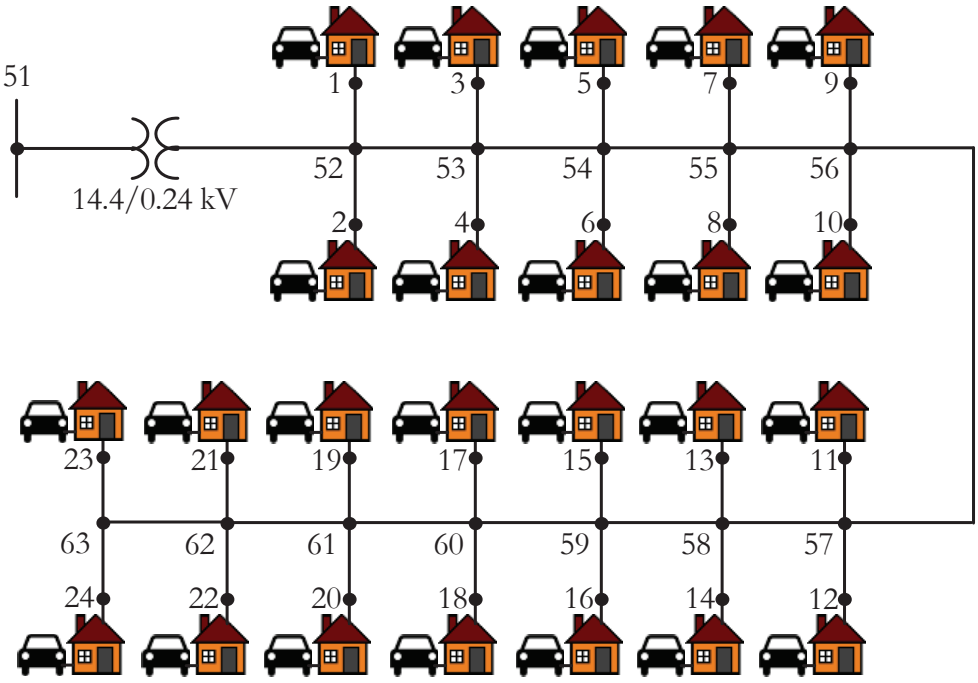

Figure 4.8: LV 240V Feeder with 24-houses used for the simulation studies.

The case studies to be discussed next demonstrates 4-quadrant operations of EVs

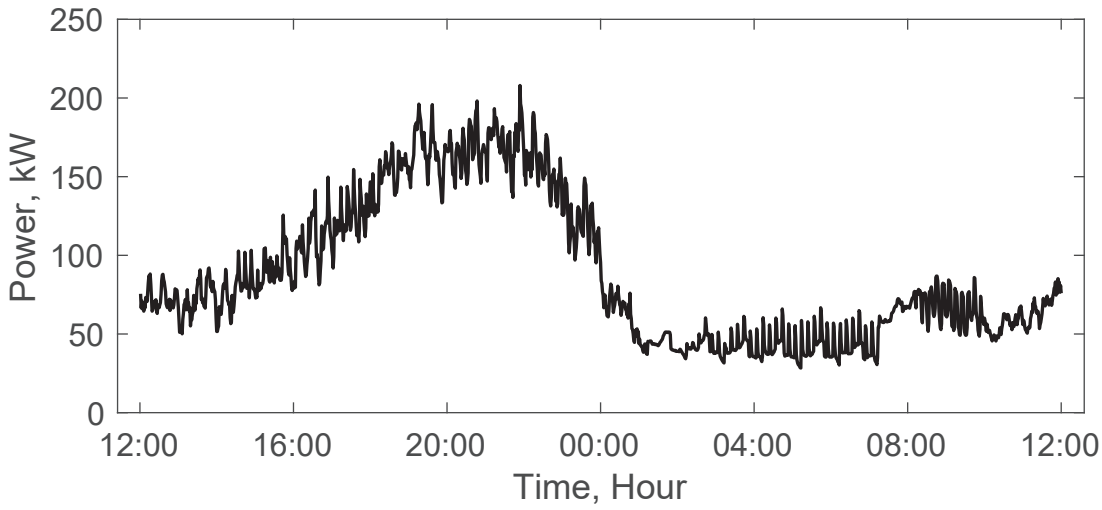

Figure 4.9: Base load profile on the feeder.

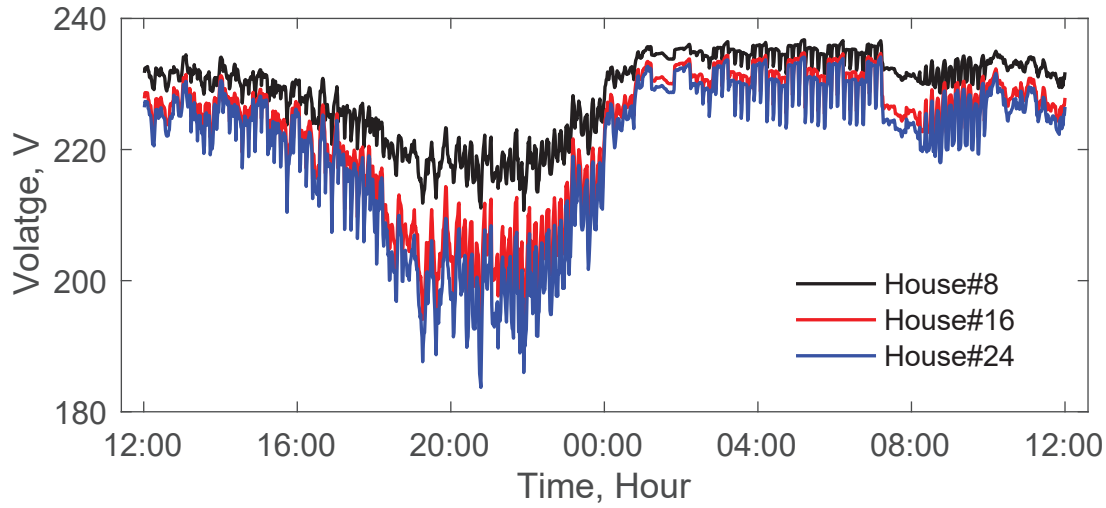

Figure 4.10: Voltage profile at selective houses (8,16,and 24) on the feeder.

showing impacts on feeder voltage and the 4-quadrant operation of EVs to maintain voltages on the feeder.

Case-A: Since the battery has limited capability, EVs can not support grid for all day long. Also, the EVs primary purpose won't let the EVs be connected to grid all the times. Therefore, one hour in a day is considered to carry out the case studies.

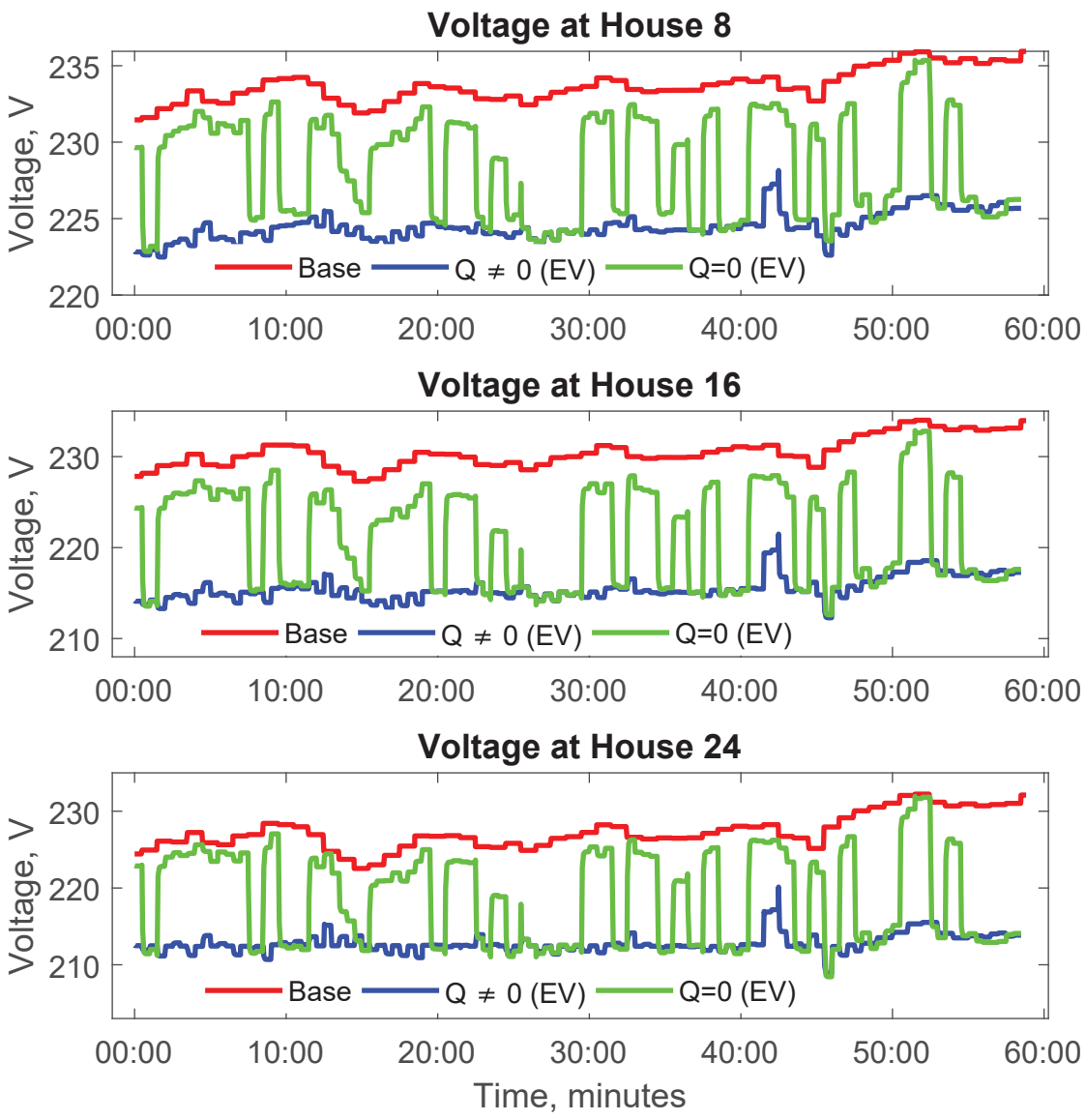

Figure 4.11: Voltage profile at House 8, 16, and 24 with base, with EV loads ($Q = 0$ and $Q \neq 0$) when most of EVs are charging on the feeder (under light loading conditions).

In Case-A, first the working of high fidelity battery model will be shown when several of EVs are connected to the feeder. 00:00 to 1:00 AM is chosen when the EVs are home and the feeder is under light load condition. The time is chosen such that the base load is low. This ensures voltage drop is not significant and the available voltage

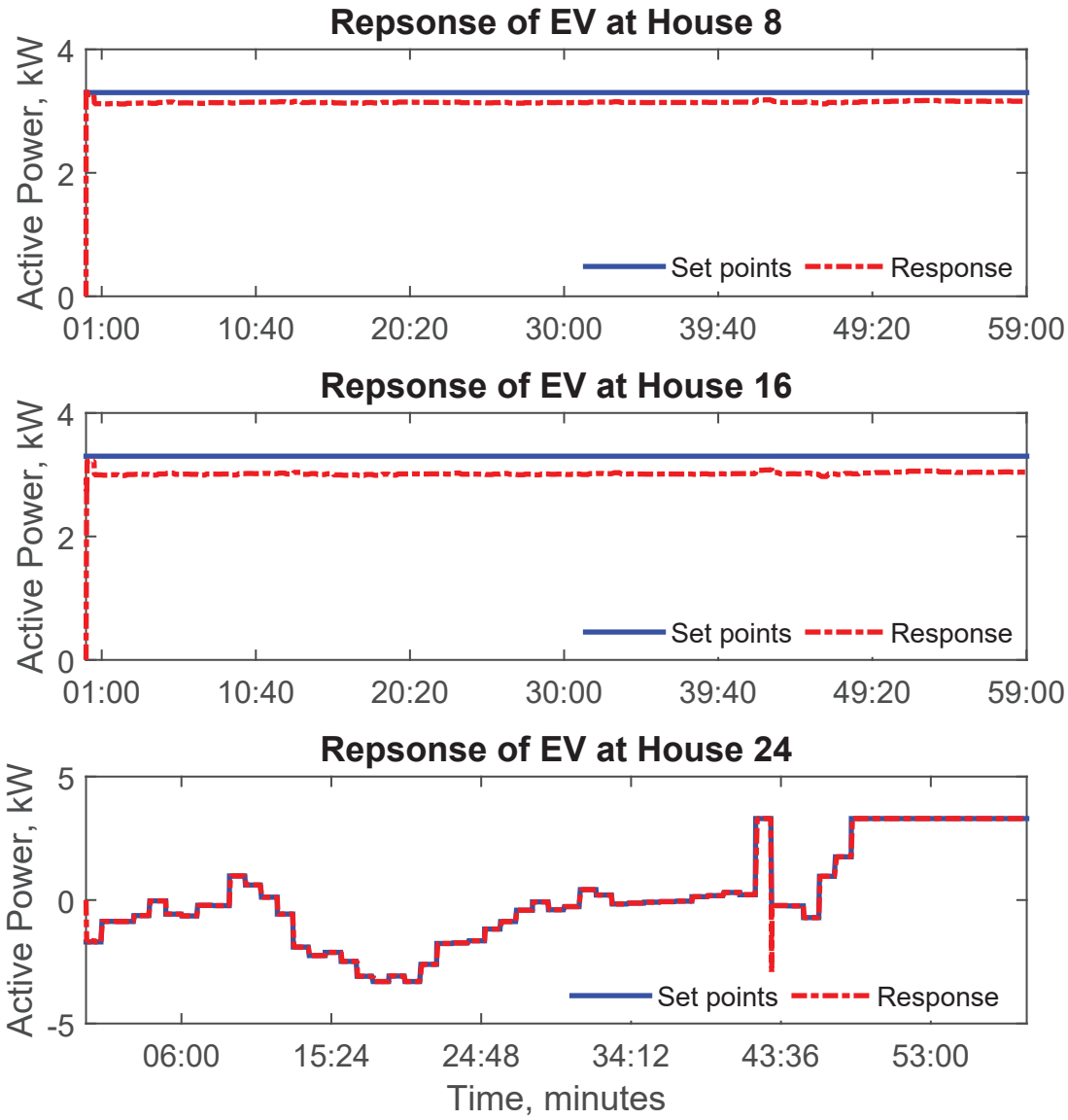

Figure 4.12: Response of active power of EVs at House 8, 16, and 24 without reactive power dispatch (under light loading conditions).

margins allow EVs to charge. For comparative analysis, EVs are dispatched with and without reactive power.

Fig. 4.11 shows voltage profiles at selective nodes (House 8, 16, 24) with and without EV reactive power dispatch. Since the voltage regulation signals (in terms of P,Q

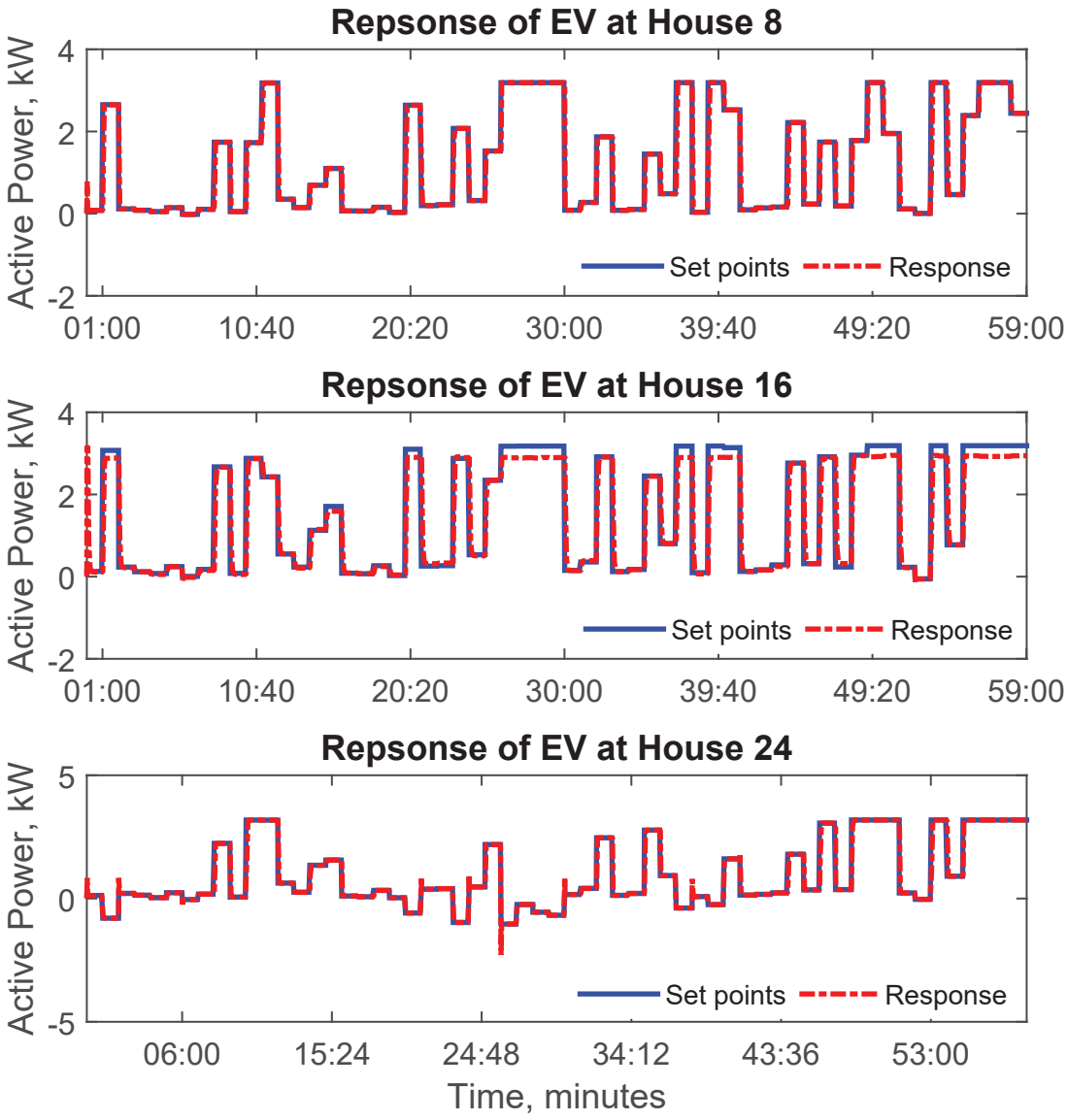

Figure 4.13: Response of active power of EVs at House 8, 16, and 24 with reactive power dispatch (under light loading conditions).

dispatch of EVs) are obtained using an optimization model, and the EVs are spread over the feeder length, EVs near to feeder head has more room to charge EVs compared to EVs downstream. This is clear from Fig. 4.11 as well, where EVs at House 8 and 16 are allowed to charge at high rate. Compared to EVs at House 8 and 16, the

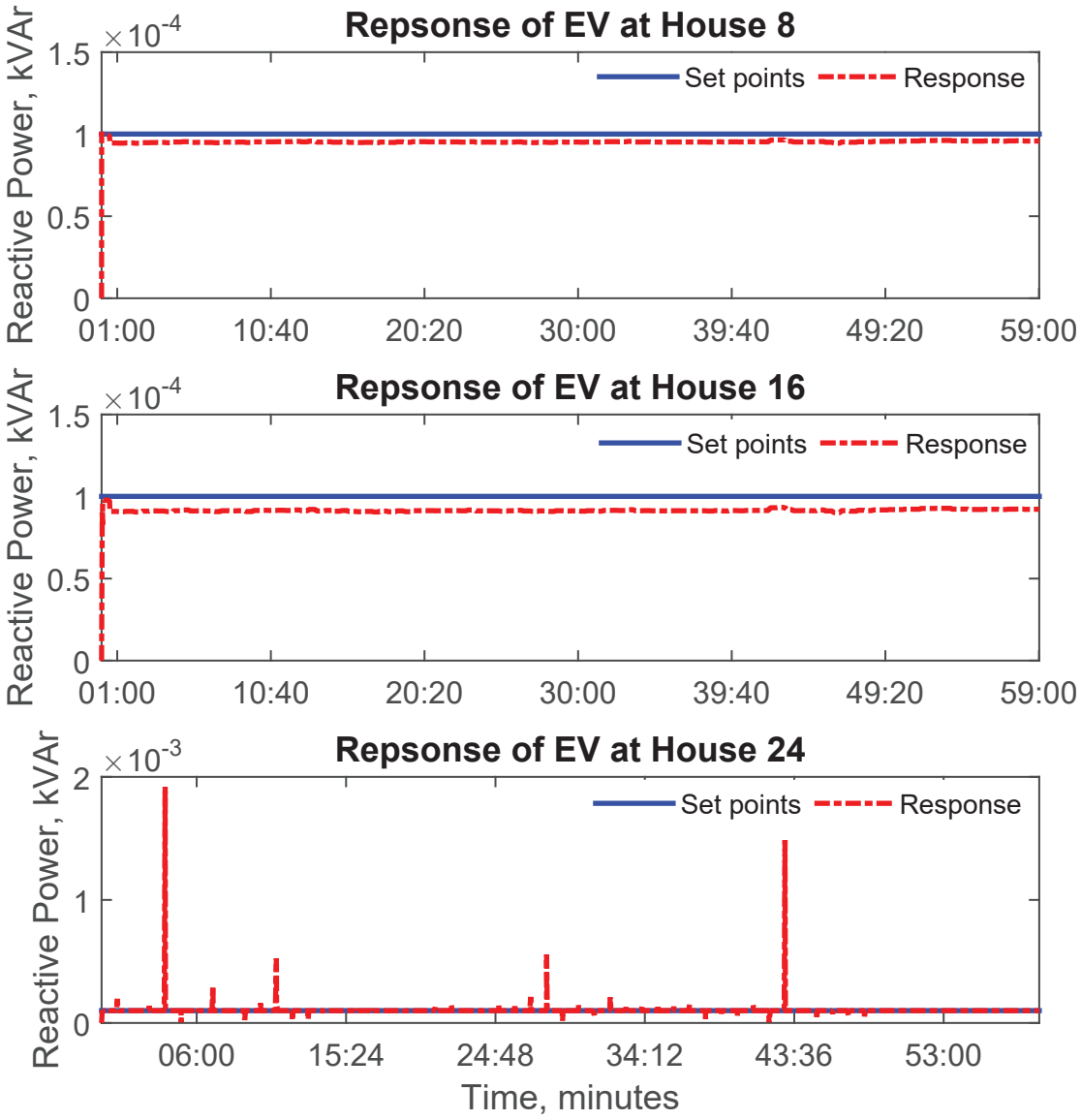

Figure 4.14: Response of reactive power of EVs at House 8, 16, and 24 without reactive power dispatch (under light loading conditions).

EV at House 24 is more constrained; hence, it allows EVs to charge at lower rate. Since most of the EVs are operating in the charging mode, the voltages decrease with reactive power dispatch as reactive power charging leads to lower voltages. However, the voltages are still within limits and satisfy constraints, which is fine.

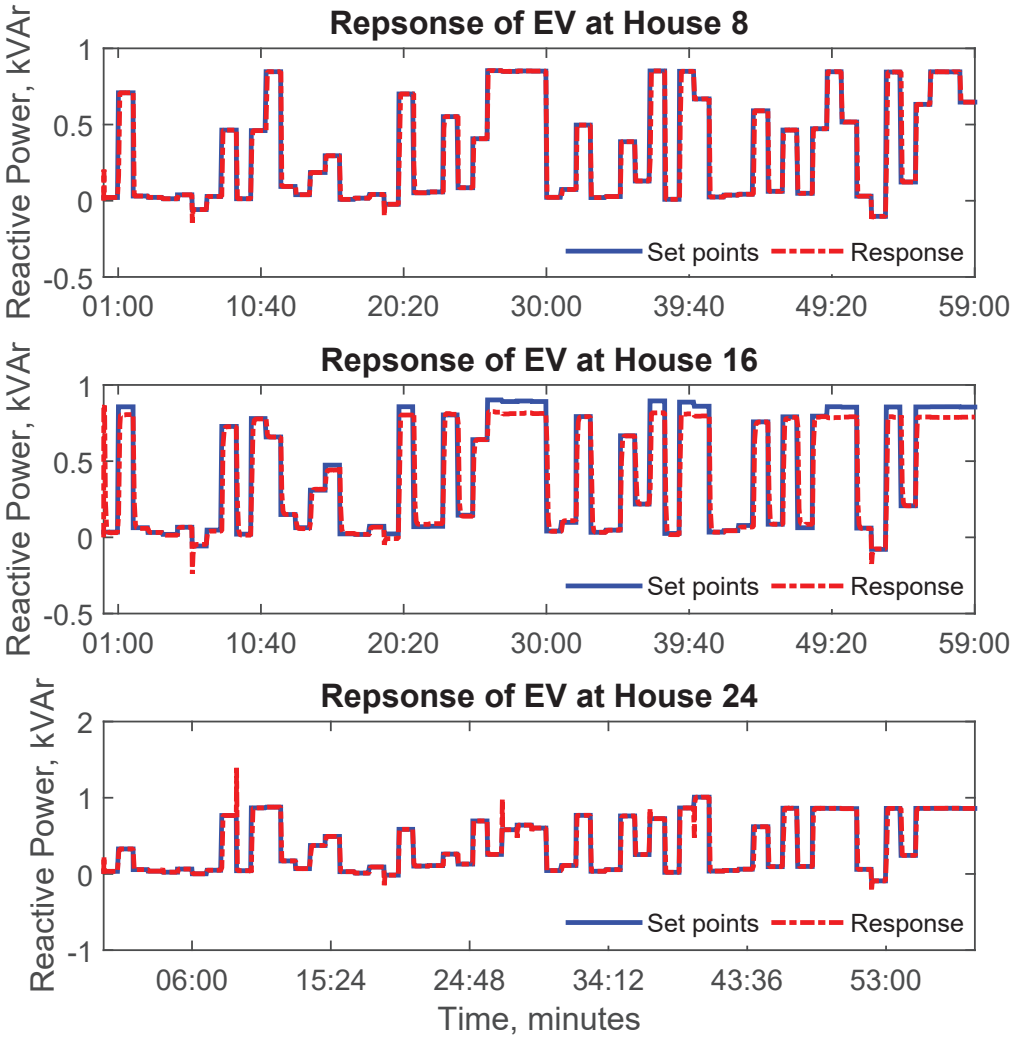

Figure 4.15: Response of reactive power of EVs at House 8, 16, and 24 with reactive power dispatch (under light loading conditions).

As EV is in charging mode for the selected hour, voltage profile is low compared to the base case. It is observed in Fig. 4.12 and 4.13 that upstream EVs, which are closer to the service transformer, has more voltage room to charge than downstream EVs. Therefore, the optimal voltage regulation signal provides higher active power set points to upstream EVs. During the EV charging, the voltage profile of House-24, which is the farthest node from the transformer becomes limiting as it hits the lower

prescribed limit first.

Fig. 4.12 and 4.13 show active power dispatch of EVs compared to the regulation signals obtained from optimization model of DSO. At House 8, the EV dispatch are positive; hence the EVs over SOC was increased. As moving towards EVs downstream the feeder, it is observed that the regulation signals from DSO are both positive and negative. For example, at House 24; the regulation signals for EVs are both charging and discharging. Fig. 4.14 and 4.15 show reactive power dispatch of EVs and the response of EVs; this shows the EVs are effectively working on 4-quadrants.

Case-B: In these case studies, how EVs can support voltage with 4-quadrant operation will be demonstrated. For these studies, one hour window during the peak load (10:00-11:00PM) is intentionally picked. This ensures most of EVs operate in discharging mode. The voltage profiles at this hour are low, however, there is still room to utilize before it hits the statutory limits. As the loading condition varies, SOC of EVs change, EVs arrive and leave on random times, some of the EVs may operate in the charging mode as well, which is acceptable as long as the voltages are maintained on the feeder. This is used to let EVs charge (with dispatch of Q) and analyze the impact on voltages on the feeder. Fig. 4.16 shows the voltage nodal voltage profiles at House 8, 16, and 24 with and without EV reactive power dispatch. It clearly shows the EVs are helping to improve the voltage profile on the feeder. Especially, on House 24 (which is furthest from head node), the nodal voltage is already

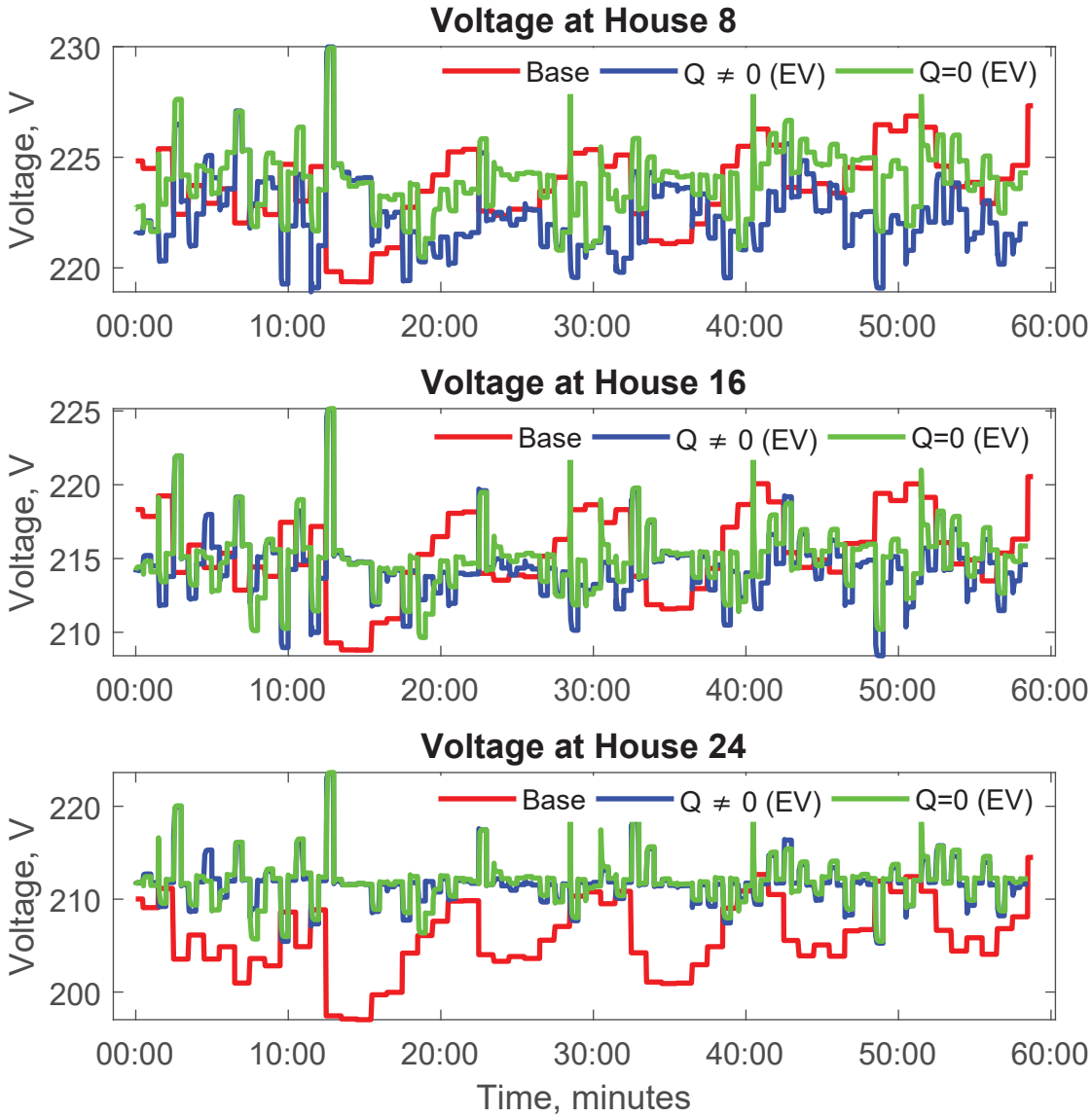

Figure 4.16: Voltage profile at House 8, 16, and 24 with base, with EV loads ($Q = 0$ and $Q \neq 0$) when most of EVs are in discharging mode (under high loading conditions).

beyond limits, hence, the optimization model forces the EVs to discharge, and hence the voltage profile at this node improves with EVs.

Fig. 4.17 and 4.18 show the responses of EVs on the optimal voltage regulation signals

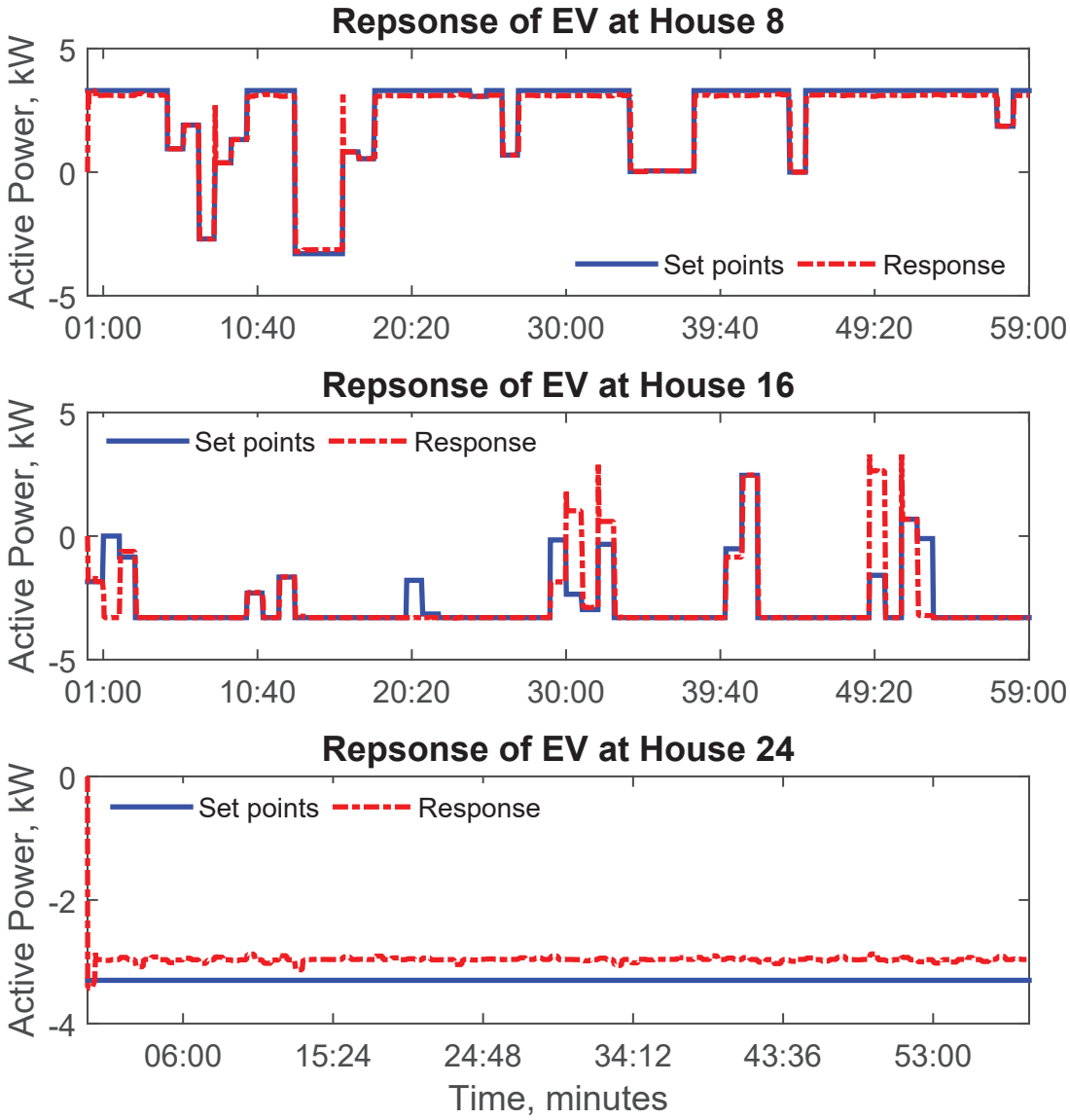

Figure 4.17: Response of active power of EVs at House 8, 16, and 24 without reactive power dispatch (under high loading conditions).

that is trying to keep the nodal voltages within the prescribed limits. Note that the EVs are in mixed mode of charging/discharging. Fig. 4.19 and 4.20 show the tracking of EVs for reactive power set points (obtained from the optimization model).

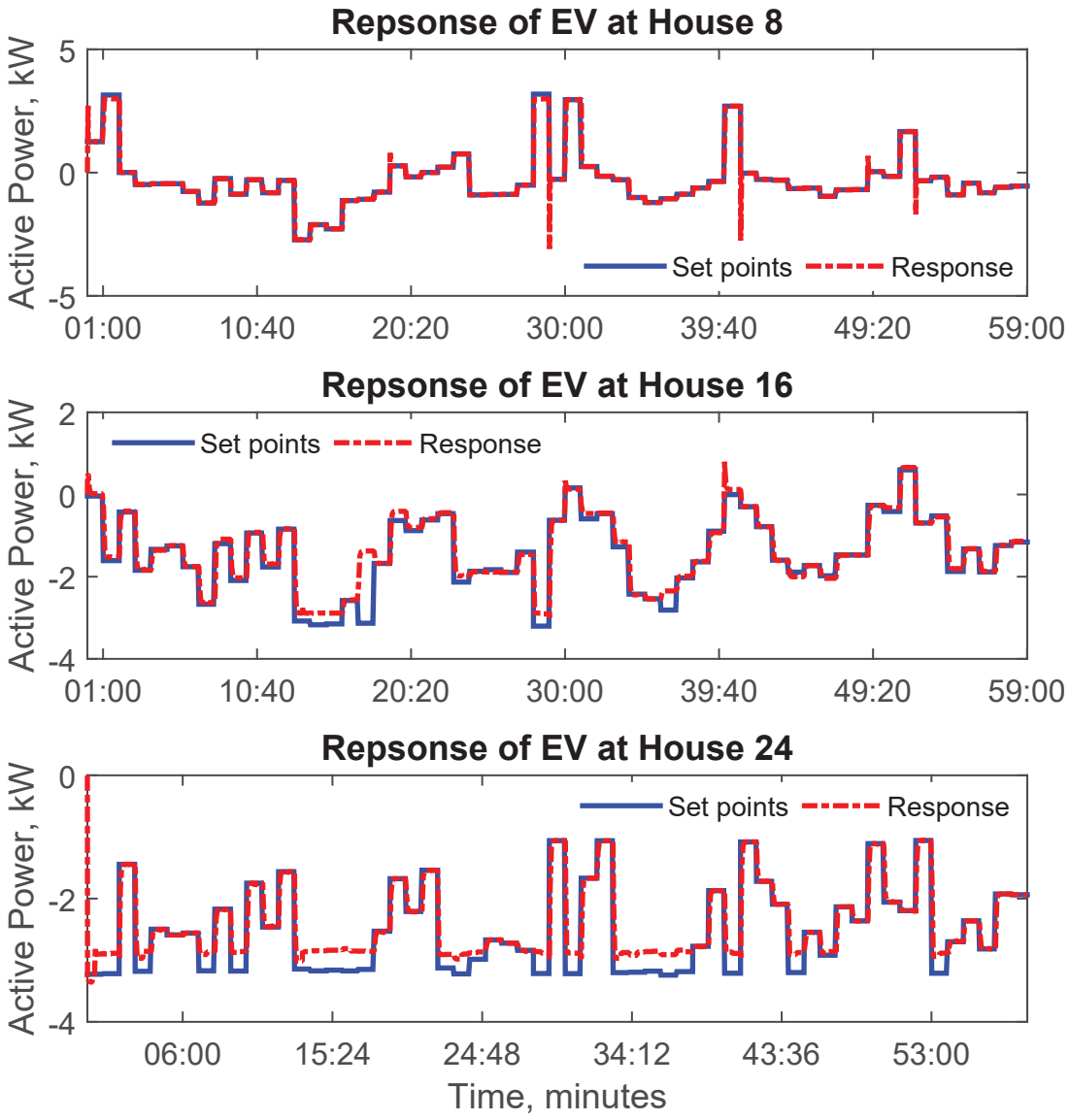

Figure 4.18: Response of active power of EVs at House 8, 16, and 24 with reactive power dispatch (under high loading conditions).

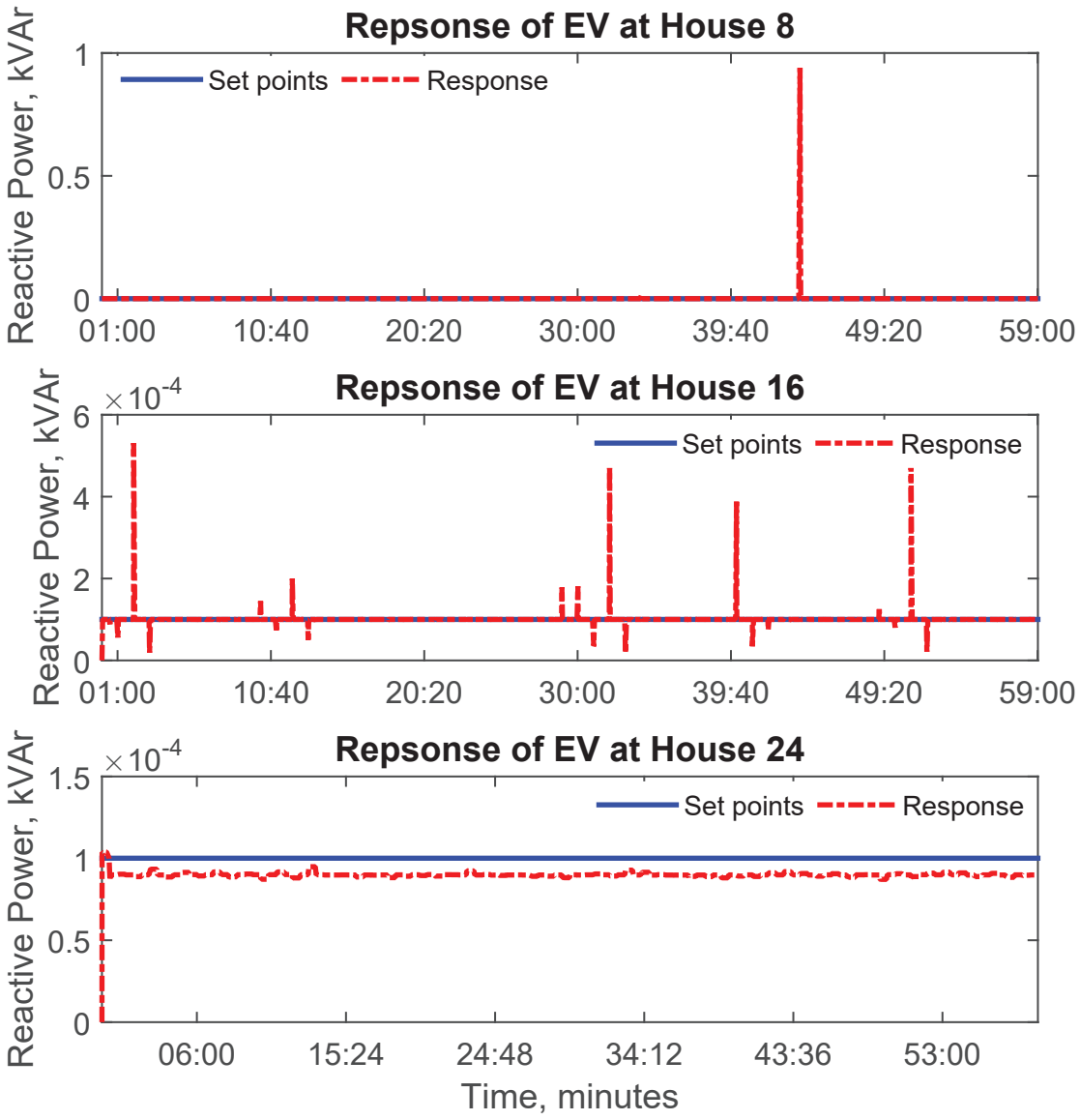

Figure 4.19: Response of reactive power of EVs at House 8, 16, and 24 without reactive power dispatch (under high loading conditions).

4.6 Conclusion

In this Chapter, the detailed high-fidelity model of battery and EV on-board charger that allows four-quadrant operation is integrated to a typical North American low

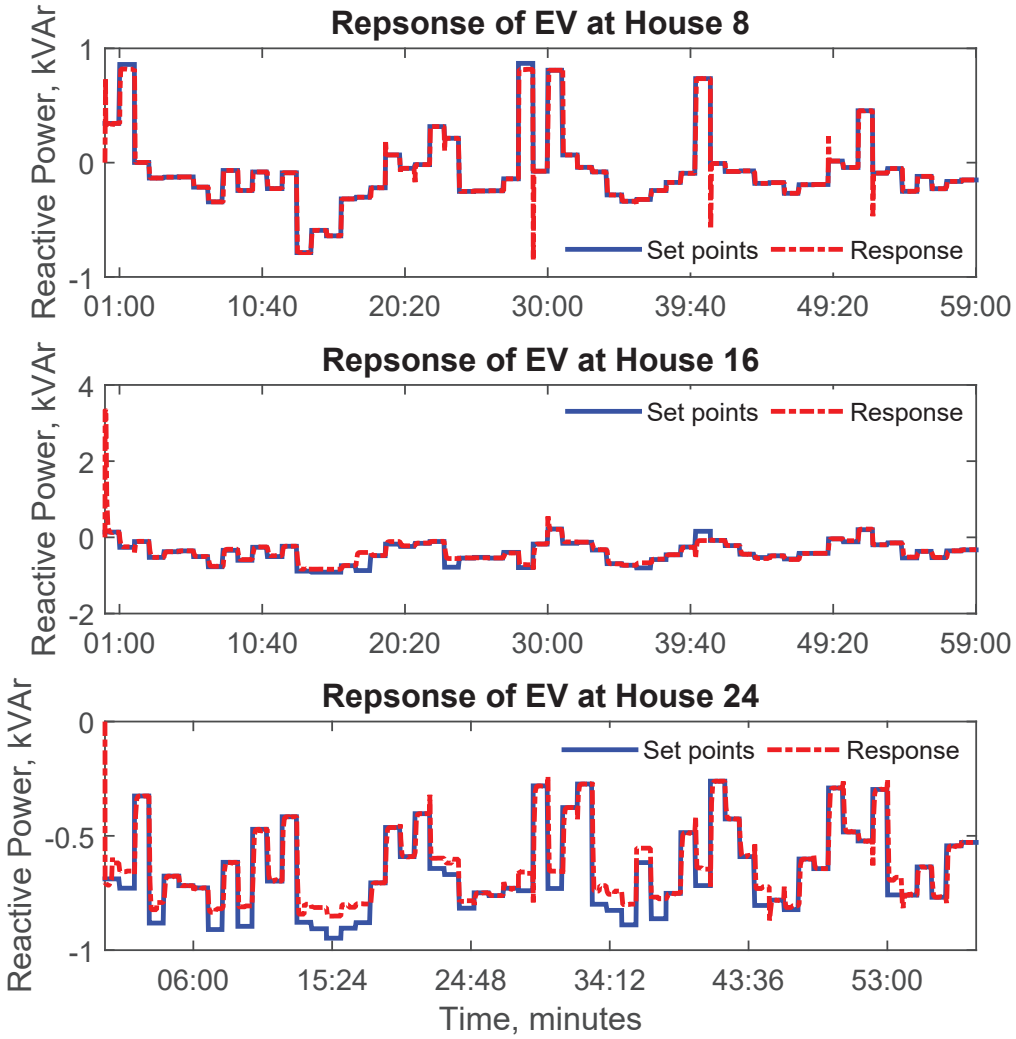

Figure 4.20: Response of reactive power of EVs at House 8, 16, and 24 without reactive power dispatch (under high loading conditions).

voltage distribution feeder to demonstrate the usefulness of four-quadrant dispatch of EVs in supporting voltage on the feeder. For this, voltage regulation signals (in terms of P,Q dispatch of EVs) are generated from an optimal power flow model and the EVs are dispatched accordingly. The real time simulation demonstrates effectiveness of dispatching EVs in 4-quadrant for supporting voltage on the distribution feeders.

Chapter 5

Real-time Virtual Power Plant Coordination at Distribution Level and HIL Implementation

5.1 Introduction

In this chapter, preliminary feasibility of virtual power plant (VPP)[1] is examined. For real time dispatch of resources in VPP, a linearized optimal power flow approach is adopted. In addition, VPP scheduling is implemented in hardware-in-the-loop (HIL)

[1]This work was carried out in collaboration with Dr. M. R. Almassalkhi and his group from the University of Vermont.

simulation with OPAL-RT's simulator in real time. Results shown in this Chapter are preliminary based on a work in progress. Readers are advised to follow publications that will contain detailed models and rigorous analyses.

5.2 VPP Coordination Model

In this work, a scalable Quadratic Programming (QP) version of VPP scheduling problem is formulated. The QP model consists of a linearized version of three-phase unbalanced power flow equations. A high level mathematical model of the QP-DOPF is provided next.

$$\text{Min} : \left(P_{track} - \sum_{vpp} P_{vpp} \right)^2 \tag{5.1}$$

The development of mathematical models is based on branch currents and nodal voltages. π-equivalent circuits are used to model cables and conductors. Detailed models are available in [108]. Sending end and receiving end currents and voltages are modeled with ABCD parameters for series elements,

$$\begin{bmatrix} V_{i,k} \\ \\ I_{s,j,k} \end{bmatrix} = \begin{bmatrix} A_j & B_j \\ \\ C_j & D_j \end{bmatrix} \begin{bmatrix} V_{i+1,k} \\ \\ I_{r,j,k} \end{bmatrix} \tag{5.2}$$

As the active power, reactive power, and voltage magnitude have relatively small and limited range of variation, they can be linearized around an estimated operation point (V_0, I_0), as shown in (5.3) and (5.4).

$$\begin{aligned} P_n = P_n \Big|_{V=V_0,I=I_0} + \frac{\partial P(V,I)}{\partial I} \Big|_{V=V_0,I=I_0} (I - I_0) \\ + \frac{\partial P(V,I)}{\partial V} \Big|_{V=V_0,I=I_0} (V - V_0) \end{aligned}$$

$$\begin{aligned} Q_n = Q_n \Big|_{V=V_0,I=I_0} + \frac{\partial Q(V,I)}{\partial I} \Big|_{V=V_0,I=I_0} (I - I_0) \\ + \frac{\partial Q(V,I)}{\partial V} \Big|_{V=V_0,I=I_0} (V - V_0) \end{aligned}$$

$$P_{vpp} = \sum_{n \in vpp} P_n \tag{5.3}$$

$$0.95^2 \leq {V_n}^2 \Big|_{V=V_0} + \frac{\partial V_n^2}{\partial V_n} \Big|_{V=V_0} (V_n - V_0) \leq 1.05^2 \tag{5.4}$$

$$P_{vpp} \leq P_{vpp}^{max} \tag{5.5}$$

where V represents three-phase voltage vector, I represents three-phase branch current vector, V_0 and I_0 represent the operating point around which the constraint set are linearized, P represents active power loads, Q represents reactive power loads, A, B, C, D are the line parameters, s, and r represent two ends of the lines, n represents node, vpp represents number of virtual power plants (VPPs), and P_{track} represents tracking reference signal for VVPs to follow.

5.3 HIL Implementation

The HIL design uses the architecture shown in Fig. 5.1. The HIL setup mainly consists of a Grid Simulator, Grid Control Center, and Load Emulator. Grid Control Center consists of Grid Optimization and VPP Coordinator models. The Grid Control Center controls the grid model built in Grid Simulator (OPAL-RT OP5600). The VPP coordinator sends dispatch signals to the loads, which are emulated using microcontrollers (ESP8266). Each ESP8266 simulates up to thousands of water heaters (load model), which is based on the Packetized Load Management Algorithm[1] [129, 130]. Output of ESP8266 is voltage proportional to the load. In Grid Control Center, a DOPF model (that consists of comprehensive mathematical model of three-phase distribution grid components, operational limits, and control variables including load tap changers, capacitor banks) is solved. This model provides set points every 15

[1]This work was done by University of Vermont, and the contents of this Chapter was developed based on the collaborative work between Michigan Tech. and the University of Vermont.

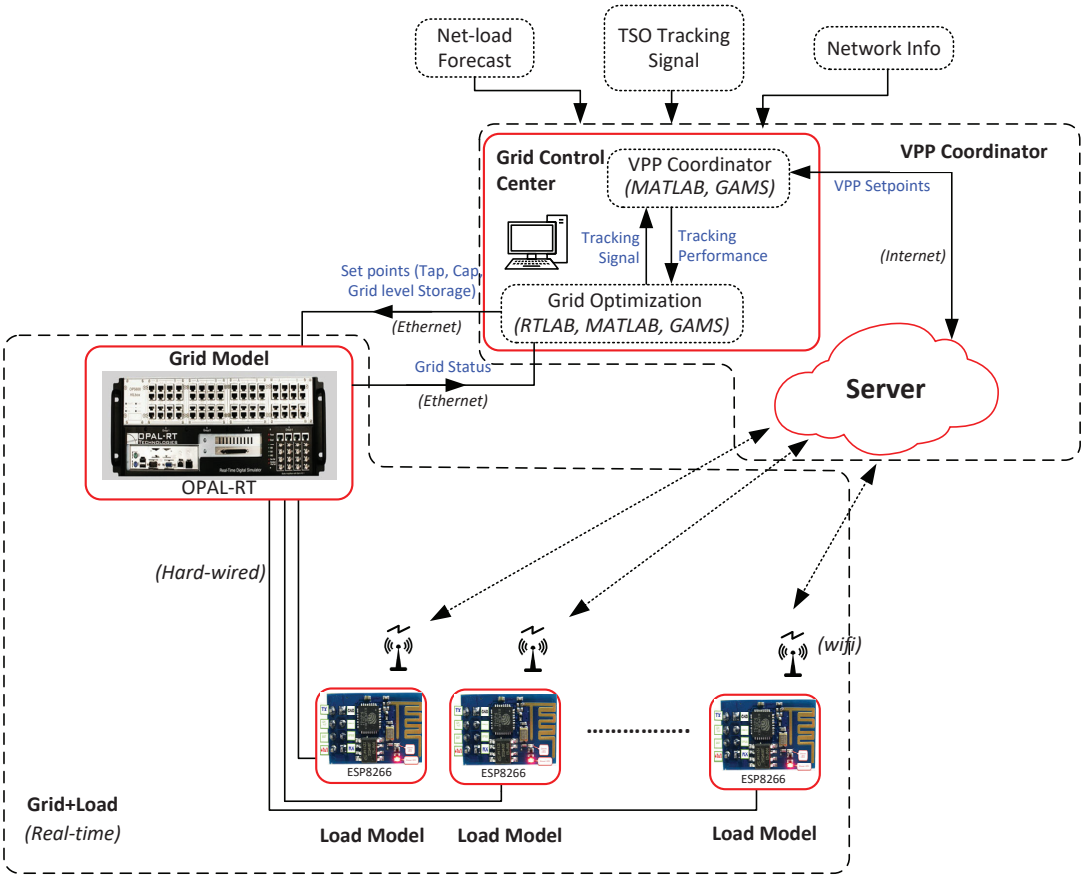

Figure 5.1: Overview of the HIL setup.

minutes. This model is built in GAMS and solved using KNITRO solver. Then, a VPP scheduler model is solved, which provides the set points of VPPs every 30 seconds.

5.4 Case Studies

5.4.1 Accuracy of QP VPP Scheduler Model

IEEE 4-node test feeder is used to show the effectiveness of the proposed model. The proposed QP and non-linear models are compared by varying the load data in the range of $\pm 10\%$ around the base load. The largest voltage difference obtained is 0.014%, which shows that the proposed QP VPP scheduler model is very accurate around the base load.

5.4.2 VPP Scheduling

The QP VPP Scheduler model is tested with 68-node feeder using CPLEX solver. The original 64-node feeder is first modified by adding LTCs, cap banks, and an energy storage device at sub-station. The resulting feeder is a 68 node circuit. On a slower time scale (15-minute resolution) for 3-hour rolling horizon full scale MINLP-DOPF model is solved, which provides set points for LTCs, cap banks, and grid level energy storage devices. In near real time, the DSO receives tracking signals from TSO to follow, which must be obtained by coordinating the resources from the VPPs within the DSO service area. To coordinate the VPPs, given the fast response

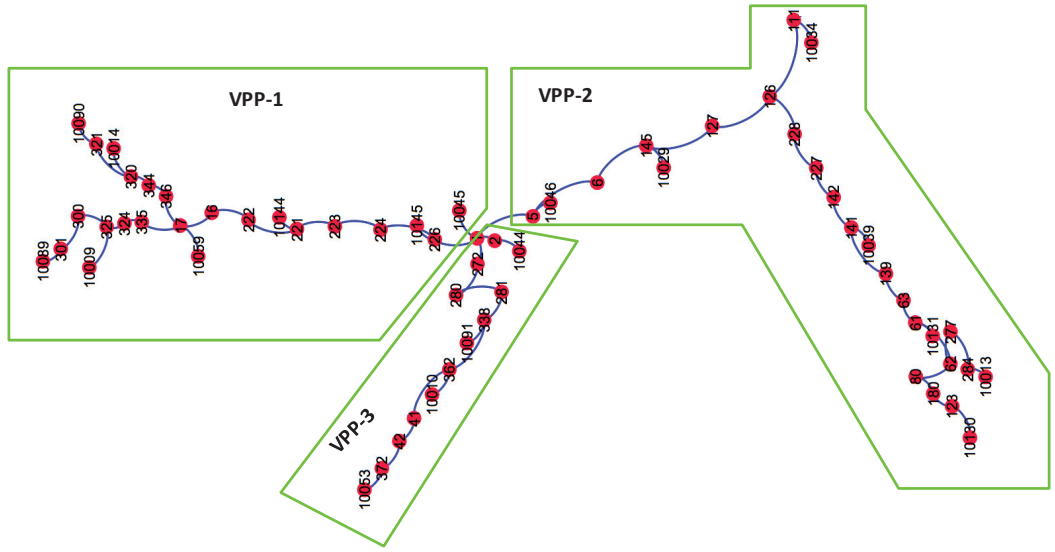

Figure 5.2: 68-node feeder to demonstrate QP-DOPF.

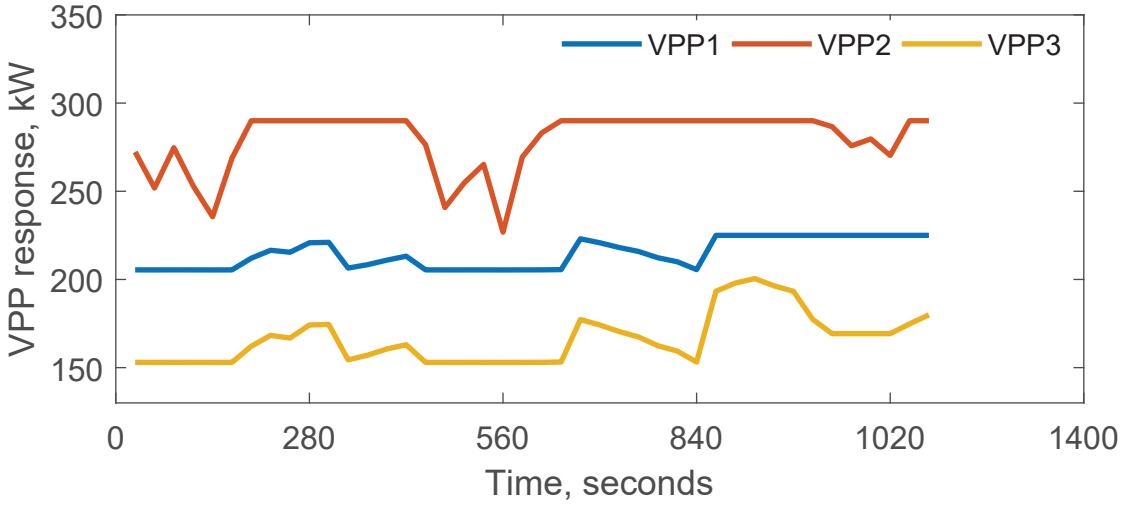

Figure 5.3: Set points of three VPPs in 68-node feeder.

needed, QP-DOPF model is used. Three VPPs are considered, as shown in Fig. 5.2, to demonstrate the concept and to demonstrate the performance of QP-DOPF model. VPP-1 and -2 have 8 load nodes and VPP-3 has 4 load nodes. Each VPP sends net load forecasting at 5-minute resolution to the DSO. DSO then solves the MINLP-DOPF and dispatches its assets. In near real time, the VPP sends updated short-term

net load prediction. Based on the tracking signal received by the DSO and the net load capabilities of the VPPs, DSO solves the QP-DOPF to track the reference signal from TSO as closely as possible. While dispatching the VPPs, the DSO ensures that the grid constraints (e.g. voltage limits, transformer capacity limits) are not violated. The QP-DOPF model is solved every 30-seconds. Solution time for each case was $<$ 2 seconds.

Fig. 5.3 shows the response of 3 VPPs for the DSO level tracking signal. From the Fig. 5.3, it can be observed that when VPP-2 can not increase kW consumption due grid constraints (eg., transformer capacity in the VPPs), the unconstrained VPPs (VPP-1 and -3) share the slack.

5.4.3 HIL Simulation in Large-Scale Feeder

A 534-node feeder is separated into three VPPs, which is shown in Fig. 5.4. There are aggregated water heater fleets connected to each VPP. In addition, there are 13 small water heater loads connected to 13 nodes in the VPP2. The small water heater loads are simulated by software-in-the-loop (SIL) and 3 large loads for 3 VPPs are simulated using HIL. The capacity of each water heater is 5kW. Since there are at most 10 houses connected to each node, there are up to 10 water heaters for each SIL node. For HIL VPPs, there are up to 300 water heaters each.

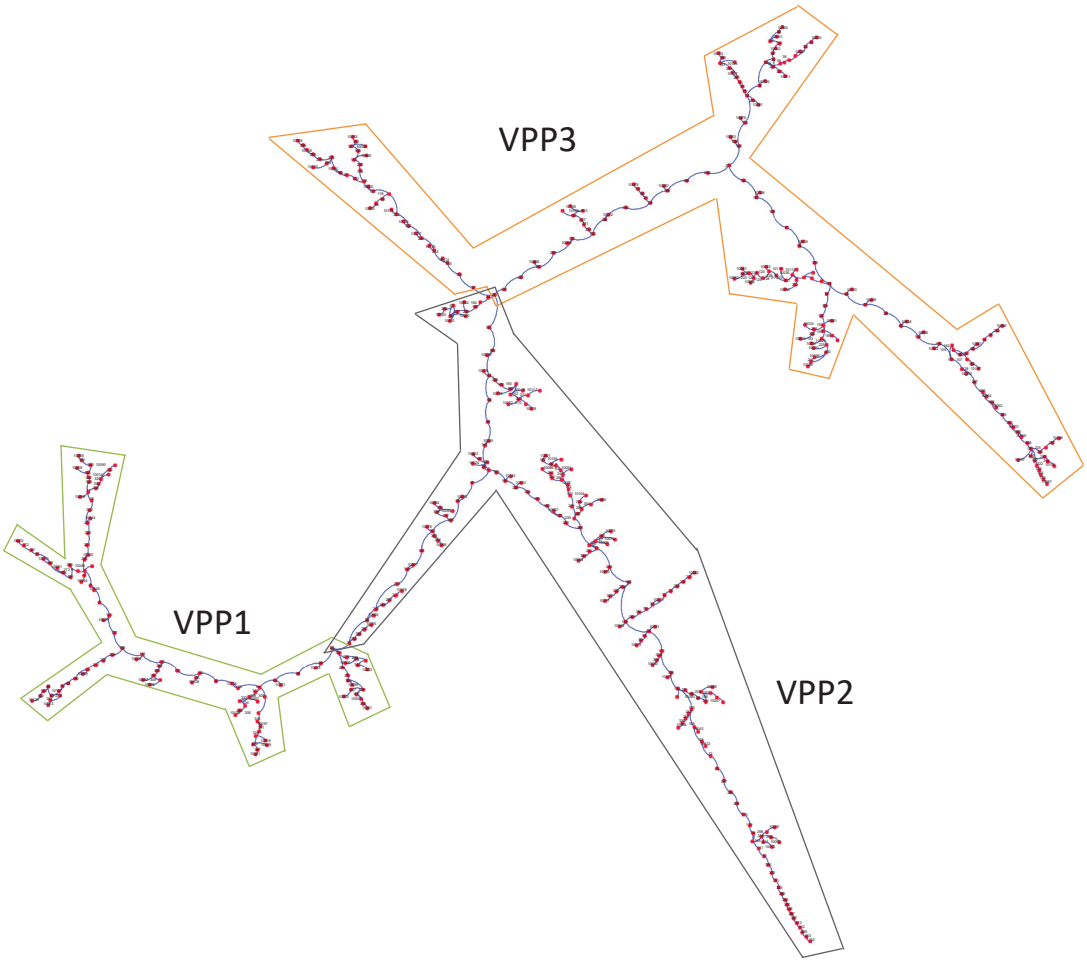

Figure 5.4: 534-node feeder to demonstrate VPPs' working in HIL.

Case I: Tracking a Step Change Signal

In this simulation studies, a step change signal from TSO is received by the DSO. DSO diaggregates the TSO level signal using VPP Scheduler model, which results in three step change signals for the three VPPs to track. The active power tracking responses of three VPPs are shown in Fig. 5.5. Voltage profile at selective nodes is

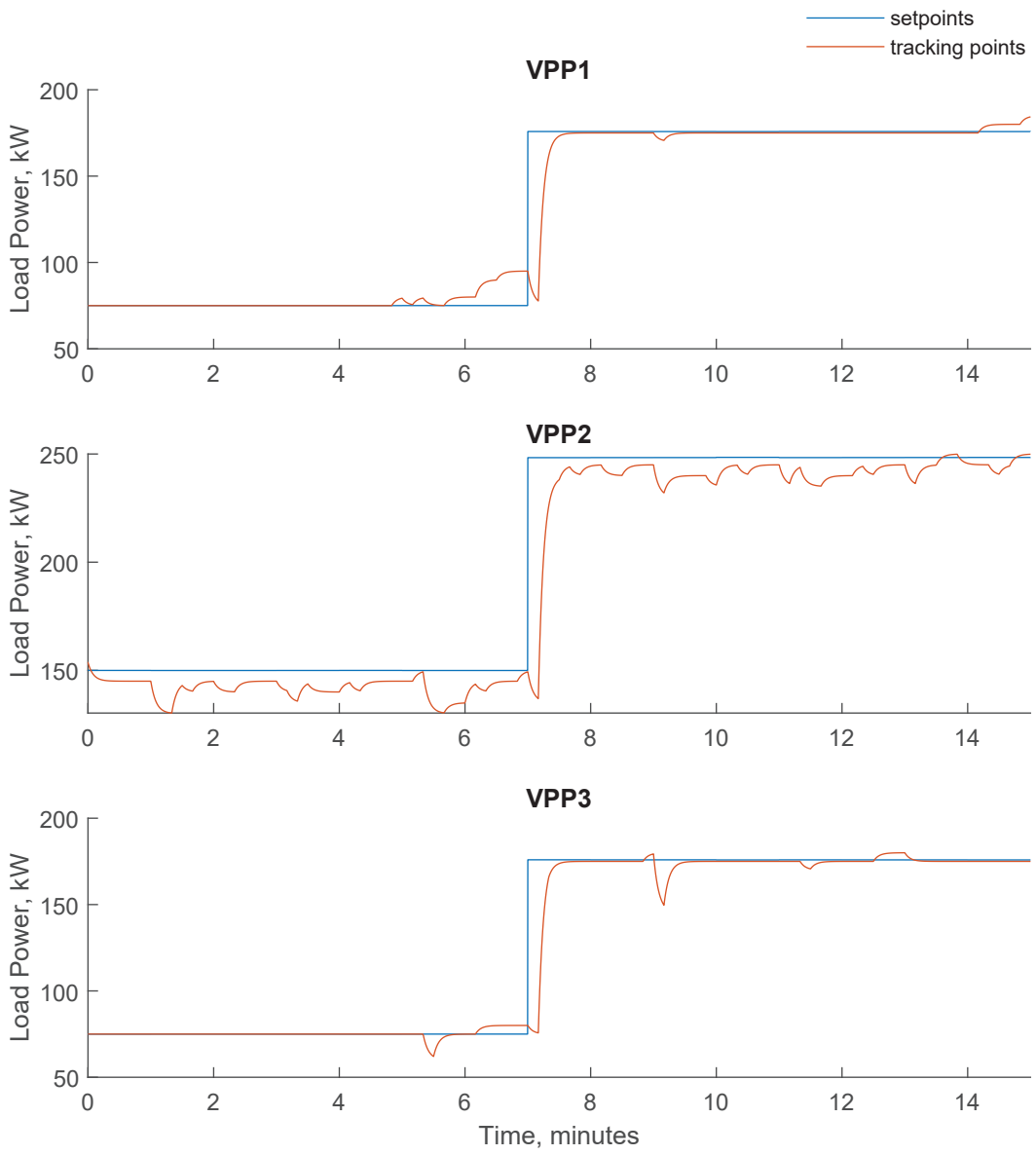

Figure 5.5: The tracking of charging set points of three VPPs for a step change signal.

shown in Fig. 5.6. This shows that three HIL VPPs are capable to track step change signals while staying within the DSO level constraints (in this case voltage bounds).

Case II: Tracking a Ramp Signal

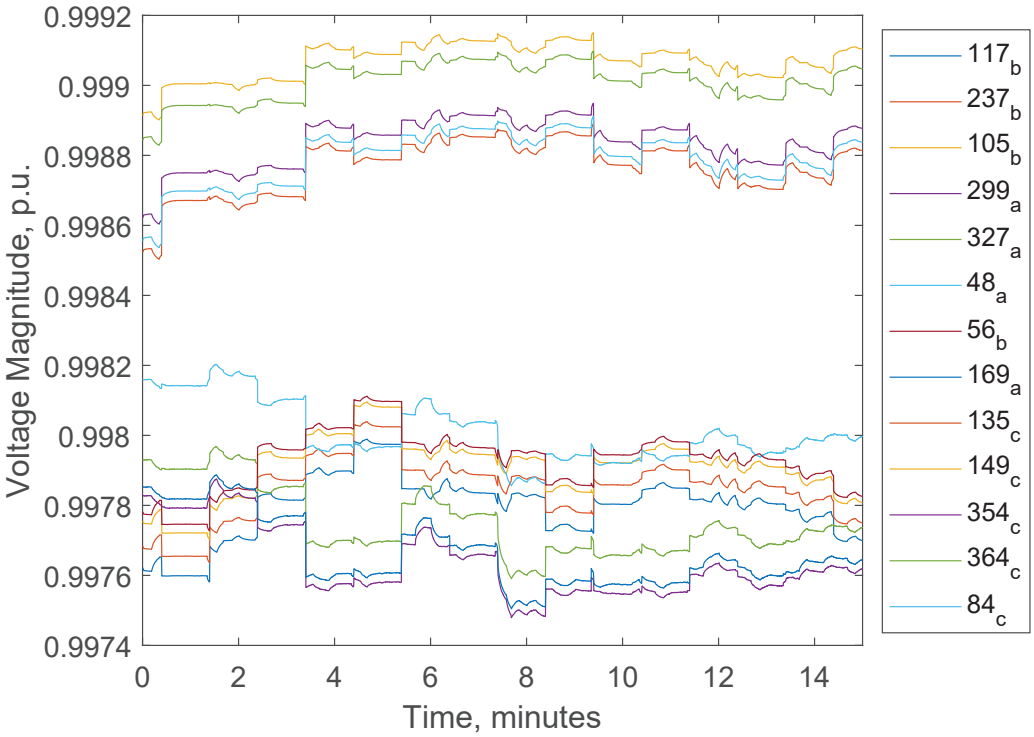

Figure 5.6: Phase voltage profile at selected three-phase nodes during VPP dispatch of distribution system Case I.

Several small step change signals are used to emulate the ramp signal. Three VPPs have their own ramp signal to track. The disaggregated responses of the distribution level VPPs and the charging signal set points are plotted for each of the three VPPs in Fig. 5.7. The corresponding node voltages are plotted in Fig. 5.8 to show three-phase feasibility of VPP dispatch in distribution feeder. All of the voltages are within limits.

Case III: VPP coordination and re-dispatch under VPP limits

If one of the VPPs is constrained, the DSO attempts to redispatch the requested

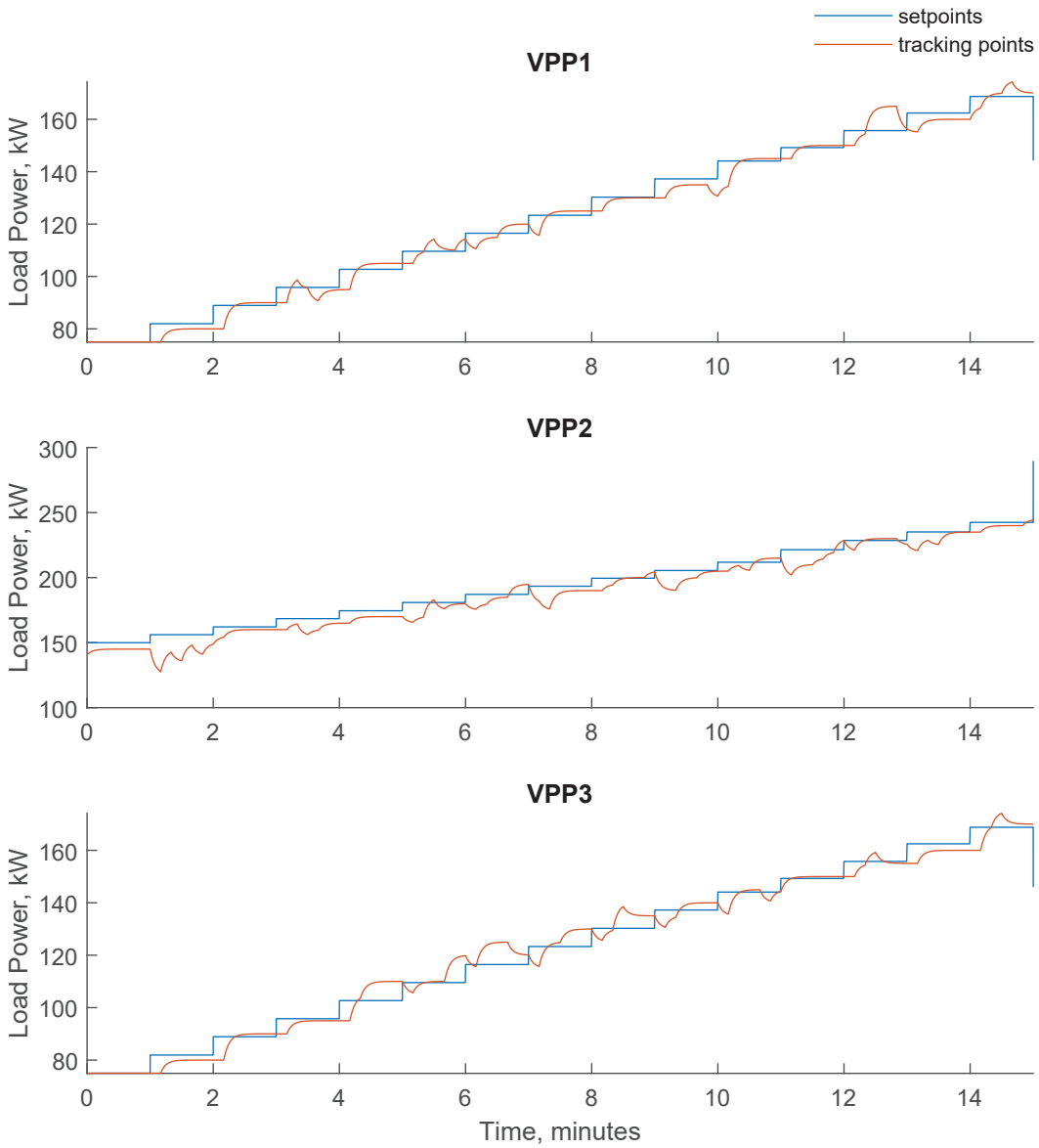

Figure 5.7: The tracking of charging set points of three VPPs Case II.

flexibility to the remaining VPPs. In case the remaining VPPs also have power limitations, the DSO sends trigger signal to redispatch at TSO level (however, this is beyond the scope of this dissertation). Fig. 5.9 shows, VPP1 saturates at 5th minute (by enforcing the bounds in the model). The remaining active power, that VPP1

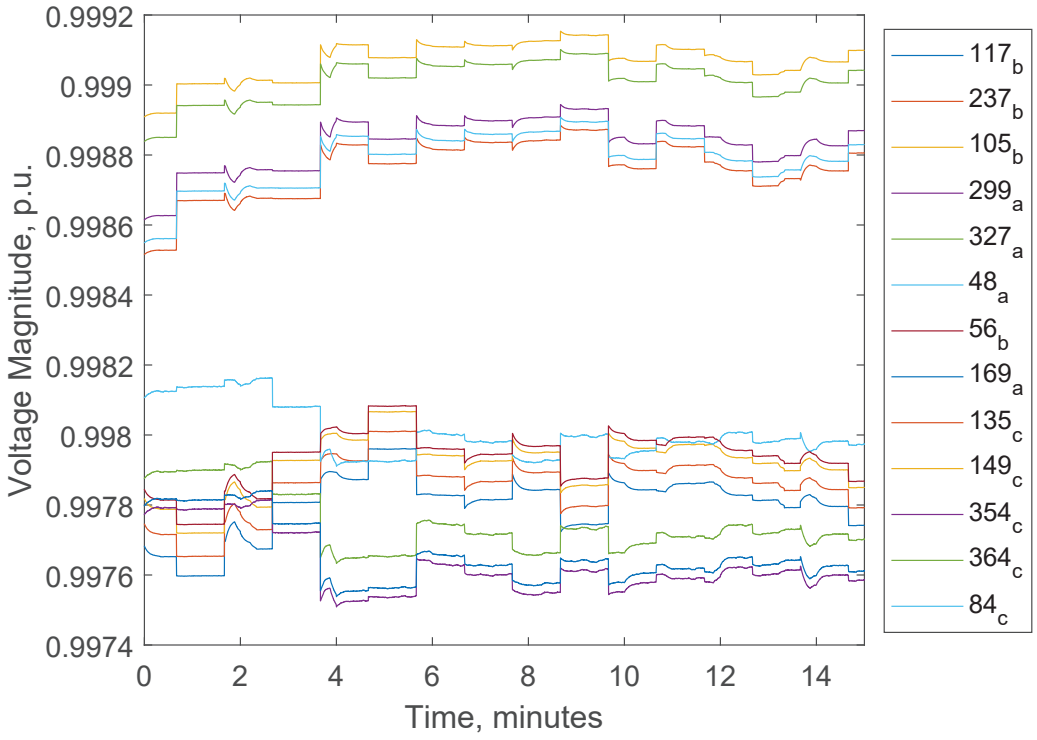

Figure 5.8: Phase voltage profile at selected three-phase nodes during VPP dispatch of distribution system Case II.

can not track, is redispatched to VPP2 and VPP3 using the QP model. Therfore, the setpoints of VPP2 and VPP3 are increased to accommodate the difference. Next, VPP3 saturates at 10th minute. The remaining active power of VPP3 is redispatched to VPP2 using the QP moddel. Voltage profile at selective nodes is shown in Fig. 5.10. They are lower than the voltages in Case II because of VPP saturation. However, they are still within the desired limits.

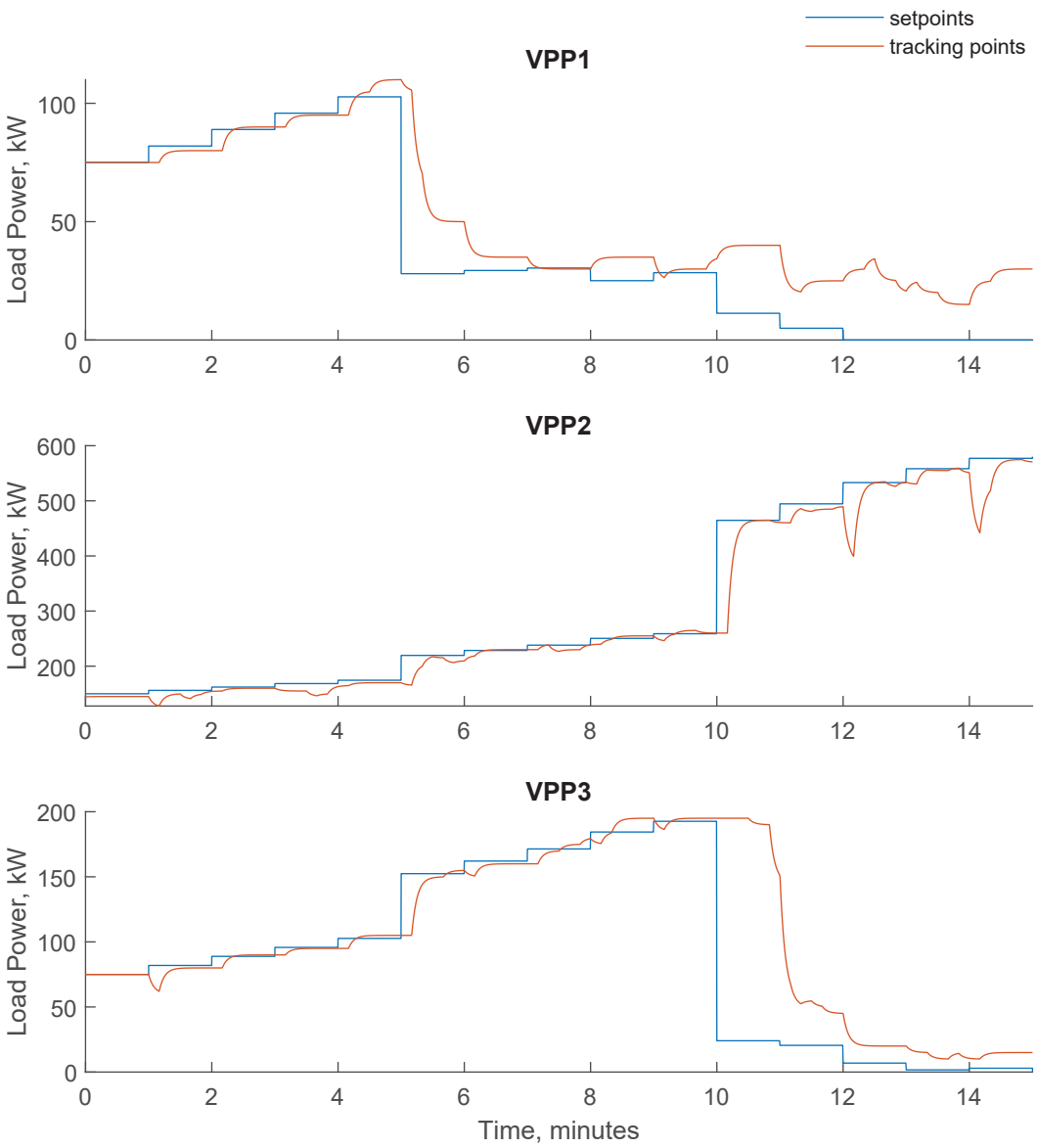

Figure 5.9: The tracking of charging set points of three VPPs Case III.

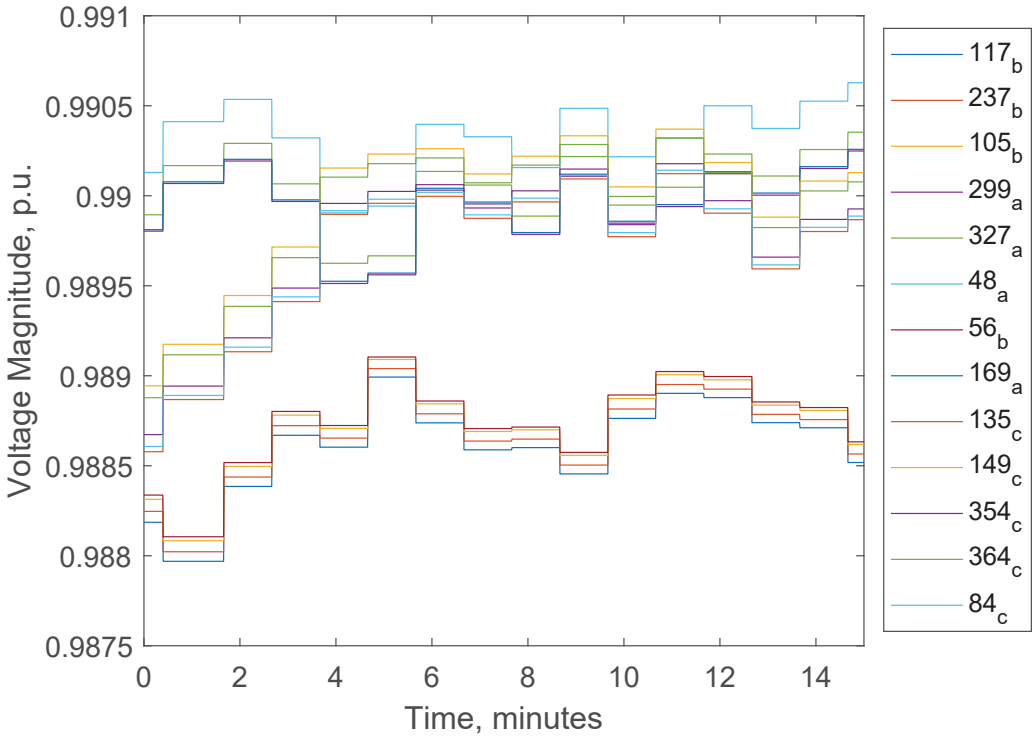

Figure 5.10: Phase voltage profile at selected three-phase nodes during VPP dispatch of distribution system Case III.

5.5 Conclusions

The HIL setup is developed for a 534-node distribution feeder using OPAL-RT OP5600 simulator with all required optimization modules built in GAMS/MATLAB and interfaced with the simulator. Distribution level VPP scheduler is developed to reschedule VPPs against distribution constraints by linearizing around the operation point of the MINLP trajectory. A QP-DOPF model of three-phase feeder is developed. The real time HIL simulation demonstrates effectiveness of the QP-DOPF model and VPP scheduler on the distribution feeders.

Chapter 6

Conclusion and Future Work

6.1 Summary

In Chapter 1, the motivation and basic concepts of this dissertation are discussed and introduced. State-of-the-art literature are reviewed.

In Chapter 2, mathematical models of distribution power flow with operational constraints, EV load model, EV charging model, and concept of VPP are introduced.

In Chapter 3, optimal distribution power flow and optimal EV charging models are first developed, which utilize reactive power injection capability of the EVs to support the grid. This work has shown that in coordinated charging scheme, if EVs agree to

inject reactive power into the grid, it benefits EVs by reducing the costs of charging the EVs in dynamic energy pricing schemes. This work also demonstrates that the reactive power injection from EVs can be coordinated with the load shifting and load curtailment in demand response applications to help accommodate increased number of EVs on constrained grids.

In Chapter 4, the detailed high-fidelity model of battery and EV on-board charger that allows four-quadrant operation is integrated to a typical North American low voltage distribution feeder to demonstrate the usefulness of four-quadrant dispatch of EVs in supporting voltage on the feeder. For this, voltage regulation signals (in terms of P,Q dispatch of EVs) are generated from an optimal power flow model and the EVs are dispatched accordingly. The real time simulation demonstrates effectiveness of dispatching EVs in 4-quadrant for supporting voltage on the distribution feeders.

In Chapter 5, the HIL setup is developed for a 534-node distribution feeder using OPAL-RT OP5600 simulator with all required optimization modules built in GAMS/MATLAB and interfaced with the simulator. More specifically, first of all, distribution level VPP coordinator is developed to reschedule VPPs against distribution constraints by linearizing around the operating point of the MINLP trajectory. Then, a quadratic programming formulation of three-phase optimal power flow using parallel computing environment is developed to ensure distribution grid operating constraints every 30 seconds. If VPPs cannot provide expected resources, distribution level finds

an optimal way of re-scheduling the VPPs requests against distribution constraints. The real time HIL simulation demonstrates effectiveness of LOPF method and VPP coordinator on the distribution feeders.

6.2 Future Work

† Evaluate and quantify the effectiveness of reactive power dispatch for voltage support on LV and MV feeder.

† Aggregate the EVs at MV level, and utilize the high fidelity battery/charger model for supporting grid services that is faster in dynamic (such as frequency regulation).

† Consider other distributed resources, such as four-quadrant operation of inverters in Chapter 3 and 4. Further consider EV and other energy storage devices in Chapter 5.

† Include transmission line model and transmission level simulation in Chapter 5.

† Consider spatial-temporal model in Chapter 3 and 4. Temporal model of EV distribution is considered in this dissertation, but not spatial model. Further research on geographic locations of EV distribution. This requires bigger power systems including transportation systems. Probability and stochastic process models of EV spatial distribution will be considered, such as Markov process model.

References

[1] Electric vehicle sales in the united states: 2016 final update. FleetCarma. [Online]. Available: http://www.fleetcarma.com/ev-sales-usa-2016-final/.

[2] M. C. Kisacikoglu, F. Erden, and N. Erdogan, "Distributed control of pev charging based on energy demand forecast," *IEEE Transactions on Industrial Informatics*, vol. 14, no. 1, pp. 332–341, Jan 2018.

[3] M. Mojdehi and P. Ghosh, "An On-Demand Compensation Function for an EV as a Reactive Power Service Provider," *IEEE Trans. Veh. Technol.*, vol. 65, no. 6, pp. 4572–4583, Jun 2016.

[4] S. Paudyal, O. Ceylan, B. P. Bhattarai, and K. S. Myers, "Optimal coordinated ev charging with reactive power support in constrained distribution grids," in *Proc. IEEE PES General Meeting*, Jul. 2017, pp. 1–5.

[5] M. E. Baran and F. F. Wu, "Network reconfiguration in distribution systems

for loss reduction and load balancing," *IEEE Transactions on Power Delivery*, vol. 4, no. 2, pp. 1401–1407, Apr. 1989.

[6] P.-Y. Kong and G. K. Karagiannidis, "Charging schemes for plug-in hybrid electric vehicles in smart grid: A survey," *IEEE Access*, vol. 4, pp. 6846–6875, 2016.

[7] S. Han, S. Han, and K. Sezaki, "Development of an optimal vehicle-to-grid aggregator for frequency regulation," *IEEE Trans. Smart Grid*, vol. 1, no. 1, pp. 65–72, Jun 2010.

[8] J. Tomić and W. Kempton, "Using fleets of electric-drive vehicles for grid support," *J. Power Sources*, vol. 168, no. 2, 2007.

[9] Y. He, B. Venkatesh, and L. Guan, "Optimal scheduling for charging and discharging of electric vehicles," *IEEE Transactions on Smart Grid*, vol. 3, no. 3, pp. 1095–1105, Sept. 2012.

[10] K. Clement-Nyns, E. Haesen, and J. Driesen, "The impact of charging plug-in hybrid electric vehicles on a residential distribution grid," *IEEE Trans. Power Syst.*, vol. 25, no. 1, pp. 371–380, Feb 2010.

[11] K. Clement, E. Haesen, and J. Driesen, "Coordinated charging of multiple plug-in hybrid electric vehicles in residential distribution grids," in *Proc. IEEE PES Power Systems Conference and Exposition*, Mar. 2009, pp. 1–7.

[12] Y. Tang, J. Zhong, and M. Bollen, "Aggregated optimal charging and vehicle-to-grid control for electric vehicles under large electric vehicle population," *IET Generation, Transmission & Distribution*, vol. 10, no. 8, pp. 2012–2018, 2016.

[13] B. P. Bhattarai, K. S. Myers, B. Bak-Jensen, and S. Paudyal, "Multi-time scale control of demand flexibility in smart distribution networks," *Energies*, vol. 10, no. 1, p. 37, 2017.

[14] S. Paudyal and S. Dahal, "Impact of plug-in hybrid electric vehicles and their optimal deployment in smart grids," in *Proc. 21st Australasian Universities Power Engineering Conference*, 2011, pp. 1–6.

[15] S. Shafiee, M. Fotuhi-Firuzabad, and M. Rastegar, "Investigating the impacts of plug-in hybrid electric vehicles on power distribution systems," *IEEE Transactions on Smart Grid*, vol. 4, no. 3, pp. 1351–1360, Sep. 2013.

[16] A. S. Masoum, A. Abu-Siada, and S. Islam, "Impact of uncoordinated and coordinated charging of plug-in electric vehicles on substation transformer in smart grid with charging stations," *Proc. IEEE PES Innovative Smart Grid Technologies (ISGT Asia)*, 2011.

[17] M. S. ElNozahy and M. M. A. Salama, "A comprehensive study of the impacts of PHEVs on residential distribution networks," *IEEE Trans. Sustainable Energy*, vol. 5, no. 1, Jan 2014.

[18] I. Beil and I. Hiskens, "Coordinated pev charging and its effect on distribution

system dynamics," in *Proc. Power Systems Computation Conference (PSCC)*, 2014, pp. 1–7.

[19] A. D. Hilshey, P. D. H. Hines, P. Rezaei, and J. R. Dowds, "Estimating the impact of electric vehicle smart charging on distribution transformer aging," *IEEE Transactions on Smart Grid*, vol. 4, no. 2, pp. 905–913, Jun. 2013.

[20] Y. Zhang, H. Yu, C. Huang, W. Zhao, and M. Luo, *Coordination of Electric Vehicles Charging to Maximize Economic Benefits*. Springer Berlin Heidelberg, 2014.

[21] M. Moghbel, M. A. S. Masoum, and A. Fereidouni, "Decentralize coordinated charging of plug-in electric vehicles in unbalanced residential networks to control distribution transformer loading, voltage profile and current unbalance," *Intelligent Industrial Systems*, vol. 1, no. 2, pp. 141–151, 2015.

[22] E. Sortomme, M. M. Hindi, S. D. J. MacPherson, and S. S. Venkata, "Coordinated charging of plug-in hybrid electric vehicles to minimize distribution system losses," vol. 2, no. 1, pp. 198–205, Mar 2011.

[23] Smart grid. Office of Electricity Delivery and Energy Reliability. [Online]. Available: http://energy.gov/oe/services/technology-development/smart-grid.

[24] The smart grid: An introduction. Office of Electricity Delivery and Energy Reliability. [Online]. Available: http://energy.gov/oe/downloads/smart-grid-introduction-0.

[25] Z. Yang, C. W. Ten, and A. Ginter, "Extended enumeration of hypothesized substations outages incorporating overload implication," *IEEE Trans. Smart Grid*, vol. 9, no. 6, pp. 6929–6938, Nov. 2018.

[26] P. Siano, "Demand response and smart gridsa survey," *Renewable and Sustainable Energy Reviews*, vol. 30, pp. 461–478, Feb. 2014.

[27] K. Spees and L. B. Lave, "Demand response and electricity market efficiency," *The Electricity J.*, vol. 20, no. 3, pp. 69–85, Apr. 2007.

[28] Demand response. Office of Electricity Delivery and Energy Reliability. [Online]. Available: http://energy.gov/oe/services/technology-development/smart-grid/demand-response.

[29] S. Shao, M. Pipattanasomporn, and S. Rahman, "Grid integration of electric vehicles and demand response with customer choice," *IEEE Trans. Smart Grid*, vol. 3, no. 1, pp. 543–550, Mar. 2012.

[30] ——, "Demand response as a load shaping tool in an intelligent grid with electric vehicles," *IEEE Trans. Smart Grid*, vol. 2, no. 4, pp. 624–631, Dec. 2011.

[31] M. Pipattanasomporn, M. Kuzlu, and S. Rahman, "An algorithm for intelligent home energy management and demand response analysis," *IEEE Trans. Smart Grid*, vol. 3, no. 4, pp. 2166–2173, Dec. 2012.

[32] W. Kempton and J. Tomić, "Vehicle-to-grid power fundamentals: Calculating

capacity and net revenue," *J. of Power Sources*, vol. 144, no. 1, pp. 268–279, 2005.

[33] W. Kempton and J. Tomić, "Vehicle-to-grid power fundamentals: Calculating capacity and net revenue," *J. power sources*, vol. 144, no. 1, pp. 268–279, Jun. 2005.

[34] J. Tomić and W. Kempton, "Using fleets of electric-drive vehicles for grid support," *J. of Power Sources*, vol. 168, no. 2, pp. 459–468, Jun. 2007.

[35] C. Guille and G. Gross, "A conceptual framework for the vehicle-to-grid (v2g) implementation," *Energy policy*, vol. 37, no. 11, pp. 4379–4390, 2009.

[36] S. Han, S. Han, and K. Sezaki, "Development of an optimal vehicle-to-grid aggregator for frequency regulation," *IEEE Trans. smart grid*, vol. 1, no. 1, pp. 65–72, Jun. 2010.

[37] S. B. Peterson, J. F. Whitacre, and J. Apt, "The economics of using plug-in hybrid electric vehicle battery packs for grid storage," *J. Power Sources*, vol. 195, no. 8, pp. 2377–2384, 2010.

[38] S. B. Peterson, J. Apt, and J. F. Whitacre, "Lithium-ion battery cell degradation resulting from realistic vehicle and vehicle-to-grid utilization," *J. Power Sources*, vol. 195, no. 8, pp. 2385–2392, 2010.

[39] K. Clement-Nyns, E. Haesen, and J. Driesen, "The impact of charging plug-in

hybrid electric vehicles on a residential distribution grid," *IEEE Trans. Power Syst.*, vol. 25, no. 1, pp. 371–380, Feb. 2010.

[40] P. Richardson, D. Flynn, and A. Keane, "Optimal charging of electric vehicles in low-voltage distribution systems," *IEEE Trans. Power Syst.*, vol. 27, no. 1, pp. 268–279, Feb. 2012.

[41] E. Sortomme and M. A. El-Sharkawi, "Optimal charging strategies for unidirectional vehicle-to-grid," *IEEE Trans. Smart Grid*, vol. 2, no. 1, pp. 131–138, Mar. 2011.

[42] S. Deilami, A. S. Masoum, P. S. Moses, and M. A. S. Masoum, "Real-time coordination of plug-in electric vehicle charging in smart grids to minimize power losses and improve voltage profile," *IEEE Trans. Smart Grid*, vol. 2, no. 3, pp. 456–467, Sept. 2011.

[43] R.-C. Leou, "Optimal charging/discharging control for electric vehicles considering power system constraints and operation costs," *IEEE Trans. Power Syst.*, vol. 31, no. 3, pp. 1854–1860, May 2016.

[44] Z. Ma, D. S. Callaway, and I. A. Hiskens, "Decentralized charging control of large populations of plug-in electric vehicles," *IEEE Trans. Control Syst. Technol.*, vol. 21, no. 1, pp. 67–78, Jan. 2013.

[45] J. A. P. Lopes, F. J. Soares, P. M. Almeida, and M. M. Da Silva, "Smart charging strategies for electric vehicles: Enhancing grid performance and maximizing

the use of variable renewable energy resources," in *Proc. Int. Battery, Hybrid and Fuell Cell Electric Vehicle Symp. Exhib.*, 2009, pp. 1–11.

[46] E. Sortomme, M. M. Hindi, S. D. J. MacPherson, and S. S. Venkata, "Coordinated charging of plug-in hybrid electric vehicles to minimize distribution system losses," *IEEE trans. smart grid*, vol. 2, no. 1, pp. 198–205, Mar. 2011.

[47] L. Gan, U. Topcu, and S. H. Low, "Optimal decentralized protocol for electric vehicle charging," *IEEE Trans. Power Syst.*, vol. 28, no. 2, pp. 940–951, May 2013.

[48] H. Xing, M. Fu, Z. Lin, and Y. Mou, "Decentralized optimal scheduling for charging and discharging of plug-in electric vehicles in smart grids," *IEEE Transactions on Power Systems*, vol. 31, no. 5, pp. 4118–4127, Sept. 2016.

[49] E. L. Karfopoulos, K. A. Panourgias, and N. D. Hatziargyriou, "Distributed coordination of electric vehicles providing v2g regulation services," *IEEE Trans. Power Syst.*, vol. 31, no. 4, pp. 2834–2846, Jul. 2016.

[50] E. L. Karfopoulos and N. D. Hatziargyriou, "Distributed coordination of electric vehicles providing v2g services," *IEEE Trans. Power Syst.*, vol. 31, no. 1, pp. 329–338, Jan. 2016.

[51] A. Ghavami, K. Kar, and A. Gupta, "Decentralized charging of plug-in electric vehicles with distribution feeder overload control," *IEEE Trans. Autom. Control*, vol. 61, no. 11, pp. 3527–3532, Nov. 2016.

[52] D. S. Callaway and I. A. Hiskens, "Achieving controllability of electric loads," *Proc. of the IEEE*, vol. 99, no. 1, pp. 184–199, Jan. 2011.

[53] Y. He, B. Venkatesh, and L. Guan, "Optimal scheduling for charging and discharging of electric vehicles," *IEEE Trans. Smart Grid*, vol. 3, no. 3, pp. 1095–1105, Sept. 2012.

[54] G. R. Bharati and S. Paudyal, "Coordinated control of distribution grid and electric vehicle loads," *Electric Power Syst. Research*, vol. 140, pp. 761–768, Nov. 2016.

[55] H. F. Farahani, H. A. Shayanfar, and M. S. Ghazizadeh, "Modeling of stochastic behavior of plug-in hybrid electric vehicle in a reactive power market," *Elect. Eng.*, vol. 96, no. 1, pp. 1–13, Mar. 2014.

[56] J. Zhong and K. Bhattacharya, "Toward a competitive market for reactive power," *IEEE Trans. Smart Grid*, vol. 17, no. 4, pp. 1206–1215, Nov. 2002.

[57] B. Bhattarai, M. Levesque, M. Maier, B. Bak-Jensen, and J. Pillai, "Optimizing electric vehicle charging coordination over a haterogeneous mesh network in a scaled-down smart grid testbed," *IEEE Transactions on Smart Grid*, vol. 6, no. 2, pp. 784–794, Jan. 2015.

[58] M. N. Mojdehi and P. Ghosh, "Modeling and revenue estimation of EV as reactive power service provider," in *Proc. IEEE PES GM*, 2014.

[59] M. C. Kisacikoglu, B. Ozpineci, and L. M. Tolbert, "Examination of a PHEV bidirectional charger system for V2G reactive power compensation," in *Proc. IEEE Applied Power Electronics Conference and Exposition*, Feb. 2010, pp. 458–465.

[60] M. Kesler, M. C. Kisacikoglu, and L. M. Tolbert, "Vehicle-to-Grid Reactive Power Operation Using Plug-In Electric Vehicle Bidirectional Offboard Charger," *IEEE Transactions on Industrial Electronics*, vol. 61, no. 12, pp. 6778–6784, Dec. 2014.

[61] B. Sun, T. Dragicevic, M. Savaghebi, J. C. Vasquez, and J. M. Guerrero, "Reactive power support of electrical vehicle charging station upgraded with flywheel energy storage system," in *Proc. IEEE PowerTech*, June 2015, pp. 1–6.

[62] M. N. Mojdehi and P. Ghosh, "An on-demand compensation function for an ev as a reactive power service provider," *IEEE Trans. Veh. Technol.*, vol. 65, no. 6, pp. 4572–4583, Jun. 2016.

[63] M. C. Kisacikoglu, B. Ozpineci, and L. M. Tolbert, "Examination of a PHEV bidirectional charger system for V2G reactive power compensation," in *Proc. IEEE Applied Power Electronics Conference and Exposition*, 2010, pp. 458–465.

[64] A. Rabiee, H. F. Farahani, M. Khalili, J. Aghaei, and K. M. Muttaqi, "Integration of plug-in electric vehicles into microgrids as energy and reactive power

providers in market environment," *IEEE Trans. Ind. Informat.*, vol. 12, no. 4, pp. 1312–1320, Aug 2016.

[65] M. C. Kisacikoglu, B. Ozpineci, and L. M. Tolbert, "Examination of a phev bidirectional charger system for v2g reactive power compensation," in *25th Annu. IEEE Appl. Power Electron. Conf. and Expo.*, Feb. 2010, pp. 458–465.

[66] M. C. Kisacikoglu, "Vehicle-to-grid (v2g) reactive power operation analysis of the ev/phev bidirectional battery charger," Ph.D. dissertation, University of Tennessee, Knoxville, 2013.

[67] Y. Du, X. Zhou, and S. Bai, "Review of non-isolated bi-directional dc-dc converters for plug-in hybrid electric vehicle charge station application at municipal parking decks," in *25th Annual IEEE Appl. Power Electron. Conf. and Expo.*, Feb. 2010, pp. 1145–1151.

[68] M. N. Mojdehi and P. Ghosh, "Estimation of the battery degradation effects on the ev operating cost during charging/discharging and providing reactive power service," in *IEEE 81st Veh. Technol. Conf.*, May 2015, pp. 1–5.

[69] B. Jiang and Y. Fei, "Decentralized scheduling of pev on-street parking and charging for smart grid reactive power compensation," in *IEEE PES Innovative Smart Grid Technologies*, Feb. 2013, pp. 1–6.

[70] S. Shao, M. Pipattanasomporn, and S. Rahman, "Demand response as a load

shaping tool in an intelligent grid with electric vehicles," *IEEE Trans. Smart Grid*, vol. 2, no. 4, pp. 624–631, Dec 2011.

[71] C. K. Wen, J. C. Chen, J. H. Teng, and P. Ting, "Decentralized plug-in electric vehicle charging selection algorithm in power systems," *IEEE Trans. Smart Grid*, vol. 3, no. 4, pp. 1779–1789, Dec 2012.

[72] J. de Hoog, T. Alpcan, M. Brazil, D. A. Thomas, and I. Mareels, "Optimal charging of electric vehicles taking distribution network constraints into account," *IEEE Trans. Power Syst.*, vol. 30, no. 1, pp. 365–375, Jan 2015.

[73] B. Bhattarai, B. Bak-Jensen, P. Mahat, J. Pillai, and M. Maier, "Hierarchical control architecture for demand response in smart grid scenario," in *Proc. IEEE PES APPEEC*, Dec 2013, pp. 1–6.

[74] G. R. Bharati and S. Paudyal, "Coordinated control of distribution grid and electric vehicle loads," *Electric Power Systems Research*, vol. 140, pp. 761 – 768, 2016.

[75] S. Paudyal and G. R. Bharati, "Hierarchical approach for optimal operation of distribution grid and electric vehicles," in *Proc. IEEE PowerTech*, Jun. 2015, pp. 1–6.

[76] Z. Li, Q. Guo, H. Sun, and S. Xin, "A decentralized optimization method to track electric vehicle aggregator's optimal charging plan," in *Proc. IEEE PES General Meeting*, July 2014, pp. 1–5.

[77] L. Gan, U. Topcu, and S. H. Low, "Optimal decentralized protocol for electric vehicle charging," *IEEE Transactions on Power Systems*, vol. 28, no. 2, pp. 940–951, May 2013.

[78] M. C. Kisacikoglu, B. Ozpineci, and L. M. Tolbert, "EV/PHEV Bidirectional Charger Assessment for V2G Reactive Power Operation," *IEEE Trans. Power Electron.*, vol. 28, no. 12, pp. 5717–5727, Dec 2013.

[79] M. C. Kisacikoglu, M. Kesler, and L. M. Tolbert, "Single-phase on-board bidirectional pev charger for v2g reactive power operation," *IEEE Transactions on Smart Grid*, vol. 6, no. 2, pp. 767–775, March 2015.

[80] L. P. Fernandez, T. G. S. Roman, R. Cossent, C. M. Domingo, and P. Frias, "Assessment of the impact of plug-in electric vehicles on distribution networks," vol. 26, no. 1, pp. 206–213, Feb 2011.

[81] E. Veldman and R. A. Verzijlbergh, "Distribution grid impacts of smart electric vehicle charging from different perspectives," *IEEE Trans. Smart Grid*, vol. 6, no. 1, pp. 333–342, Jan 2015.

[82] S. Shafiee, M. Fotuhi-Firuzabad, and M. Rastegar, "Investigating the impacts of plug-in hybrid electric vehicles on power distribution systems," *Smart Grid, IEEE Transactions on*, vol. 4, no. 3, pp. 1351–1360, 2013.

[83] E. Ucer, M. C. Kisacikoglu, and M. Yuksel, "Analysis of an internet-inspired

EV charging network in a distribution grid," in *IEEE Transmiss. Distr. Conf.*, Apr 2018.

[84] Z. Wang and S. Wang, "Grid power peak shaving and valley filling using vehicle-to-grid systems," vol. 28, no. 3, pp. 1822–1829, Jul 2013.

[85] M. J. E. Alam, K. M. Muttaqi, and D. Sutanto, "A controllable local peak-shaving strategy for effective utilization of PEV battery capacity for distribution network support," vol. 51, no. 3, pp. 2030–2037, 2015.

[86] M. C. Kisacikoglu, M. Kesler, and L. M. Tolbert, "Single-phase on-board bidirectional PEV charger for V2G reactive power operation," vol. 6, no. 2, pp. 767–775, Mar 2015.

[87] M. Singh, P. Kumar, and I. Kar, "A multi charging station for electric vehicles and its utilization for load management and the grid support," *IEEE Trans. Smart Grid*, vol. 4, no. 2, pp. 1026–1037, 2013.

[88] A. Di Giorgio, F. Liberati, and S. Canale, "Electric vehicles charging control in a smart grid: A model predictive control approach," *Control Engineering Practice*, vol. 22, pp. 147–162, 2014.

[89] J. Wang, G. R. Bharati, S. Paudyal, O. Ceylan, B. P. Bhattarai, and K. S. Myers, "Coordinated electric vehicle charging with reactive power support to distribution grids," *IEEE Trans. Ind. Informat.*, to be published.

[90] Y. He, B. Venkatesh, and L. Guan, "Optimal scheduling for charging and discharging of electric vehicles," *IEEE Trans. Smart Grid*, vol. 3, no. 3, pp. 1095–1105, Sep 2012.

[91] Y. Tang, J. Zhong, and M. Bollen, "Aggregated optimal charging and vehicle-to-grid control for electric vehicles under large electric vehicle population," *IET Generation, Transmission Distribution*, vol. 10, no. 8, pp. 2012–2018, 2016.

[92] I. Vittorias, M. Metzger, D. Kunz, M. Gerlich, and G. Bachmaier, "A bidirectional battery charger for electric vehicles with V2G and V2H capability and active and reactive power control," in *Proc. IEEE Transportation Electrification Conference and Expo.*, 2014, pp. 1–6.

[93] M. Kesler, M. C. Kisacikoglu, and L. M. Tolbert, "Vehicle-to-grid reactive power operation using plug-in electric vehicle bidirectional offboard charger," *IEEE Trans. Ind. Electron.*, vol. 61, no. 12, pp. 6778–6784, Dec 2014.

[94] W. Zheng, W. Wu, B. Zhang, H. Sun, and Y. Liu, "A fully distributed reactive power optimization and control method for active distribution networks," *IEEE Trans. Smart Grid*, vol. 7, no. 2, pp. 1021–1033, Mar 2016.

[95] T. Ding, S. Liu, W. Yuan, Z. Bie, and B. Zeng, "A two-stage robust reactive power optimization considering uncertain wind power integration in active distribution networks," *IEEE Trans. Sustainable Energy*, vol. 7, no. 1, pp. 301–311, Jan 2016.

[96] M. A. Azzouz, M. F. Shaaban, and E. F. El-Saadany, "Real-time optimal voltage regulation for distribution networks incorporating high penetration of pevs," *IEEE Trans. Power Syst.*, vol. 30, no. 6, pp. 3234–3245, Nov 2015.

[97] J. Wang, G. R. Bharati, S. Paudyal, O. Ceylan, B. P. Bhattarai, and K. S. Myers, "Coordinated electric vehicle charging with reactive power support to distribution grids," *IEEE Trans. Ind. Informat.*, pp. 1–1, 2018.

[98] N. Mehboob, M. Restrepo, C. A. Caizares, C. Rosenberg, and M. Kazerani, "Smart operation of electric vehicles with four-quadrant chargers considering uncertainties," *IEEE Trans. Smart Grid*, pp. 1–1, 2018.

[99] M. Restrepo, C. A. Caizares, and M. Kazerani, "Three-stage distribution feeder control considering four-quadrant EV chargers," *IEEE Trans. Smart Grid*, vol. 9, no. 4, pp. 3736–3747, Jul 2018.

[100] E. G. Kardakos, C. K. Simoglou, and A. G. Bakirtzis, "Optimal offering strategy of a virtual power plant: A stochastic bi-level approach," *IEEE Transactions on Smart Grid*, vol. 7, no. 2, pp. 794–806, 2016.

[101] A. T. Al-Awami, N. A. Amleh, and A. M. Muqbel, "Optimal demand response bidding and pricing mechanism with fuzzy optimization: Application for a virtual power plant," *IEEE Transactions on Industry Applications*, vol. 53, no. 5, pp. 5051–5061, 2017.

[102] H. Yang, D. Yi, J. Zhao, and Z. Dong, "Distributed optimal dispatch of virtual

power plant via limited communication," *IEEE Transactions on power systems*, vol. 28, no. 3, pp. 3511–3512, 2013.

[103] E. DallAnese, S. S. Guggilam, A. Simonetto, Y. C. Chen, and S. V. Dhople, "Optimal regulation of virtual power plants," *IEEE Transactions on Power Systems*, vol. 33, no. 2, pp. 1868–1881, 2018.

[104] M. Abdolrasol, M. Hannan, A. Mohamed, U. Amiruldin, I. Abidin, and M. Uddin, "An optimal scheduling controller for virtual power plant and microgrid integration using binary backtracking search algorithm," *IEEE Transactions on Industry Applications*, 2018.

[105] Z. Liang, Q. Alsafasfeh, T. Jin, H. Pourbabak, and W. Su, "Risk-constrained optimal energy management for virtual power plants considering correlated demand response," *IEEE Transactions on Smart Grid*, 2017.

[106] A. Bagchi, L. Goel, and P. Wang, "Adequacy assessment of generating systems incorporating storage integrated virtual power plants," *IEEE Transactions on Smart Grid*, 2018.

[107] V. A. Evangelopoulos, P. S. Georgilakis, and N. D. Hatziargyriou, "Optimal operation of smart distribution networks: A review of models, methods and future research," *Electric Power Systems Research*, vol. 140, pp. 95–106, 2016.

[108] S. Paudyal, C. Cañizares, and K. Bhattacharya, "Optimal operation of distribution feeders in smart grids," *IEEE Transactions on Industrial Electronics*, vol. 58, no. 10, pp. 4495–4503, Oct. 2011.

[109] J. Franco, L. Ochoa, and R. Romero, "Ac opf for smart distribution networks: An efficient and robust quadratic approach," *IEEE Transactions on Smart Grid*, 2017.

[110] P. L. Cavalcante, J. C. López, J. F. Franco, M. J. Rider, A. V. Garcia, M. R. Malveira, L. L. Martins, and L. C. M. Direito, "Centralized self-healing scheme for electrical distribution systems," *IEEE Transactions on Smart Grid*, vol. 7, no. 1, pp. 145–155, 2016.

[111] L. H. Macedo, J. F. Franco, M. J. Rider, and R. Romero, "Optimal operation of distribution networks considering energy storage devices," *IEEE Transactions on Smart Grid*, vol. 6, no. 6, pp. 2825–2836, 2015.

[112] J. F. Franco, M. J. Rider, and R. Romero, "A mixed-integer linear programming model for the electric vehicle charging coordination problem in unbalanced electrical distribution systems," *IEEE Transactions on Smart Grid*, vol. 6, no. 5, pp. 2200–2210, 2015.

[113] G. Liu, M. Starke, X. Zhang, and K. Tomsovic, "A milp-based distribution optimal power flow model for microgrid operation," in *Power and Energy Society General Meeting (PESGM)*. IEEE, 2016, pp. 1–5.

[114] H. Ahmadi, J. R. Martı, and A. von Meier, "A linear power flow formulation for three-phase distribution systems," *IEEE Transactions on Power Systems*, vol. 31, no. 6, pp. 5012–5021, 2016.

[115] F. Pilo, G. Pisano, and G. G. Soma, "Optimal coordination of energy resources with a two-stage online active management," *IEEE Transactions on Industrial Electronics*, vol. 58, no. 10, pp. 4526–4537, 2011.

[116] G. Liu, Y. Xu, O. Ceylan, and K. Tomsovic, "A new linearization method of unbalanced electrical distribution networks," in *North American Power Symposium (NAPS)*. IEEE, 2014, pp. 1–6.

[117] M. E. Baran and F. F. Wu, "Network reconfiguration in distribution systems for loss reduction and load balancing," *IEEE Transactions on Power delivery*, vol. 4, no. 2, pp. 1401–1407, 1989.

[118] J. Xu and H. Sun, "Admm-based coordinated decentralized voltage control meets practical communication systems," in *IEEE International Conference on Communications Workshops (ICC Workshops)*. IEEE, 2017, pp. 1–5.

[119] H. Zhu and H. J. Liu, "Fast local voltage control under limited reactive power: Optimality and stability analysis," *IEEE Transactions on Power Systems*, vol. 31, no. 5, pp. 3794–3803, 2016.

[120] H. Zhu and N. Li, "Asynchronous local voltage control in power distribution

networks," in *IEEE International Conference on Acoustics, Speech and Signal Processing (ICASSP)*. IEEE, 2016, pp. 3461–3465.

[121] W. Lin and E. Bitar, "Decentralized control of distributed energy resources in radial distribution systems," in *IEEE International Conference on Smart Grid Communications (SmartGridComm)*. IEEE, 2016, pp. 296–301.

[122] H. E. Farag and E. F. El-Saadany, "A novel cooperative protocol for distributed voltage control in active distribution systems," *IEEE Transactions on Power Systems*, vol. 28, no. 2, pp. 1645–1656, 2013.

[123] B. A. Robbins and A. D. Domínguez-García, "Optimal reactive power dispatch for voltage regulation in unbalanced distribution systems," *IEEE Transactions on Power Systems*, vol. 31, no. 4, pp. 2903–2913, 2016.

[124] W. H. Kersting, *Distribution System Modeling and Analysis*, 3rd ed. CRC Press, 2012.

[125] F. Erden, M. C. Kisacikoglu, and O. H. Gurec, "Examination of EV-grid integration using real driving and transformer loading data," in *Proc. 9th International Conference on Electrical and Electronics Engg.*, 2015.

[126] S. I. Vagropoulos and A. G. Bakirtzis, "Optimal bidding strategy for electric vehicle aggregators in electricity markets," *IEEE Transactions on Power Systems*, vol. 28, no. 4, pp. 4031–4041, Nov 2013.

[127] S. H. Low, "Convex relaxation of optimal power flow–Part I: Formulations and equivalence," *IEEE Transactions on Control of Network Systems*, vol. 1, no. 1, pp. 15–27, Mar. 2014.

[128] R. Tonkoski, L. A. Lopes, and T. H. El-Fouly, "Coordinated active power curtailment of grid connected pv inverters for overvoltage prevention," *IEEE Trans. Sustainable Enery*, vol. 2, no. 2, pp. 139–147, Apr 2011.

[129] M. Almassalkhi, L. D. Espinosa, P. D. H. Hines, J. Frolik, S. Paudyal, and M. Amini, *Asynchronous Coordination of Distributed Energy Resources with Packetized Energy Management*. New York, NY: Springer New York, 2018, pp. 333–361.

[130] L. A. D. Espinosa, M. Almassalkhi, P. Hines, and J. Frolik, "Aggregate modeling and coordination of diverse energy resources under packetized energy management," in *2017 IEEE 56th Annual Conference on Decision and Control (CDC)*, Dec 2017, pp. 1394–1400.

Appendix A

Letters of Permission

Thesis / Dissertation Reuse

The IEEE does not require individuals working on a thesis to obtain a formal reuse license, however, you may print out this statement to be used as a permission grant:

Requirements to be followed when using any portion (e.g., figure, graph, table, or textual material) of an IEEE copyrighted paper in a thesis:

1) In the case of textual material (e.g., using short quotes or referring to the work within these papers) users must give full credit to the original source (author, paper, publication) followed by the IEEE copyright line © 2011 IEEE.
2) In the case of illustrations or tabular material, we require that the copyright line © [Year of original publication] IEEE appear prominently with each reprinted figure and/or table.
3) If a substantial portion of the original paper is to be used, and if you are not the senior author, also obtain the senior author's approval.

Requirements to be followed when using an entire IEEE copyrighted paper in a thesis:

1) The following IEEE copyright/ credit notice should be placed prominently in the references: © [year of original publication] IEEE. Reprinted, with permission, from [author names, paper title, IEEE publication title, and month/year of publication]
2) Only the accepted version of an IEEE copyrighted paper can be used when posting the paper or your thesis on-line.
3) In placing the thesis on the author's university website, please display the following message in a prominent place on the website: In reference to IEEE copyrighted material which is used with permission in this thesis, the IEEE does not endorse any of [university/educational entity's name goes here]'s products or services. Internal or personal use of this material is permitted. If interested in reprinting/republishing IEEE copyrighted material for advertising or promotional purposes or for creating new collective works for resale or redistribution, please go to http://www.ieee.org/publications_standards/publications/rights/rights_link.html to learn how to obtain a License from RightsLink.

If applicable, University Microfilms and/or ProQuest Library, or the Archives of Canada may supply single copies of the dissertation.